NASA CR-]32355

(NASA-CR-132355) EFFECT OF SWEEP ANGLE ON THE PRESSURE DISTRIBUTIONS AND EFFECTIVENESS OF THE OGEE TIP IN (Rochester Applied Science Associates, Inc.) 123 p HC $8.25 CSCL 01A

N74-11822

Unclas G3/01 23759

EFFECT OF SWEEP ANGLE ON THE PRESSURE DISTRIBUTIONS AND EFFECTIVENESS OF THE OGEE TIP IN DIFFUSING A LINE VORTEX

By John C. Balcerak and Raymond F. Feller

Issued by Originator as RASA Report No. 73-07

Prepared under Contract No. NAS1-12012 by
ROCHESTER APPLIED SCIENCE ASSOCIATES, INC.
Rochester, N.Y.

for Langley Research Center

NATIONAL AERONAUTICS AND SPACE ADMINISTRATION

TABLE OF CONTENTS

EFFECT OF SWEEP ANGLE ON THE PRESSURE DISTRIBUTIONS AND EFFECTIVENESS OF THE OGEE TIP IN DIFFUSING A LINE VORTEX

By John C. Balcerak and Raymond F. Feller
ROCHESTER APPLIED SCIENCE ASSOCIATES, INC.

SUMMARY

Low-speed wind tunnel tests were conducted to study the influence of sweep angle on the pressure distributions of an ogee-tip configuration with relation to the effectiveness of the ogee tip in diffusing a line vortex. In addition to the pressure data, performance and flow-visualization data were obtained in the wind tunnel tests to evaluate the application of the ogee tip to aircraft configurations. The effect of sweep angle on the performance characteristics of a conventional-tip model, having equivalent planform area, was also investigated for comparison with the ogee-tip configuration.

Results of the investigation generally indicate that sweep angle has little effect on the characteristics of the ogee in diffusing a line vortex. In addition, the performance characteristics of the ogee were generally superior to those of the conventional-tip configuration. The performance data also indicate that changes in the outermost tip geometry of the ogee may be required for application at high subsonic speeds.

INTRODUCTION

The further development of the helicopter is, to a large extent, dependent upon the improvement of the performance, blade life and acoustic characteristics of the rotor system. One of the primary problems that has hindered the improvement of the rotor systems is the proximity of a vortex that is trailed off a blade to a following blade or to itself in a succeeding passage, or actual blade-vortex intersections. In recent years, the concern over this problem area has led to expanded research involving both active and passive vortex-modification systems. Among the various passive systems that have been investigated for application to the helicopter, the ogee-tip configuration appears to hold the most promise for implementation within the immediate future. In nonrotating systems, this promise has been supported by performance and wake-survey data (ref. 1), performance and flow-visualization data (ref. 2) and by performance data in a rotating system (ref. 3).

As a helicopter blade rotates, say in hover, the peak in the lift distribution of the blade is far outboard, and if the tip is squared off with respect to the blade radius as in a conventional blade, a steep gradient in the lift distribution exists between this peak and the tip of the blade. This gradient in the lift distribution leads to the formation of a separation vortex which trails off the tip of the blade. The principle underlying some of the passive vortex-modification systems for helicopter applications was to prevent this steep gradient in the local lift distribution which, in turn, would prevent the formation of the separation vortex. Attempts to effect these favorable gradients by tapering the blade, or otherwise modifying the blade to accommodate swept-forward or swept-aft pointed tips or other tip shapes have generally led to unacceptable penalties in performance or in overall systems applications. The ogee tip, which was developed by NASA, also prevents the steep gradient in the local lift distribution, but the basic goal of the ogee-tip design was to modify the formation mechanism of the tip vortex. In a conventional-tip rotor blade, a concentrated tip vortex is formed by the interaction of the intense core of the separation vortex with the vortex sheet shed from the trailing edge of the airfoil. The ogee-tip shape modifies this process so that the vortex trailed off the tip would roll up more as a sheet, and thus constrains the mechanism associated with the formation of the separation vortex.

One of the problems in adapting a vortex-modification system to the helicopter is that the system must operate in a rotating framework, where in forward flight, the blade is subjected to an effective sweep angle because of the radial component of flow. This component of flow may have a beneficial or adverse effect in regard to the application of a vortex-modification system for helicopters. Thus, the evaluation of a vortex-modification system for helicopter applications has to be made from test data either in a rotating system or in a stationary system which accounts for the radial component of flow.

On the basis of the results which were obtained in reference 2, in which the ogee-tip configuration showed favorable characteristics in regard to performance and vortex diffusion at zero sweep, NASA/Langley sponsored the research effort whose objectives were to determine the effects of the sweep angle on the performance and vortex-modification characteristics of the ogee-tip configuration. These objectives were attained by the collection of performance data, flow-visualization data and pressure data for the ogee-tip configuration in a stationary system by accounting for sweep angle in the range $-20 \leq \Lambda \leq +30°$.

LIST OF SYMBOLS

AA	angle of attack at root, degrees
AR	model aspect ratio, $2b^2/S$, dimensionless
AY	yaw angle, degrees
b	model semispan, cm (or in.)
CCP	chordwise center of pressure, dimensionless
C_D	drag coefficient, dimensionless
C_L	lift coefficient, dimensionless
C_N	normal force coefficient, dimensionless
c	blade chord, cm (or in.)
D	drag force, newtons (or lb)
L	lift force, newtons (or lb)
ΔP	differential pressure, dimensionless meter units
PM	pitching moment, newton-meters (or ft-lb)
P_n	pressure tap reading at port "n", dimensionless meter units
P_s	tunnel-centerline static pressure, dimensionless meter units
P_t	tunnel total pressure, dimensionless meter units
q	dynamic pressure dimensionless meter units or newtons/meter^2 (or lb/ft^2)
R_N	Reynolds number, dimensionless
RM	rolling moment, newton-meters (or ft-lb)
S	model planform area, cm^2 (or in.^{2})

S CP	spanwise center of pressure, dimensionless
SF	side force, newtons (or lb)
V	freestream or tunnel velocity, meters/sec (or ft/sec)
x	streamwise or chordwise ordinate, cm (or in.)
YM	yawing moment, newton-meters (or ft-lb)
y	spanwise ordinate, cm (or in.)
α_R	angle of attack at model root, degrees
Λ	sweep angle, positive for sweepback, degrees

DESCRIPTION OF MODELS AND WIND TUNNEL INSTALLATION

Ogee Model #1

Ogee Model #1 was fabricated as an attachment to the tip of a UH-1D helicopter blade. The basic blade section was untapered, had a NACA 0012 airfoil section with a chord of 53.6 cm (21.1 in.), and a measured twist of 0.0082 deg/cm (0.0208 deg/in.). The ogee-tip section was fabricated from wood and was not twisted. Planform coordinates of the ogee-tip section are presented in Table I. The 0012 airfoil section was maintained to station 168.15 (66.20), and outboard from this point, the airfoil section was contoured smoothly to a complete elliptical section at station 188.85 (74.35). Figures 1 and 2 show sketches of the ogee planform with the layout of the 148 pressure taps incorporated within the model. A tabular listing of the pressure-tap locations and their designation is given in Table II. The pressure taps on the upper surface of the model were numbered from 1 through 74, while the pressure taps on the lower surface were numbered from 101 through 174.

Grooves were routed out on both the upper and lower surfaces of the ogee-tip section for installation of the pressure taps and associated tubing, then filled in with potting compound and sanded to maintain smooth section contours. The ogee section was attached to the blade section by a 20.3 cm (8 in.) extended piece at the base of the wooden section which was fitted snugly into the D-spar and attached to it with thru-bolts. Aft of the D-spar, the ogee section was recessed to fit between the upper and lower skins of the UH-1D blade section by routing out the honeycomb material to a depth of approximately 2.54 cm (1 inch). It was secured to the blade skin with wood screws. The outermost section of the ogee-tip was mortised at station 167.77 (66.05) to accommodate various tip shapes. The station numbers refer to spanwise locations on the model with reference to the tunnel floor at zero sweep. The measurements are in centimeters and, parenthetically, in inches. Provision was made to accommodate pressure taps in the outermost tip region. The outermost section of section of the ogee shown in Figure 1 was instrumented with pressure taps, but the one additional tip shape which was tested was not instrumented with pressure taps.

Ogee Model #2

The model designation, Ogee Model #2, refers to the ogee model which was fabricated and tested under a previous program (ref. 2). In the present test program, the model was used solely for conducting flow-visualization studies using the helium-bubble technique to minimize the possibility of plugging the pressure taps on Ogee Model #1 with the soap solution used in the bubble-generating process. Ogee Model #2 was identical in planform to Ogee Model #1, but the measured twist of the UH-1D blade section comprising Model #2 was 0.0046 deg/cm (0.0117 deg/in.)

Model #3

Model #3 was a conventional-tip model, also fabricated and tested under a previous program (ref. 2). The model was fabricated from an outboard section of a UH-1D helicopter blade which had a measured twist of 0.0046 deg/cm (0.0117 deg/in.). The tip of the model was fitted with a "half-round" cap whose shape was obtained by rotating an airfoil template 180 degrees about the centerline of the chord. Figure 3 shows schematic diagrams of the ogee and conventional-model planforms.

Installation of Models

The wind tunnel installation of all three models was identical. Provisions were made for varying the sweep angle of each model manually by bolting an existing model base support to a plate which pivoted within a jig assembly. The jig contained pre-set positions for securing the models at the requisite sweep angles. Each sweep-angle condition required separate floor plates which were fitted around the base of the models to provide a gap of approximately 0.635 cm (0.25 in.).

Table III presents a comparison of the planform geometries associated with the ogee-tip and conventional-tip models for the reflection-plane installation in the wind tunnel. Although the exposed planform area varied with sweep angle, it was identical for the ogee-tip and conventional-tip models for all sweep angles tested. Since the areas were equal for both models, the aspect ratio of the ogee-tip model was higher than that of the conventional-tip model. The differences in aspect ratio for these models were exaggerated in comparison to those which would be realized on full-scale helicopter blades. The performance characteristics of the models were not corrected for the differences in aspect ratio as precise quantitative comparisons of the performance characteristics were not a primary objective of the research program.

Photographs of Ogee Model #1 installed in the test section at two sweep positions are shown in Figures 4 and 5 for sweep angles of +20 and -20 degrees, respectively. Photographs of Ogee Model #2 at Λ = +30° and Model #3 at Λ = -15° are shown as Figures 6 and 7, respectively.

A "reverse ogee" configuration was achieved by rotating the turntable 180° in the test section. Ogee Models #1 and #2 were tested in this manner at Λ = 0°.

TESTING PROCEDURES AND DATA ACQUISITION

Balance Data

The wind tunnel test program was conducted in the University of Maryland wind tunnel facility at College Park, Maryland. The wind tunnel test section is 2.36 x 3.35 m (7.75 x 11 ft) and 4.57 m (15 ft) long. Model forces and moments were measured by a six-component yoke-type balance located beneath the floor of the test section. Balance data for the models was monitored on-line in the wind-axes system of the wind tunnel with the forces and moments resolved relative to axes parallel and perpendicular to the tunnel centerline. The recorded balance data in this wind-axes system were transformed into a wind-axes system with its origin located on the model quarter-chord at the tunnel floor for any sweep position of the model. A sketch of the coordinate system and the balance data in this reference system are presented in Appendix A. A summary of the model configurations and test conditions for which balance data were obtained is presented in Table IV.

In the plan of test, it was desired to obtain data at the same value of lift at a given angle of attack and sweep angle for both the ogee and conventional-tip models. Baseline data were obtained at $\Lambda = 0°$ and a dynamic pressure of 1842 newtons/meter^2 (38.5 lb/ft^2) by pitching the ogee model through an angle-of-attack range at the model root from -2 to +14 degrees in 2-degree increments. The Reynolds number for these conditions based on the model chord was 1.9×10^6. Balance data were recorded for all the other model test conditions by varying the dynamic pressure in order to generate the same lift that was obtained for the baseline condition at a given angle of attack. This method of testing was adopted to establish a basis for comparison of the circulation strength of the tip vortex, that is, for a given value of lift, it was assumed that the same percentage of vorticity would be rolled up into the tip vortex. Because of differences in twist, the average angle of attack of the conventional model was approximately 0.2 degree less than the ogee model. This slight difference in the average angle of attack was neglected since it would effect only minor differences in the comparison of the performance characteristics between the models. For some test conditions above stall, it was not possible to attain the required lift within the limits of the wind tunnel. For these conditions, testing was conducted by oeprating at a constant dynamic pressure which was maintained at its pre-stall value. Tests of the reverse-ogee configuration were conducted at a constant dynamic pressure of 1842 newtons/meter^2 throughout the angle-of-attack range tested.

Pressure Data

Pressure data from the 148 pressure taps located on Ogee Model #1 were obtained concurrently with the performance data. The test conditions for which pressure data were obtained with Ogee Model #1 are summarized in Table V.

The pressure data were recorded from four, 48-port scanivalves. Three ports on each scanivalve monitored the tunnel total, tunnel static, and tunnel-centerline static pressures, respectively, so that a maximum number of 45 taps were connected to a scanivalve. Pressure transducers with a sensitivity of ±17228 newtons/meter^2 (±2.5 lb/in.^{2}) were used to cover the range of differential pressure ratio, $\Delta P/q$, for all the test conditions. The pressure data were recorded in meter units on punched cards, and converted to coefficient form, $\Delta P/q$, as follows:

$$q = \left| P_t - P_s \right|$$

$$\Delta P/q = \frac{(P_s - P_n)}{q}$$

where P_t = tunnel total pressure,

P_s = static pressure at tunnel centerline,

P_n = pressure at each port.

All the pressure data recorded during the test are listed in Appendix B.

Flow-Visualization Data

Two methods of flow-visualization were used during the wind tunnel test program. Indications of the swirl in the trailing tip vortex from Ogee Model #1 were observed on a tuft grid, of 5.08 x 5.08 cm (2 x 2 in.) grid size, which was installed 13 chord lengths downstream in the tunnel. Still photographs of the tuft grid were taken with a remotely-operated 35 mm camera concurrently for each test condition during which balance and pressure data were obtained.

Flow-visualization studies in the proximity of the tip regions of both the ogee and conventional configurations were made with Models #2 and #3 using the helium-bubble technique.

In this technique, neutrally-buoyant, helium-filled soap bubbles were produced and released upstream of the model, and illuminated with a collimated beam of light. Flow patterns produced by the helium bubbles were observed and photographs for various views of the models in the test section with 35 mm cameras for all sweep angles at angles of attack of +8, +10, +12, and +14 degrees.

DISCUSSION OF WIND TUNNEL TEST RESULTS

The wind tunnel tests were conducted to determine the effects of sweep angle on the pressure distributions of the ogee-tip configuration, and on the effectiveness of the ogee tip in diffusing a line vortex. Flow-visualization studies were conducted using tuft grids and the helium-bubble technique. Performance data were also obtained for the ogee-tip configuration and for a conventional-tip configuration of equivalent area. Performance data were obtained for both models in the angle-of-attack range $-2° \leq \alpha_R \leq 14°$ in 2-degree increments. Initially, baseline performance data were obtained for the ogee-tip configuration at $\Lambda=0$ and subsequent data for both models were obtained at the same lift as that obtained for the ogee at $\Lambda=0$ for each angle of attack tested by changes in wind-tunnel velocity. Discussions of the results on the basis of performance characteristics, pressure distributions and flow visualization follows.

Performance Characteristics

Figure 8 shows the variation of the drag coefficient of the ogee model at constant angle of attack versus sweep angle. The drag coefficient was consistently higher at angles of forward sweep than for comparable angles of aft sweep, and the minimum values of the drag coefficient at each angle of attack tested were generally obtained with the ogee model at a sweep angle of approximately +10 degrees. At high positive (or negative) sweep angles, a larger (chordwise) gap existed between the model and the wind-tunnel floorplate, and the gap is known to effect changes in the drag. This condition may account for the general higher drag coefficients at $\Lambda=-20$, +20 and +30 degrees. The consistent trend in the data, however, suggests that the phenomenon is primarily related to aerodynamic characteristics other than that associated with this gap.

The variation of drag coefficient with sweep angle for the conventional tip configuration (fig. 9) also shows that the minimum drag occurs at low angles of positive sweep. The variation of the drag coefficient with sweep angle for the conventional-tip configuration also shows more nonuniformity than that exhibited by the ogee-tip confirguration, but the general trend shows that the drag coefficient is higher for forward sweep angles up to an angle of attack of approximately 8 degrees. At higher angles of attack, the drag coefficient is minimum at Λ=+5 degrees, and rises in much the same manner as the ogee-tip configuration as the model is swept forward. The drag data at α=10 degrees for positive sweep angles shows a wide scatter as the model approaches stall, and these results are surprising at this relatively low angle of attack. However, the model is completely stalled at α=12 degrees, and lift could not be maintained at the baseline values at angles of attack of 12 and 14 degrees and at sweep angles of +10, +20 and +30 degrees due to stall. The difference in the stalling characteristics between the ogee-tip and the conventional-tip configuration is unusual in that the inboard sections of both the ogee and the conventional-tip configurations are identical, such that the noted variations in the drag characteristics are due solely to the differences of the outermost sections of the models. Differences in comparable (inboard) model properties are also small. The twist of the ogee model, for example, is slightly higher, but the twist extends only to 94 cm (37 in.) above the tunnel floor at Λ=0, such that any effects due to differences in twist become minimized. The absolute values of the drag coefficient are generally lower for the ogee-tip configuration in the angle-of-attack range tested, and the drag coefficient for the conventional-tip configuration generally rises more rapidly with sweep than the ogee-tip configuration above α=6°. An overall comparison of these drag characteristics indicates that the primary improvement in the performance characteristics of the ogee-tip configuration in application to helicopter rotor systems would be shown in the reduction of dynamic loads due to its more gradual approach to stall.

The lift-to-drag ratios versus angle of attack at a given sweep angle for the ogee-tip configuration are shown in figure 10, and those for the conventional-tip configuration are shown in figure 11. At a constant angle of attack, the L/D reflects the changes in drag with sweep angle since the lift was maintained constant at each angle of attack for both configurations. For the ogee-tip configuration, the peak values of L/D are higher for the aft-sweep conditions than for the forward-sweep conditions and the highest L/D values occur at sweep angles of +5 and +10 degrees. Increasing the sweep angle further aft to angles of +20 and +30 degrees tends to decrease the L/D throughout the angle-of-attack range tested, but the L/D at these conditions remain higher than at zero or negative sweep. Very little change in the shapes and peak levels of the L/D curves occurred between zero sweep and sweep angles of -5 and -10 degrees, while the peak L/D at sweep angles of -15 and -20 degrees was much lower. The lower peak L/D ratios also occurred at lower angles of attack than the higher peak L/D ratios.

For the conventional-tip configuration (fig. 11), the data exhibited more variation in the effects of sweep than that exhibited by the ogee-tip configuration. With respect to zero sweep, higher peak values of L/D were obtained at all sweep angles except at Λ=-15 and -20 degrees, and the peak L/D's tended to occur at approximately the same angle of attack. The overall optimum L/D variation occurred at Λ=+5 degrees. Although higher peak L/D ratios were obtained above Λ=+5 degrees, the L/D for these conditions dropped sharply above an angle of attack of approximately 8 degrees.

Comparison of the variation in L/D between the ogee-tip and conventional-tip configurations shows that higher L/D's are generally attainable with the ogee-tip throughout the angle-of-attack range tested such that overall improvement in performance would be expected in helicopter applications. This result is in variance with that reported in reference 3, which showed a degradation in hover performance characteristics of the ogee with respect to a conventional-tip rotor in small-scale rotor tests. The comparison of the performance characteristics in these tests was made on the basis of equivalent blade radii, in contrast to equivalent planform area as reported herein. Data presented in reference 1 also show improved performance characteristics of the ogee in comparison to a conventional-tip model where the basis for comparison was the equivalent area.

Previous performance tests conducted with Ogee Model #2 at zero sweep (ref. 2) showed a lower value in peak L/D than that which was indicated with Ogee Model #1 during this test program. The observed difference in L/D levels between the two tests was attributed to the fact that a closer gap was maintained between the base of the model and tunnel floor during the current testing, thereby resulting in a "cleaner" model installation and improved performance in terms of the lift and drag measured by the balance. Slight differences in model geometry between the two models could also effect slight differences in the L/D curves with angle of attack. Comparative data which was obtained for the ogee and conventional-tip configuration at zero sweep in reference 2 also showed that the higher peak L/D's were obtained with the ogee.

The spanwise variation in the center of lift versus angle of attack for the ogee configuration is shown in figure 12. The effect of sweep angle on the lift-center variation is negligible, and the center-of-lift location was approximately 43 percent of the semispan of the ogee model outboard of the tunnel floor.

The spanwise variation in center of lift versus angle of attack for the conventional-tip model is presented in figure 13.

The spanwise lift center for the conventional-tip model shows slightly more variation with sweep angle and angle of attack than the ogee-tip configuration, and was generally inboard of that shown for the ogee-tip configuration with respect to the floor of the wind tunnel for comparable test conditions as might be expected, since the area of both models is equivalent. If nondimensionalized by the semispan of the models, however, the spanwise center of pressure of the conventional-tip model would be outboard of the ogee-tip model since the outboard section of the ogee carries a lower percentage of the total lift.

Modified Ogee Tip

A modified (pointed, see figure 26) ogee tip was installed on model No. 1 and tested at $\Lambda=-20°$. The modified tip was tested previously (ref. 2) at zero sweep and had shown slight improvements in the L/D characteristics over a conventional-tip model. As shown in figure 14, only marginal differences in L/D were also found at $\Lambda=-20°$. Figure 15 shows a comparison of the spanwise drag center of the modified ogee tip and the unmodified elliptical ogee tip at the -20° sweep position. The modified tip shows a reduction in drag in the angle-of-attack range $0° \leq \alpha \leq 8°$, as evidenced by the inboard shift of the spanwise drag center such that this drag reduction was due to the reduction of the tip drag. Little difference in the drag center between the modified and the unmodified ogee-tip configurations was shown for angles of attack above 8°. At the lower angles of attack, a larger percentage of the total drag is due to profile drag, such that in helicopter applications, modifications in the outermost tip region of the ogee would be beneficial in those portions of the disk such as the advancing side, where tip angles of attack are small.

Ogee Pressure Data

The pressure taps on the ogee model were positioned such that a series of taps at six spanwise stations were aligned parallel to the airstream at $\Lambda=0$, -20 and +20 degrees (fig. 1). The absolute pressure distributions for these spanwise stations at $\Lambda=0$, -20 and +20 degrees are shown in figures 16, 17 and 18, respectively. At $\Lambda=0$ degrees, there was a drop in the pressure peak at the leading edge at $\alpha=14°$ near station 136.14(53.60), and at $\alpha=12$ degrees farther outboard. At $\Lambda=+20$ degrees, the drop in the pressure peak at the leading edge occurs at $\alpha=14$ degrees at approximately the same spanwise station as at $\Lambda=0$ degrees, and also at $\alpha=12$ degrees farther outboard. At $\Lambda=-20$ degrees, the outermost sections of the ogee do not show this characteristic drop in the pressure peaks up to $\alpha=14$ degrees. Farther inboard, however, the differences in the pressure peaks between $\alpha=12$ degrees and $\alpha=14$ degrees are less than those at $\Lambda=0$ degrees or $\Lambda=+20$ degrees for these angles of attack. At angles of attack less than 12 degrees, the streamwise pressure distributions are representative of those normally observed farther inboard from the tip of a lifting surface. For all sweep angles, the distortion in the pressur distributions at angles of attack near 12 degrees are associated with the formation of more distinct vortices at this angle of attack, while at higher angles of attack, the lifting surface experiences the onset of stall.

Balance data in the angle-of-attack range $12° \le \alpha \le 14°$ shows that the onset of stall for the ogee-tip configuration was more gradual than for the conventional-tip configuration at all sweep angles, and the pressure data support these results as seen that not all sections of the ogee stalled simultaneously.

Because of the limited number of pressure taps that could be installed in streamwise alignment at all sweep angles, indications of vortex formation were not conveniently discerned from the streamwise pressure distributions. Contour plots showing lines of constant pressure for the upper surfaces of the ogee were generated from cross plots of the chordwise and spanwise pressure distributions. In these plots, evidence of vortex formation can be easily discerned by the distortion of the contours as shown for a conventional-tip configuration in figure 19 (fig. 3 of ref. 4). Contour plots at α=8 degrees for Λ=-20, 0, and +20 degrees are shown in figures 20, 21 and 22, respectively. At an angle of attack of 8 degrees, the lines of constant pressure tended to retain a constant chordwise position from the inboard to the outermost regions of the ogee, and this uniformity was negligibly affected as the sweep angle was varied from -20 degrees to +20 degrees. As the sweep angle was varied, however, there was a chordwise shift in the lines of constant pressure, which was most noticeable nearer the trailing edge of the surface. The uniformity of the contours, however, indicates that the vorticity in the tip region tends to trail off as a sheet, since the contours are typical of those inboard of the tip of a lifting surface.

Contour plots for α=12 degrees and Λ=-20, 0, and +20 degrees are shown in figures 23, 24, and 25, respectively. As the angle of attack was increased from 8 to 12 degrees, the uniformity in the lines of constant pressure that was seen at α=8 degrees became distorted, particularly in the region near spanwise station 159.51(62.80). The shift in the lines of constant pressure as sweep angle was varied at α=8 degrees became more pronounced at α=12 degrees, and the peak pressures near the leading edge at Λ=-20 degrees were higher than at Λ=0 degrees or Λ=+20 degrees. The reason for these characteristics are unknown. The contour plots indicate the formation of a vortex in the region near station 159.21 (62.80) and the characteristic patterns of the contours also suggest that the vortex for the swept-forward configuration would tend to be more distinct than for zero or aft-sweep configurations.

Figure 26 shows the contour pressure plot for Λ=-20 degrees and α=12 degrees using a modified ogee tip. Comparison of figure 23 with figure 26 shows that the nonuniform flow region which existed in the area near station 159.51 (62.80) for the elliptical ogee finger became more uniform with the modified ogee tip. The modified tip would thus show less tendency to form a concentrated vortex than the elliptical ogee finger at the same conditions. The contours for the modified tip also show a chordwise shift in lines of constant pressure, and higher peak pressures were obtained at the leading edge of this configuration than for the elliptical ogee finger for the same conditions.

Pressure data were also obtained for spanwise locations along the upper and lower surfaces of the ogee model at the 19% chord, and figure 27 shows these pressure distributions at α=8 degrees for sweep angles of -20, 0, and +20 degrees. An indication of the spanwise loading distribution for the ogee-tip configuration is given in Figure 28, which shows the integrated chordwise pressures in the form of the normal force coefficient, C_N, for spanwise stations of the ogee section at Λ=0 and α=8°. Comparison of figures 27 and 28 shows that the characteristic shape of the spanwise pressures at the 19% chord was similar to the loading distribution based on the integrated chordwise distributions. On this basis the spanwise pressures at the 19% chord were considered representative of the spanwise loading distribution. The gradients of the loading distributions from the base of the ogee section, station 116.59 (45.90) were approximately the same for all sweep angles, which suggests that little difference would be expected in the vortices that would be trailed off the lifting surfaces. This observation was supported by the tuft-grid and helium-bubble flow-visualization data which showed only slight differences in the swirl patterns for the same conditions. The pressure distributions at all sweep angles also exhibited a distortion which was approximately coincident with the base of the ogee section. This distortion in the pressure distribution was attributed to the marked change in planform at this spanwise position.

The sharp drop in the pressure coefficient near the root of the ogee model shown in figure 27 was due to the gap between the model and the wind tunnel floor plates, which created a region of low pressure near the root of the model. This gap was maintained larger than had been desired because the deflections of the model on the support system were larger than anticipated. The presence of this gap, however, did not compromise the balance nor the pressure data, since all of the model configurations were consistently subjected to the same gap at all sweep angles. The primary pressure data that were obtained were also far removed from the gap.

Tuft-Grid Flow Visualization

The effectiveness of the ogee tip in diffusing the concentrated trailing tip vortex was observed qualitatively from indications of swirl motions on a tuft grid. The tuft grid was positioned 13 chord lengths downstream of the model. Tuft-grid photographs were taken and analyzed for each test condition during which balance and pressure data were obtained, and representative tuft-grid photographs are shown for sweep positions of -20, 0, and +20 degrees.

Figure 29 shows a series of tuft photographs of the ogee model at sweep angles of -20, 0, and +20 degrees for angles of attack of +4, +8, and +12 degrees. The photographs can be viewed in two aspects, as either the change in swirl motion with variation in angle of attack or with variation in sweep angle. At 4 degrees angle of attack, the tuft photos indicate almost no sign of swirl motion throughout the sweep-angle range investigated. At 8 degrees angle of attack, only slight evidence of swirl motion in the tuft grid can be seen for a sweep angle of -20 degrees, and almost no swirl is evident for sweep angles of 0 or +20 degrees. These observations indicate that the vorticity tends to trail off the ogee tip as a sheet and does not form a concentrated vortex up to a position of 13 chord lengths downstream. As the angle of attack was increased to 12 degrees, the swirl motion in the tufts became more evident for all sweep angles. For $\Lambda=-20°$ the swirl motion was more typical of that associated with vortex motion. At $\Lambda=0°$ and $+20°$, the swirl motion was again only slightly discernible in the tufts.

The tuft photos thus show that a slightly more concentrated vortex tended to form at the large angles of forward sweep, while it remained diffuse at conditions of aft sweep. These observations support the data shown in the contour pressure plots which showed that a more concentrated vortex tended to form at $\Lambda=-20°$ than for $\Lambda=0$ or $+20°$.

Figure 30 shows a series of tuft photographs comparing the conventional-tip model with the ogee-tip model at a sweep angle of -20 degrees for +4, +8, and +12 degrees of angle of attack. The existence of the concentrated trailing tip vortex for the conventional-tip model was clearly evident as indicated by the swirl motion in the tuft grid. In contrast, the ogee tip showed a much lower extent of swirl motion in the tufts. Good resolution of the conventional-tip model was not obtained in these photographs because the model was painted black for helium-bubble flow-visualization studies.

Helium-Bubble Flow Visualization

Flow-visualization studies were conducted using the helium-bubble technique to observe the flow fields across the lifting surfaces and in the near wake. In the helium-bubble technique, neutrally-buoyant, helium-filled soap bubbles are released upstream of the model, and the bubbles are illuminated by a collimated beam of light emanating from a downstream position, which permits visual observation and photographic documentation of the flow field. In the present program, helium bubbles were released from a dual source which allowed more concentration of bubbles at various sections of the ogee tip.

Figures 31, 32 and 33 are photographs of the flow field of the ogee tip for sweep angles of -20, 0, and +20 degrees respectively. The following characteristics of the flow field were observed at the noted angles of attack.

Flow field at α = 8 degrees: At Λ=-20 degrees, the flow had a marked inboard spanwise component which was less pronounced at Λ=0 degrees and virtually nonexistent at Λ=+20 degrees. At Λ=0 and +20 degrees, the flow on the outermost section of the ogee exhibited more turbulence in comparison to that seen at Λ=-20 degrees. No indication of the formation of a concentrated vortex could be noted in the proximity of the lifting surface for any of the sweep angles tested.

Flow field at α = 10 degrees: At Λ=-20 degrees, the inboard spanwise component of flow was more distinct than at α=8 degrees. At Λ=0 degrees, there was noticeably more turbulence in the outermost section of the ogee than at α=8 degrees, and the turbulent flow also exhibited an inboard spanwise component. The flow at Λ=+20 degrees was basically the same as that at α=8 degrees, except that the turbulent region in the outermost section of the ogee became enlarged.

Flow field at α = 12 degrees: At Λ=-20 degrees, the flow in almost the entire region of the ogee tip was turned inboard, and was noticeably more turbulent than at α=8 degrees. The flow at Λ=0 degrees also exhibited an inboard spanwise component of flow, but to a much lesser extent than at Λ=-20 degrees. At Λ=+20 degrees, the flow field across the ogee was almost the same as at α=8 and 10 degrees, that is, the flow across the lower section of the ogee was primarily parallel to the stream, with a separate, distinct turbulent area across the outermost section of the surface.

The inboard spanwise component of flow that was noted at α=10 degrees and 12 degrees was highly turbulent and was confined to the immediate proximity of the lifting surface. The helium-bubble streaks which depict the streamwise flow field in the photographs occur farther out from the surface. A photograph depicting this flow field for α=12 degrees and Λ=0 degrees is shown as figure 34. This photograph was taken from a point slightly behind and outboard of the ogee such that the trailing edge of the ogee is in the foreground of the photograph. In this view the separation of the turbulent flow field from the nonturbulent flow field can be more easily discerned. As can be seen in figures 31, 32 and 33, this turbulent spanwise type of flow did not occur at positive sweep angles, and was also noted to be absent at sections of the model farther inboard of the ogee tip section.

Visualization of the flow field farther downstream of the ogee model at Λ=-20 degrees is shown in figure 35 for angles of attack of +8, +10, and +12 degrees. Only at the 12 degree angle-of-attack position can evidence of vortex swirl motion be noted in the photographs. The observed swirl motion at the farther downstream position, however, was not as sharply defined as for a conventional-tip model (e.g. ref. 2).

Comparison of the flow fields for the conventional and ogee-tip configurations are shown in figure 36 for the models at Λ=-15° and at angles of attack of +8, +10, and +12 degrees. The presence of a concentrated vortex trailing from the conventional-tip model was clearly evident at each angle-of-attack position as the helium bubbles were tightly entrained within the vortex. In contrast, the ogee tip showed markedly less tendency of the flow to develop this distinctive concentrated pattern. The indications of turbulence and the inboard spanwise flow that were noted at α=8, 10 and 12 degrees for Λ=-20 degrees were also evident at Λ=-15 degrees.

A "reverse-ogee" configuration was achieved during the test program by rotating the turntable 180° in the test section so that the trailing edge of the ogee was upstream. The purpose of this test was to obtain a qualitative indication of the flow field of this type of planform by means of flow visualization. The model was tested in this attitude at Λ=0°.

Photographs of the flow field of this reverse-ogee configuration as depicted by the helium bubbles at angles of attack of 8, 10 and 12 degrees are shown in figure 37. At α=8 and 10 degrees, a vortex formed along the upstream edge of the reverse ogee near station 116.59 (45.90). This station was coincident with the juncture of the constant-chord blade section and the ogee section. The vortex then trailed off from the reverse ogee at approximately three quarters of the distance outboard of this juncture to the tip. From this three-quarter position and outboard, the flow over the airfoil was highly turbulent, while the flow over the inboard section remained relatively parallel to the stream. At α=12 degrees, the vortex which formed over the upstream edge (at α=8 and 10 degrees) became obscured as the turbulent-flow region extended over a wider area of the ogee section. Although it is recognized that the airfoil section was reversed in the airstream, it appears that a reverse ogee shape would be more apt to form a concentrated vortex because of the abrupt change in the planform at the leading edge. The formation of this vortex can be related to that exhibited by delta wings or to leading-edge "spikes" of (otherwise) conventional swept wings.

The quantitative results which were obtained in the test program were confirmed qualitatively by the flow visualization data in several aspects. Observation of the flow field, for example, showed an area of turbulent flow over the outermost sections of the ogee, which became gradually more pronounced as the angle of attack was increased. The pressure distributions reflected this phenomenon in that the peak pressures at the leading edge of the model dropped off along the span of the ogee in much the same manner. These phenomena were also reflected in the balance data as the drag of the ogee increased noticeably more gradually than the conventional tip model at angles of attack below stall. The tendency of the ogee to form a vortex at $\Lambda=-20$ degrees which was noted in the contour plots of the pressure data was also reflected in the tuft-grid data and in the downstream helium-bubble visualization of the flow field.

CONCLUSIONS

On the basis of the research effort that was conducted, it was concluded that the ogee-tip configuration shows good promise toward application to helicopter rotor systems both in regard to the diffusion of the trailed tip vortex and in performance characteristics. The pressure and flow-visualization data showed that the vorticity tends to trail off the ogee tip as a sheet rather than in a concentrated form as in a conventional-tip configuration. This characteristic was minimally affected by changes in sweep angle in the range -20 degrees $\leq \Lambda \leq +30$ degrees. The performance data showed that higher L/D's were attained with the ogee-tip configuration than for the conventional-tip configuration for comparable test conditions. The ogee also exhibited a more gradual approach to stall in comparison to the conventional-tip model, and this characteristic would tend to alleviate the high dynamic loads that are encountered by conventional rotor blades at stall.

RECOMMENDATIONS

Wind tunnel tests should be conducted at high subsonic speeds to determine the effects of compressibility on the performance characteristics of the ogee-tip configuration in relation to the conventional-tip configuration. These tests should provide for variation in the outermost tip geometry of the ogee.

Effort should continue to implement the application of the ogee tip to flight hardware. This supportive effort should include the comparative analysis of performance, acoustic and rotor-downwash characteristics between the ogee and conventional-tip rotor systems from whirl-tower and/or wind-tunnel test data.

REFERENCES

1. Rorke, J.B., Moffitt, R.C., and Ward, F.J., "Wind Tunnel Simulation of Full-Scale Vortices", Preprint No. 623, 28th Annual National Forum of the American Helicopter Society, Washington, D.C., May 1972.

2. Balcerak, J.C., and Feller, R.F., "Vortex Modification by Mass Injection and by Tip Geometry Variation", Rochester Applied Science Associates, Inc., RASA Report 73-01, USAAMRDL Technical Report 73-45, to be published, 1973.

3. Landgrebe, A.J., and Bellinger, E.D., "Experimental Investigation of Model Variable-Geometry and Ogee Tip Rotors', United Aircraft Research Laboratories, NASA Contract No. NAS1-10906, to be published, 1973.

4. Chigier, N.A., and Corsiglia, V.R., "Tip Vortices - Velocity Distributions", Preprint No. 522, 27th Annual National V/STOL Forum of the American Helicopter Society, Washington, D.C., May 1971.

TABLE I

OGEE-TIP PLANFORM COORDINATES

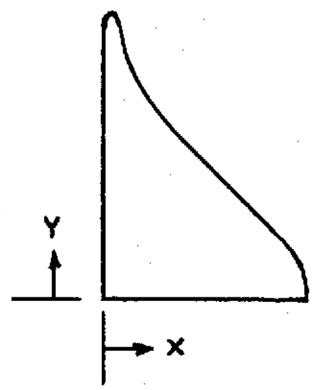

x-Coordinate cm (in.)	y-Coordinate cm (in.)*
2.06 (0.81)	188.85 (74.35)
2.67 (1.05)	185.65 (73.09)
3.18 (1.25)	183.54 (72.26)
3.76 (1.48)	181.41 (71.42)
4.32 (1.70)	179.78 (70.78)
5.69 (2.24)	176.07 (69.32)
6.65 (2.62)	173.91 (68.47)
8.03 (3.16)	171.55 (67.54)
9.37 (3.69)	169.42 (66.70)
10.52 (4.14)	167.77 (66.05)
12.04 (4.74)	165.56 (65.18)
13.36 (5.26)	164.06 (64.59)
15.88 (6.25)	161.54 (63.60)
↑ linear variation ↓	↑ linear variation ↓
47.83 (18.83)	129.54 (51.00)
48.26 (19.00)	129.08 (50.82)
49.33 (19.42)	128.02 (50.40)
50.90 (20.04)	126.09 (49.64)
52.25 (20.57)	124.00 (48.82)
53.09 (20.90)	121.64 (47.89)
53.59 (21.10)	116.59 (45.90)

*Station reference at tunnel floor.

TABLE II

MODEL #1 PRESSURE TAP LOCATIONS AND DESIGNATION

STATION cm(in.)		CHORD LOCATION									
		1.00%	4.75%	9.50%	19.0%	28.4%	37.9%	57.0%	66.5%	76.0%	85.0%
178.31	(70.20)	1	14	—	—	—	—	—	—	—	—
175.01	(68.90)	2	—	—	—	—	—	—	—	—	—
173.23	(68.20)	—	—	16	—	—	—	—	—	—	—
171.45	(67.50)	3	—	—	—	—	—	—	—	—	—
168.15	(66.20)	4	—	17	—	—	—	—	—	—	—
164.85	(64.90)	5	—	—	—	—	—	—	—	—	—
163.20	(64.25)	—	—	18	—	—	—	—	—	—	—
161.29	(63.50)	—	—	—	26	—	—	—	—	—	—
159.51	(62.80)	6	—	19	27	43	—	—	—	—	—
158.62	(62.45)	—	15	—	—	—	—	—	—	—	—
155.19	(61.10)	7	—	—	—	—	—	—	—	—	—
151.77	(59.75)	—	—	—	—	—	49	—	—	—	—
149.86	(59.00)	8	—	20	—	44	50	—	—	—	—
148.08	(58.30)	—	—	—	28	—	—	—	—	—	—
145.29	(57.20)	—	—	21	—	—	—	—	—	—	—
144.78	(57.00)	9	—	—	—	—	—	—	—	—	—
143.51	(56.50)	—	—	—	29	—	—	58	—	—	—
139.70	(55.00)	—	—	—	—	—	51	—	—	—	—
137.67	(54.20)	—	—	—	—	45	—	—	—	—	—
136.14	(53.60)	10	—	—	30	—	52	59	64	—	—
132.33	(52.10)	11	—	—	—	—	—	—	—	67	—
130.56	(51.40)	—	—	22	—	—	—	—	—	—	—
128.78	(50.70)	—	—	—	31	—	—	60	—	—	71
127.00	(50.00)	—	—	—	—	46	—	—	—	—	—
125.10	(49.25)	—	—	—	—	—	53	—	—	—	—
121.92	(48.00)	—	—	—	—	—	—	—	—	—	72
121.29	(47.75)	—	—	—	32	—	—	—	—	—	—
119.63	(47.10)	—	—	23	—	—	—	—	65	—	—
117.86	(46.40)	12	—	—	33	47	54	61	—	68	—
116.08	(45.70)	—	—	24	—	—	—	—	—	—	—
114.81	(45.20)	—	—	—	—	—	—	—	—	—	73
114.30	(45.00)	—	—	—	34	—	—	—	—	—	—
111.13	(43.75)	—	—	—	—	—	—	—	66	—	—
110.62	(43.55)	—	—	—	—	—	55	—	—	—	—
106.93	(42.10)	—	—	—	—	—	—	62	—	—	—
105.66	(41.60)	—	—	—	—	—	56	—	—	—	—
103.89	(40.90)	—	—	—	—	48	—	—	—	—	—
103.29	(40.65)	—	—	—	—	—	—	—	—	69	—
101.98	(40.15)	—	—	—	35	—	—	—	—	—	—
100.33	(39.50)	—	—	25	—	—	—	—	—	—	—
98.55	(38.80)	13	—	—	36	—	57	63	—	70	74
72.39	(28.50)	—	—	—	37	—	—	—	—	—	—

TABLE II. - Concluded

MODEL #1 PRESSURE TAP LOCATIONS AND DESIGNATION

STATION cm(in.)		CHORD LOCATION									
		1.00%	4.75%	9.50%	19.0%	28.4%	37.9%	57.0%	66.5%	76.0%	85.0%
60.33	(23.75)	--	--	--	38	--	--	--	--	--	--
48.26	(19.00)	--	--	--	39	--	--	--	--	--	--
36.20	(14.25)	--	--	--	40	--	--	--	--	--	--
24.13	(9.50)	--	--	--	41	--	--	--	--	--	--
12.07	(4.75)	--	--	--	42	--	--	--	--	--	--

TABLE III

COMPARISON OF MODEL GEOMETRY

Λ degrees	S cm^2 (in.^{2})		Ogee-Tip Model b cm(in.)		Ogee-Tip Model AR	Conventional-Tip Model b cm(in.)		Conventional-Tip Model AR
-20	8544	(1324)	176.7	(69.6)	7.31	159.0	(62.6)	5.92
-15	8434	(1307)	182.1	(71.7)	7.86	159.0	(62.6)	5.99
-10	8319	(1289)	186.0	(73.2)	8.31	157.6	(62.0)	5.97
-5	8201	(1271)	188.2	(74.1)	8.63	154.8	(60.9)	5.84
0	8069	(1250)	188.9	(74.4)	8.84	150.6	(59.3)	5.62
5	8026	(1244)	189.6	(74.7)	8.96	151.5	(59.7)	5.72
10	7971	(1235)	188.9	(74.4)	8.95	151.2	(59.5)	5.73
20	7826	(1213)	182.4	(71.8)	8.50	146.4	(57.7)	5.48
30	7676	(1189)	168.8	(66.5)	7.42	135.7	(53.4)	4.79

TABLE IV

BALANCE DATA TEST CONDITIONS

Test Run No.	Model Configuration	Sweep Angle Λ, degrees	Angle of Attack Series α_K, degrees
1	Model #1	0	-2,0,2,4,6,8,10,12,14
2	Model #1	+30	-2,0,2,4,6,8,10,12,14
3	Model #1	+20	-2,0,2,4,6,8,10,12,14
5	Model #1	+10	-2,0,2,4,6,8,10,12,14
7	Model #1	+ 5	-2,0,2,4,6,8,10,12,14
12	Model #1	-5	-2,0,2,4,6,8,10,12,14
13	Model #1	-10	-2,0,2,4,6,8,10,12,14
14	Model #1	-20	-2,0,2,4,6,8,10,12,13,14
18	Model #3	-20	-2,0,2,4,6,8,10,12,13,14 15,16,17,18
19	Model #3	-15	-2,0,2,4,6,8,10,12,13,14 15,16,17
32	Model #1 Rotated 180°	0	-2,0,2,4,6,8,10,12
33	Model #1	-15	-2,0,2,4,6,8,10,12,13,14, 15,16
34	Model #1 With Modified Tip	-20	-2,0,2,4,6,8,10,12,13,14
35	Model #3	0	-2,0,2,4,6,8,10,12,14
36	Model #3	+5	-2,0,2,4,6,8,10,12,14
37	Model #3	+10	-2,0,2,4,6,8,10,12,14
38	Model #3	+20	-2,0,2,4,6,8,10,12,14
39	Model #3	+30	-2,0,2,4,6,8,10,12,14
40	Model #3	-10	-2,0,2,4,6,8,10,12,14
41	Model #3	-5	-2,0,2,4,6,8,10,12,14
42	Model #3	-20	-2,0,2,4,6,8,10,12,14,15

TABLE V

PRESSURE DATA TEST CONDITIONS

Test Run No.	Model Configuration	Sweep Angle Λ, degrees	Angle of Attack Series α_R, degrees
1	Model #1	0	-2,2,4,6,8,10,12,14
2	Model #1	30	-2,2,4,6,8,10,12,14
3	Model #1	20	-2,2,4,6,8,10,12,14
5	Model #1	10	-2,2,4,6,8,10,12,14
7	Model #1	5	-2,2,4,6,8,10,12,14
12	Model #1	-5	-2,2,4,6,8,10,12,14
13	Model #1	-10	-2,2,4,6,8,10,12,14
14	Model #1	-20	-2,2,4,6,8,10,12,13,14
32	Model #1 Rotated 180°	0	-2,4,8,12
33	Model #1	-15	-2,2,4,6,8,10,12,14
34	Model #1 With Modified Tip	-20	4,12

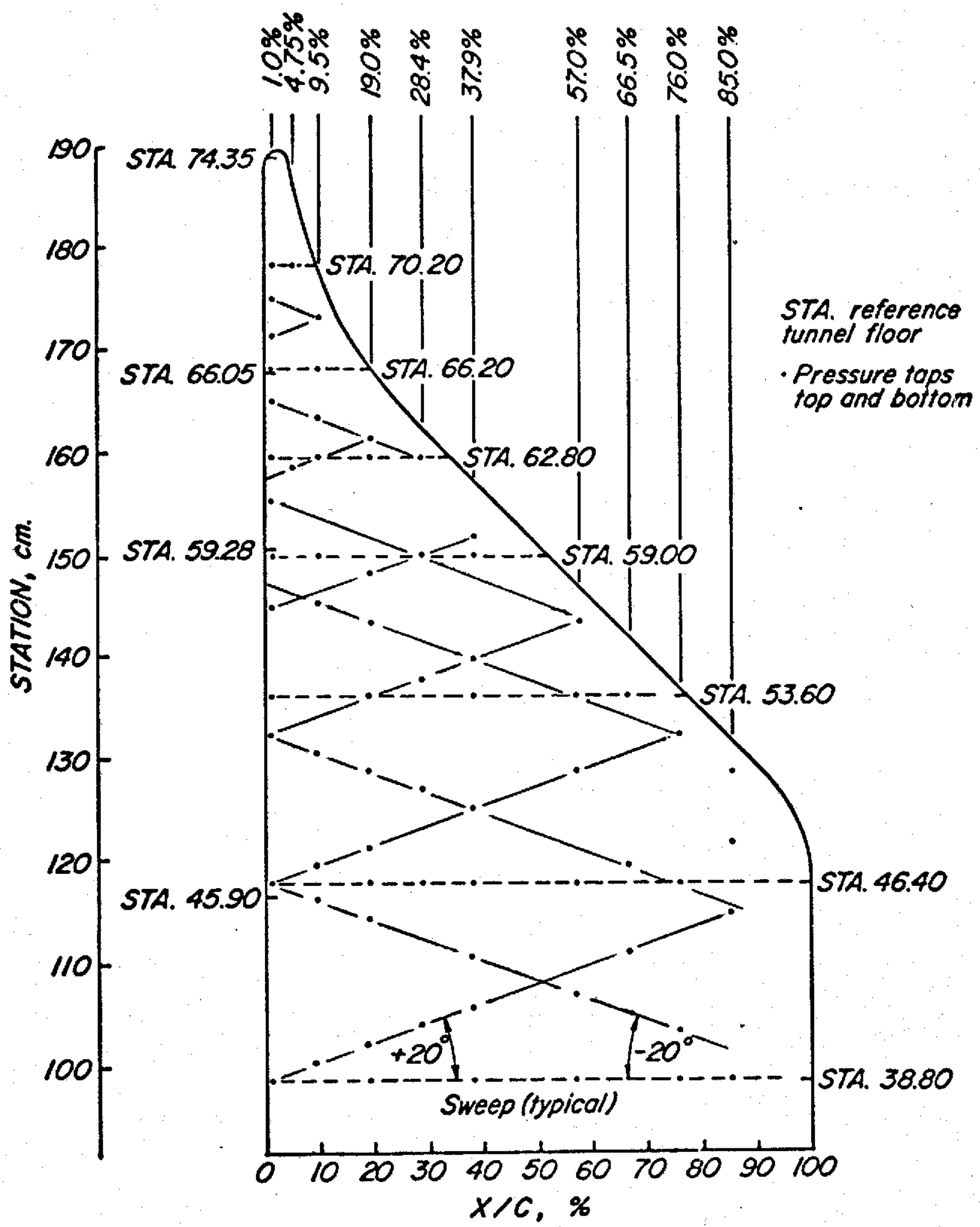

Figure 1. Model #1 ogee-tip planform

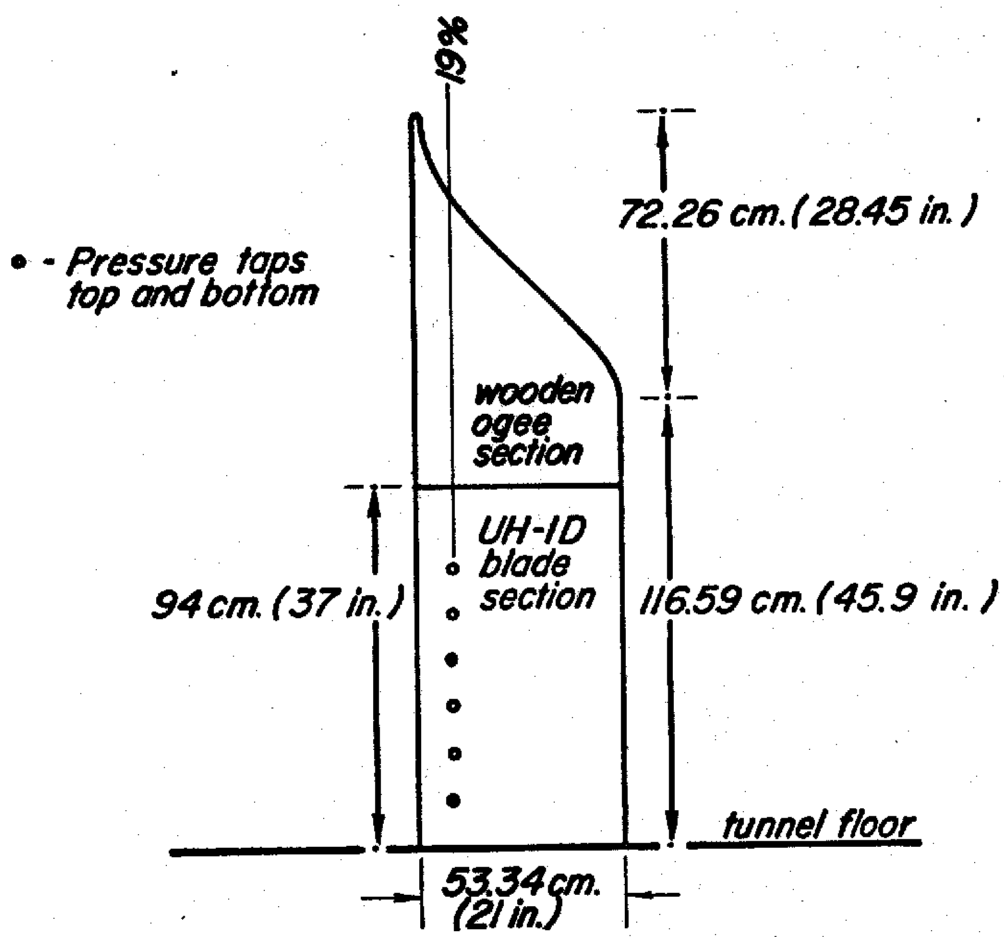

Figure 2. Model #1 planform

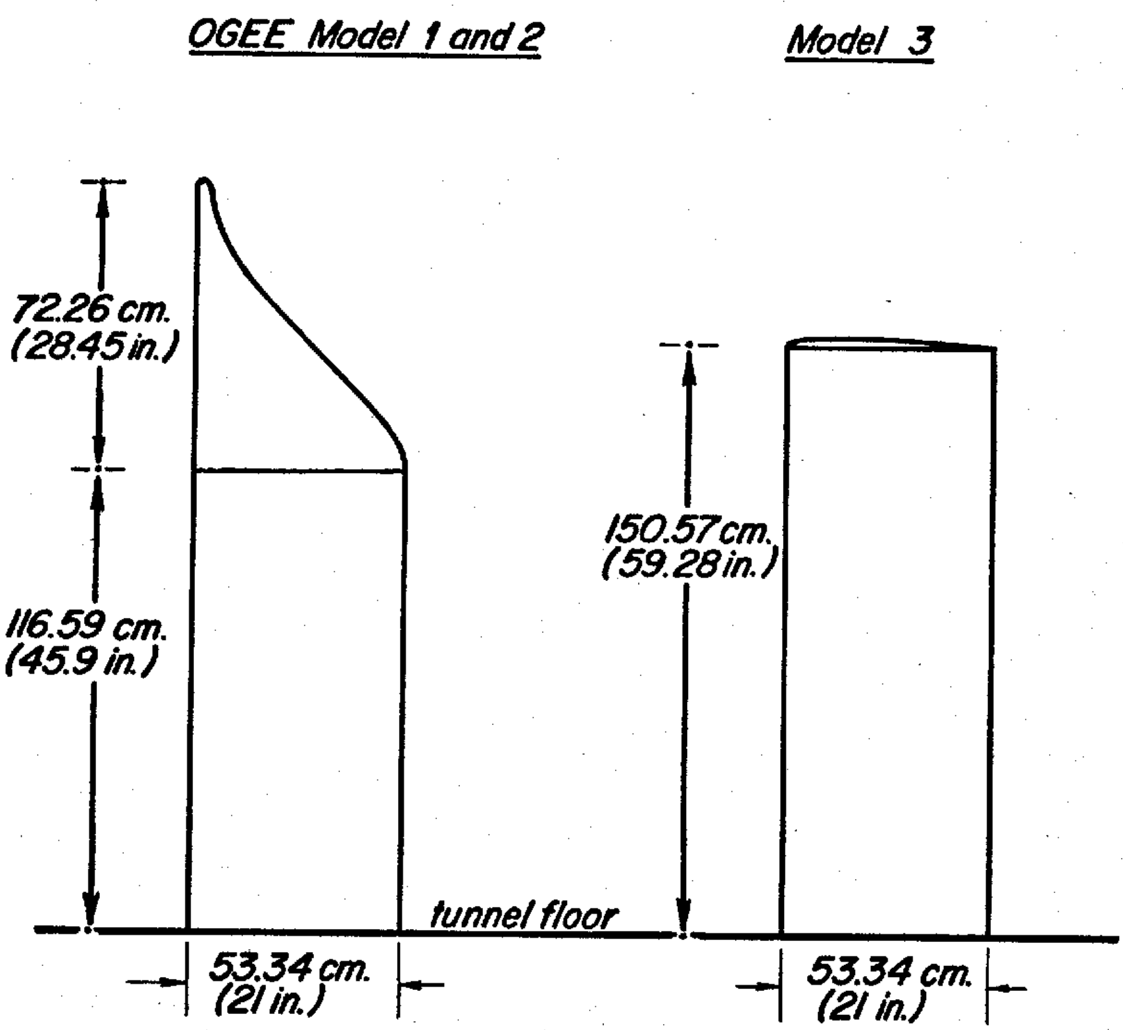

Figure 3. Schematic diagram of the ogee and conventional model planforms

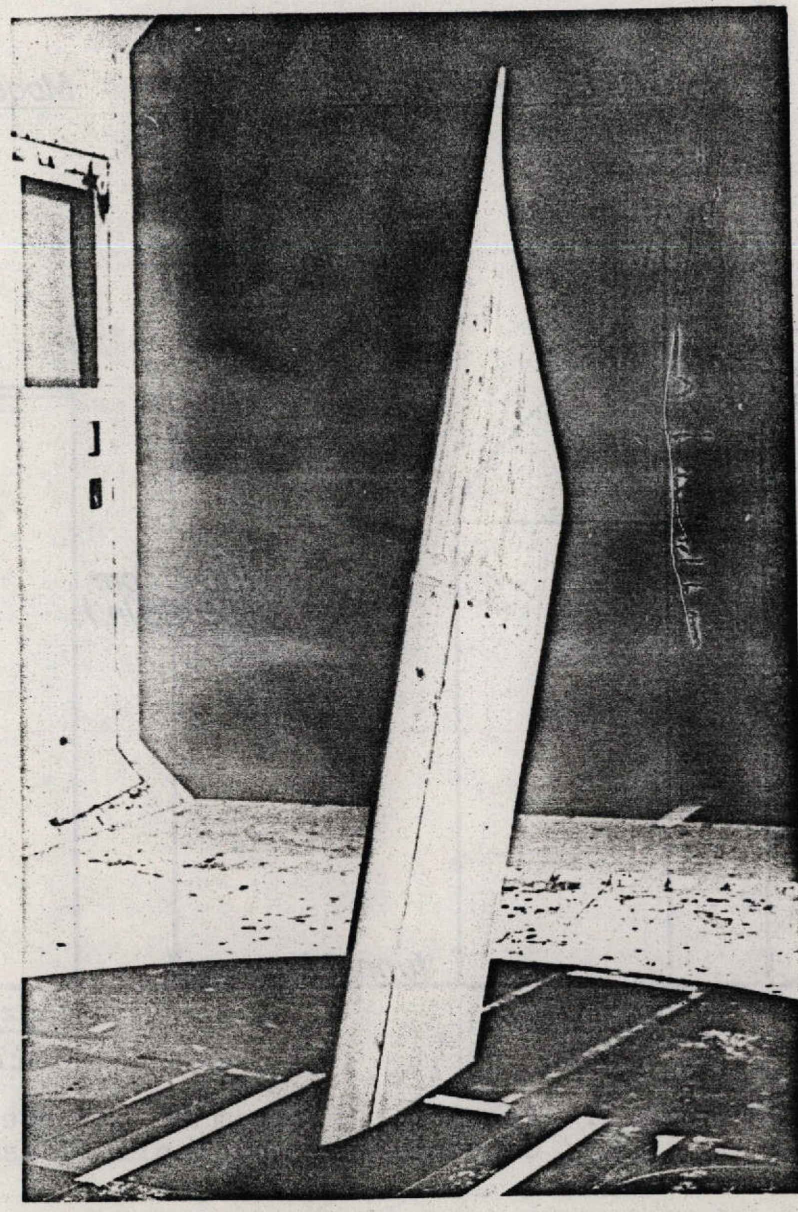

Figure 4. Wind tunnel installation of Ogee Model #1, $\Lambda = +20°$

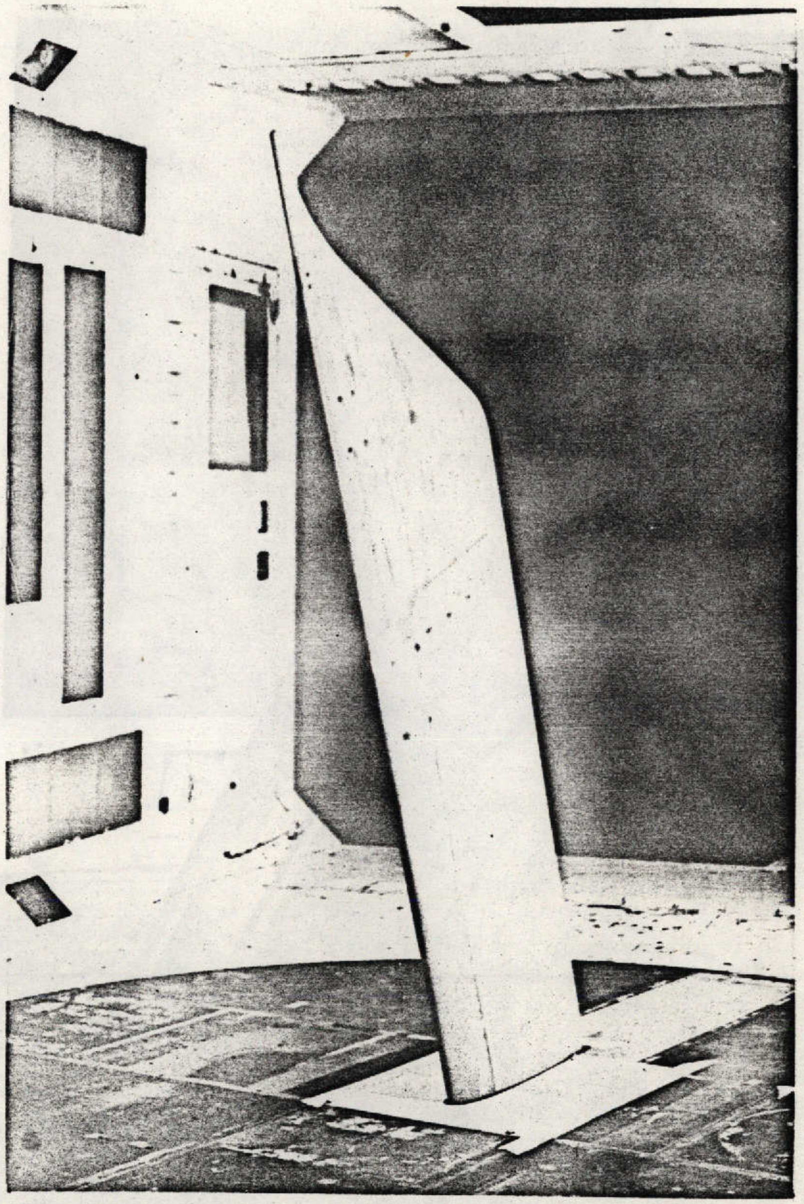

Figure 5. Wind tunnel installation of Ogee Model #1, $\Lambda = -20°$

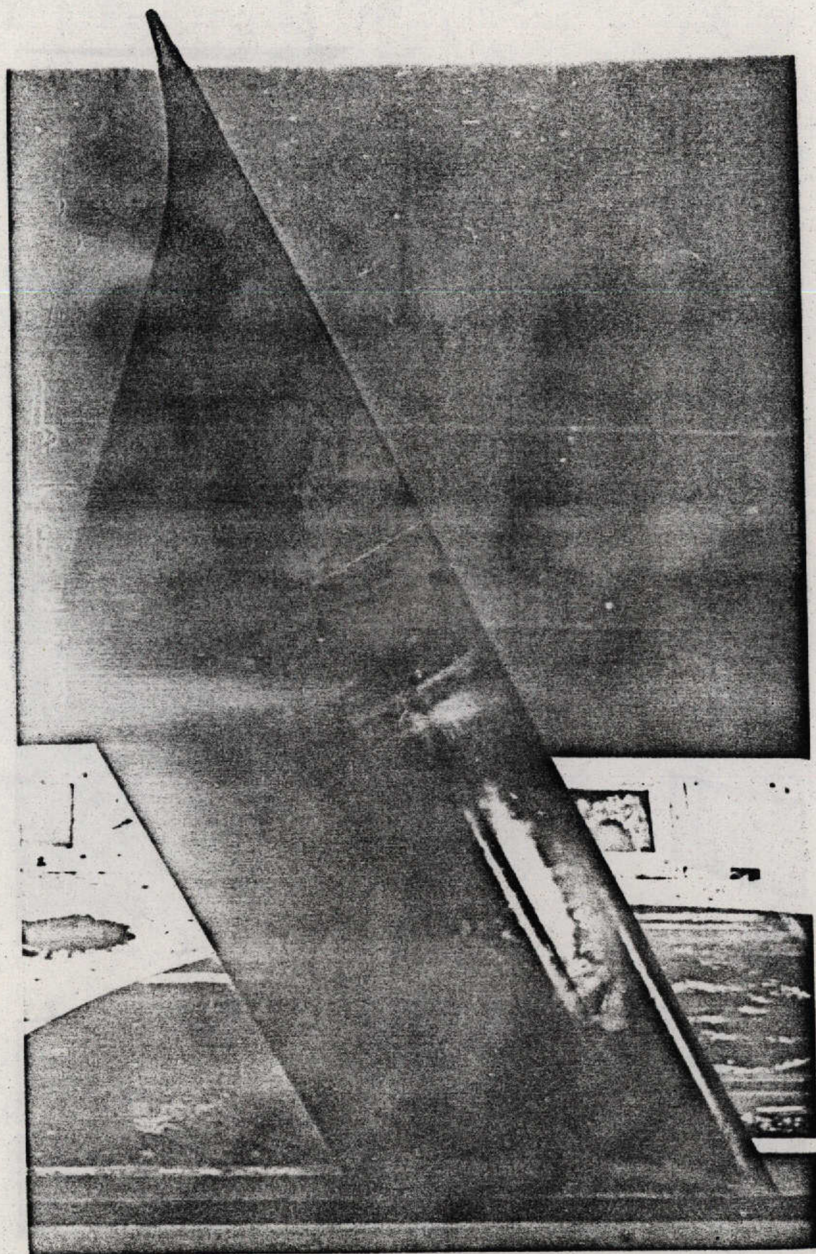

Figure 6. Wind Tunnel Installation of Ogee Model #2, $\Lambda = +30°$

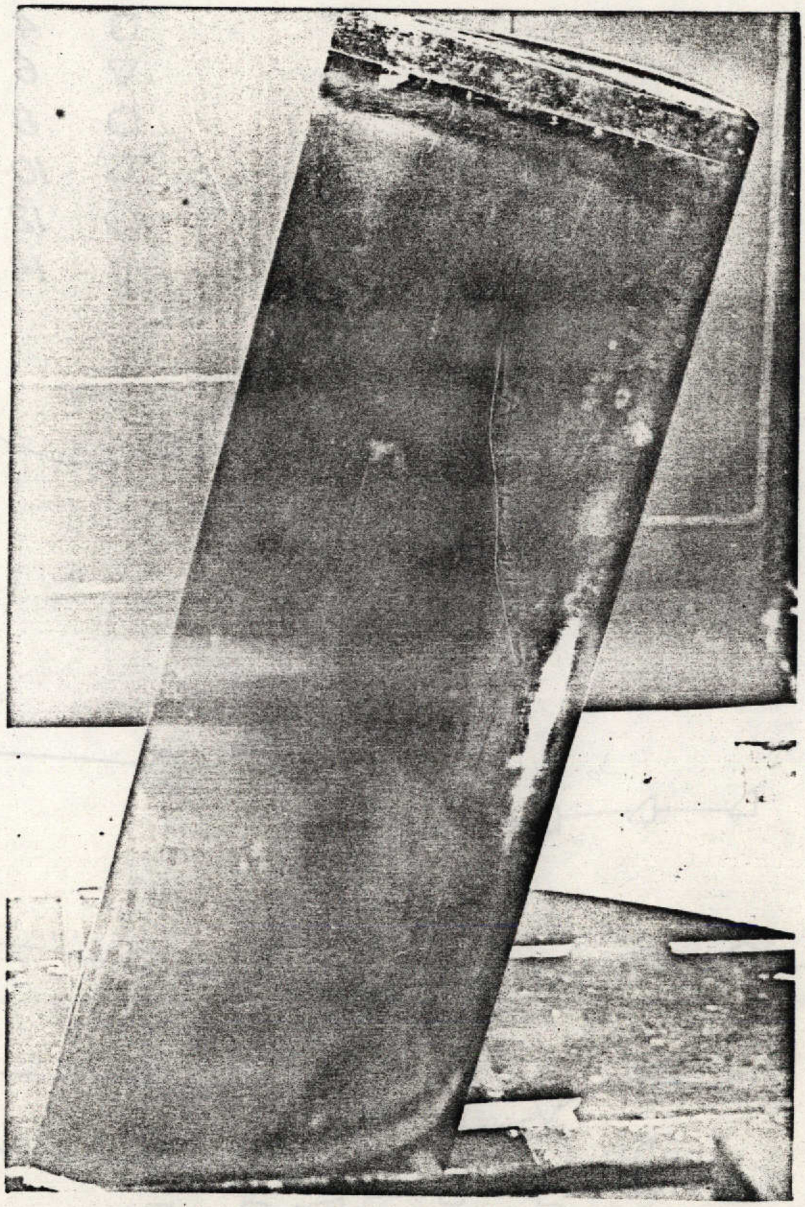

Figure 7. Wind tunnel installation of Model #3, $\Lambda = -15°$

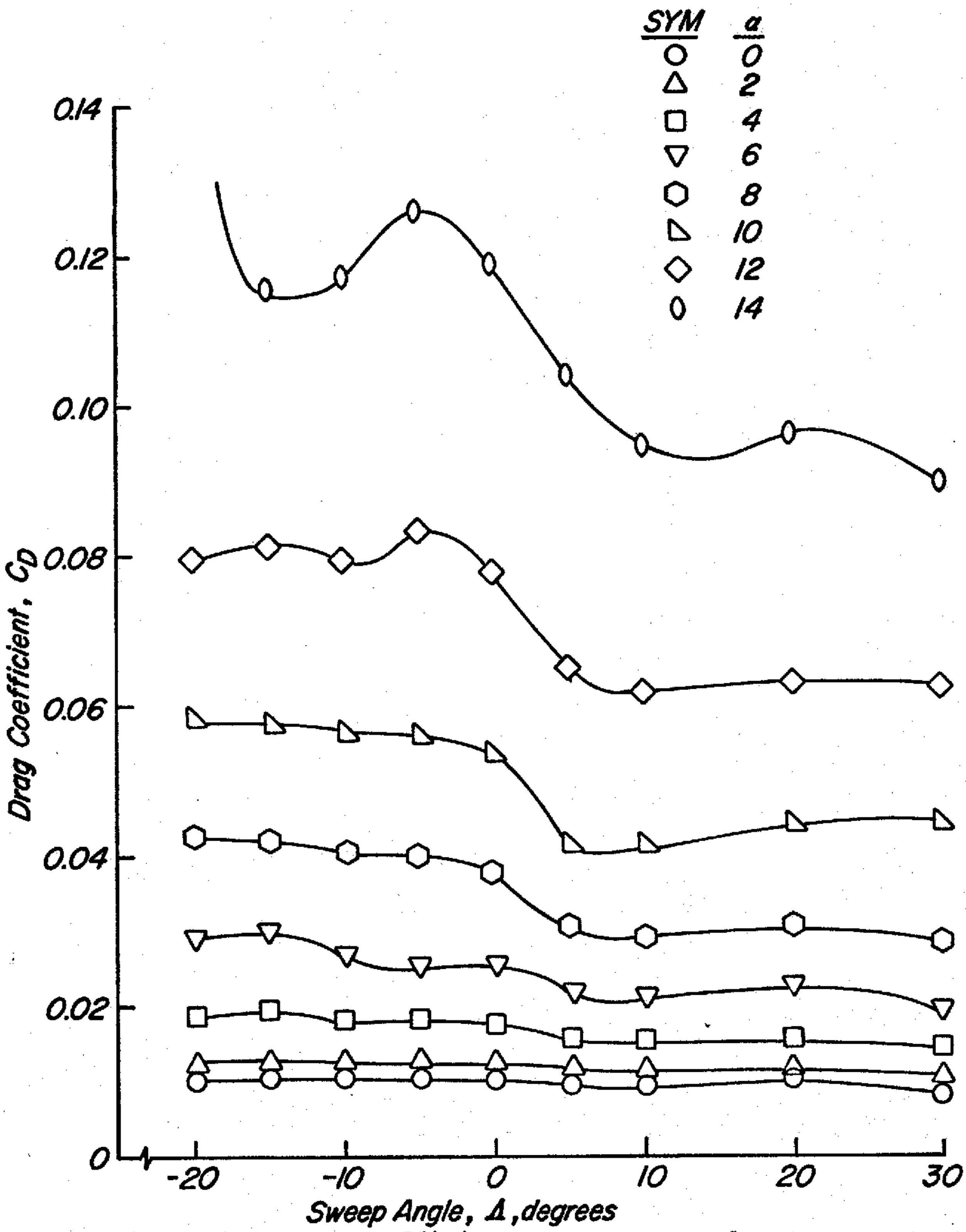

Figure 8. Drag coefficient vs. sweep angle at a constant angle of attack for the ogee model

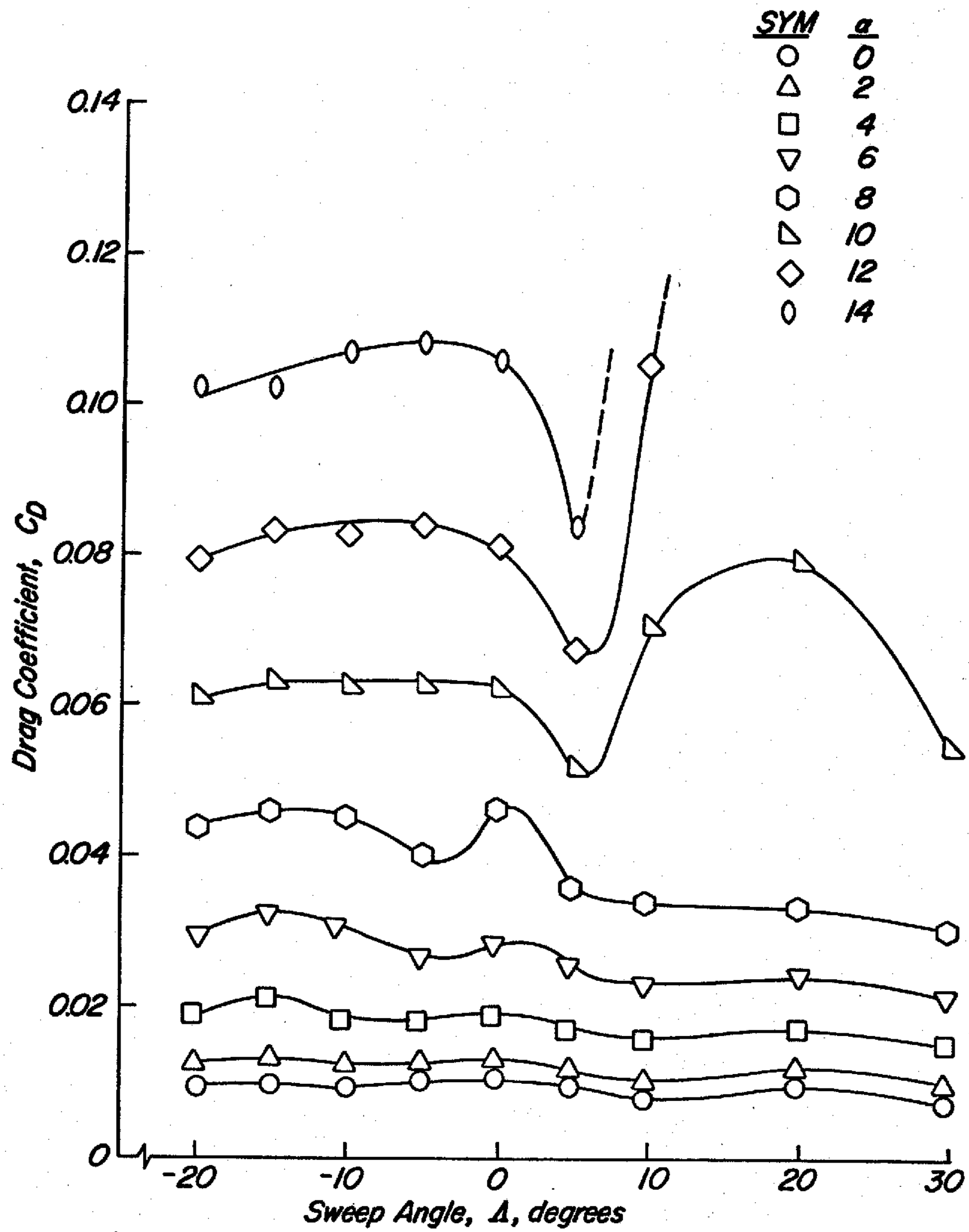

Figure 9. Drag coefficient vs. sweep angle at a constant angle of attack for the conventional-tip model

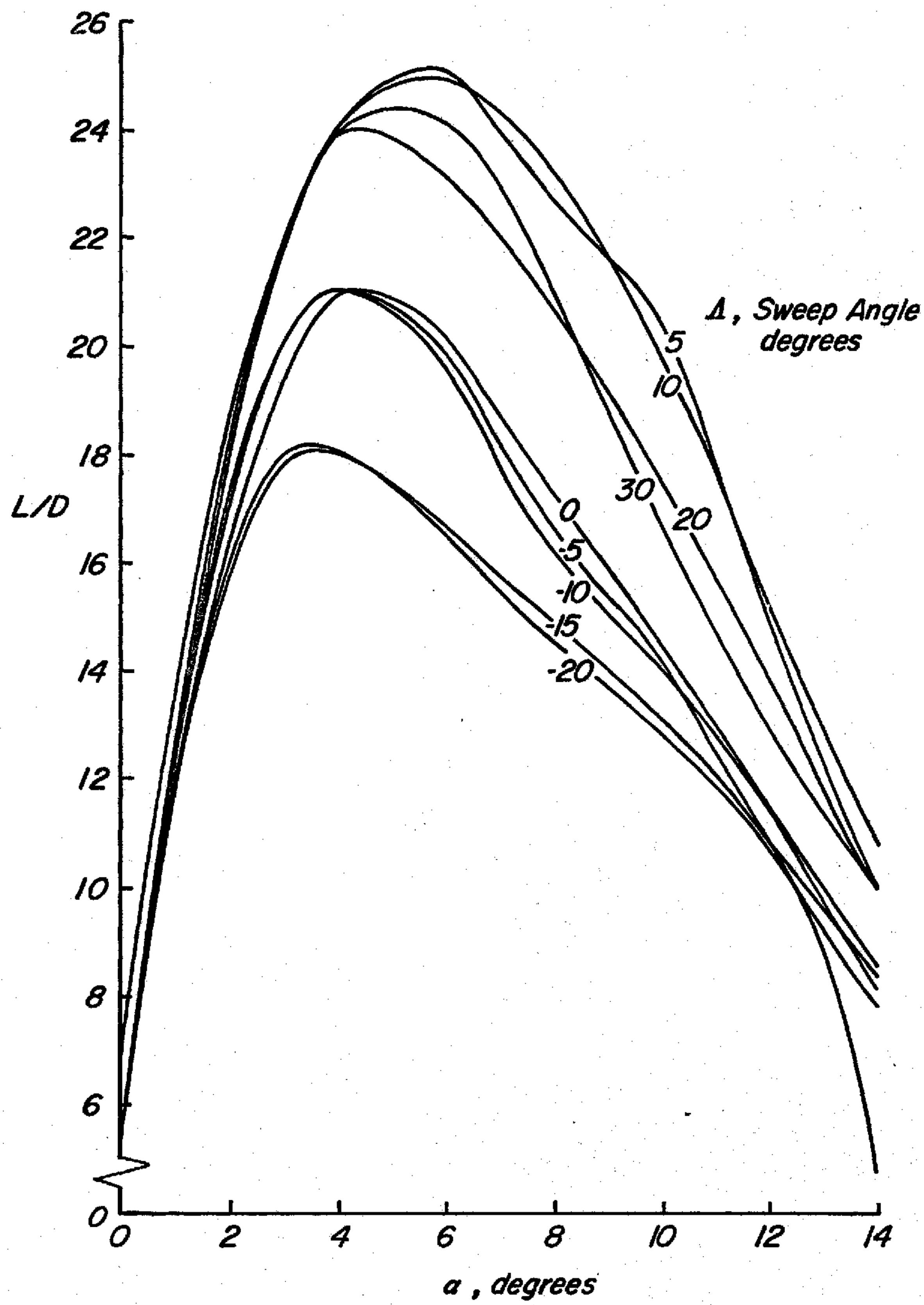

Figure 10. Lift-to-drag ratios vs. angle of attack for sweep variation of the ogee model

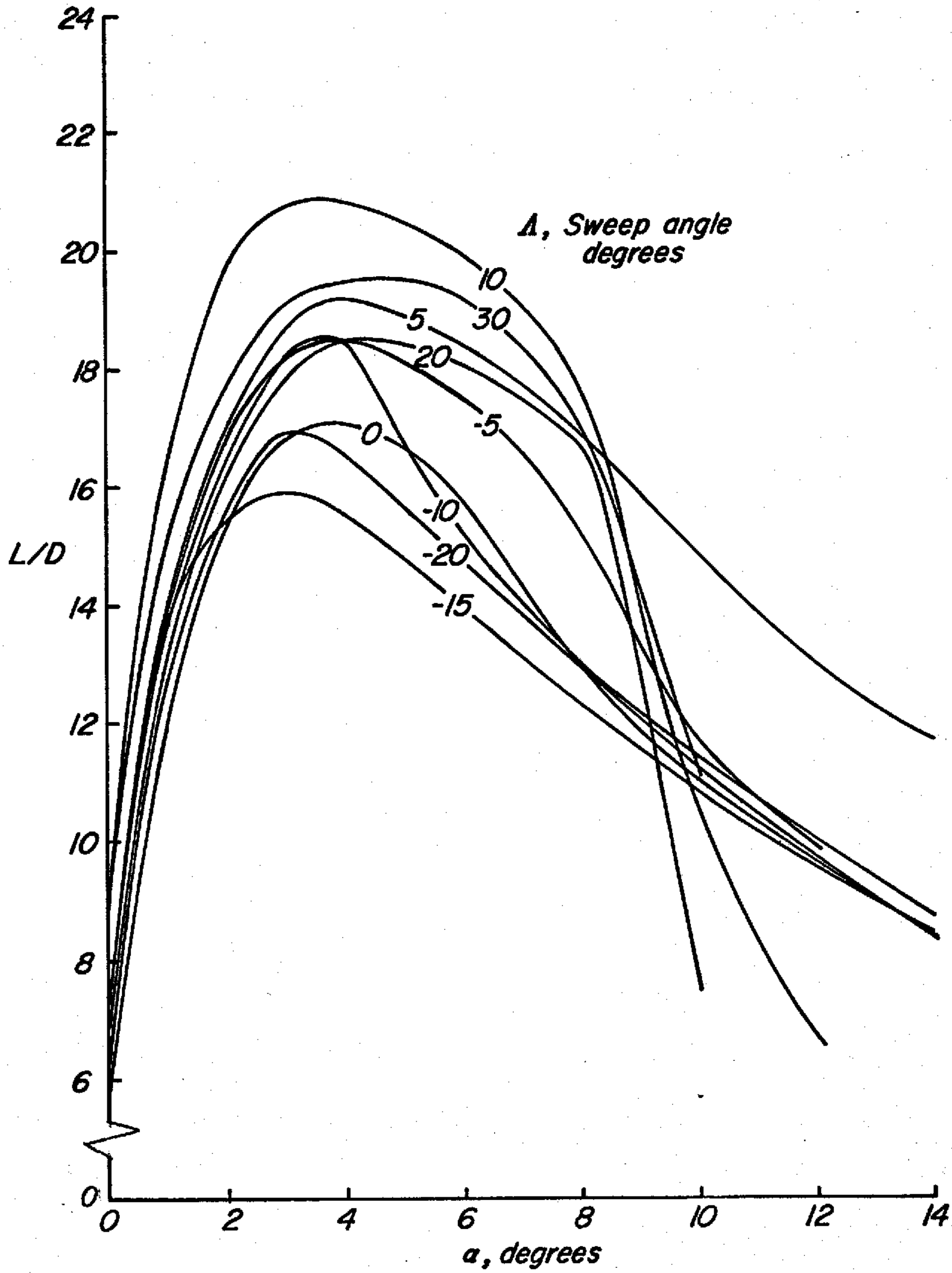

Figure 11. Lift-to-drag ratios vs. angle of attack for sweep variation of the conventional-tip model

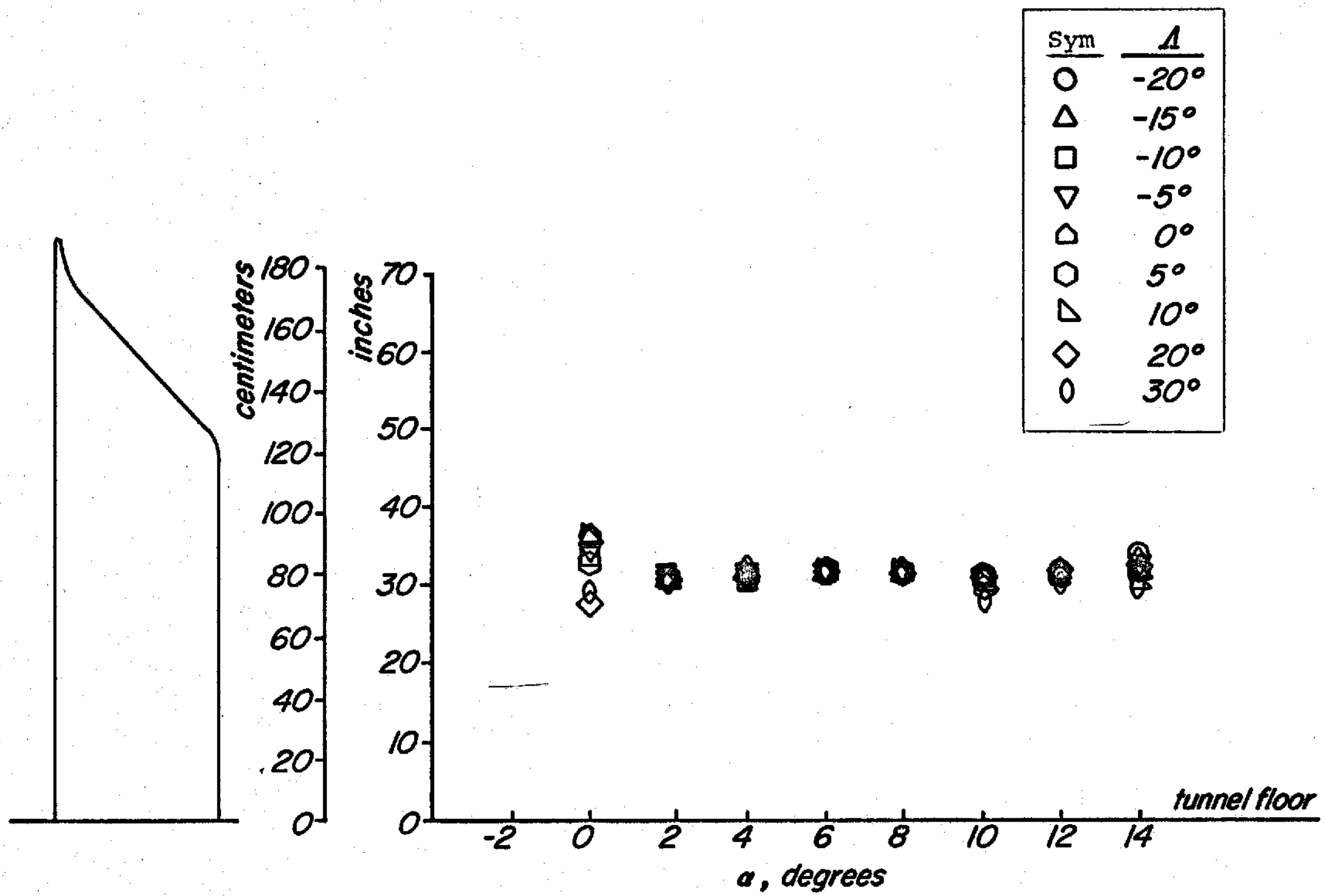

Spanwise Lift Center vs. Angle of Attack

Figure 12. Spanwise lift center vs. angle of attack for sweep variation of the ogee model

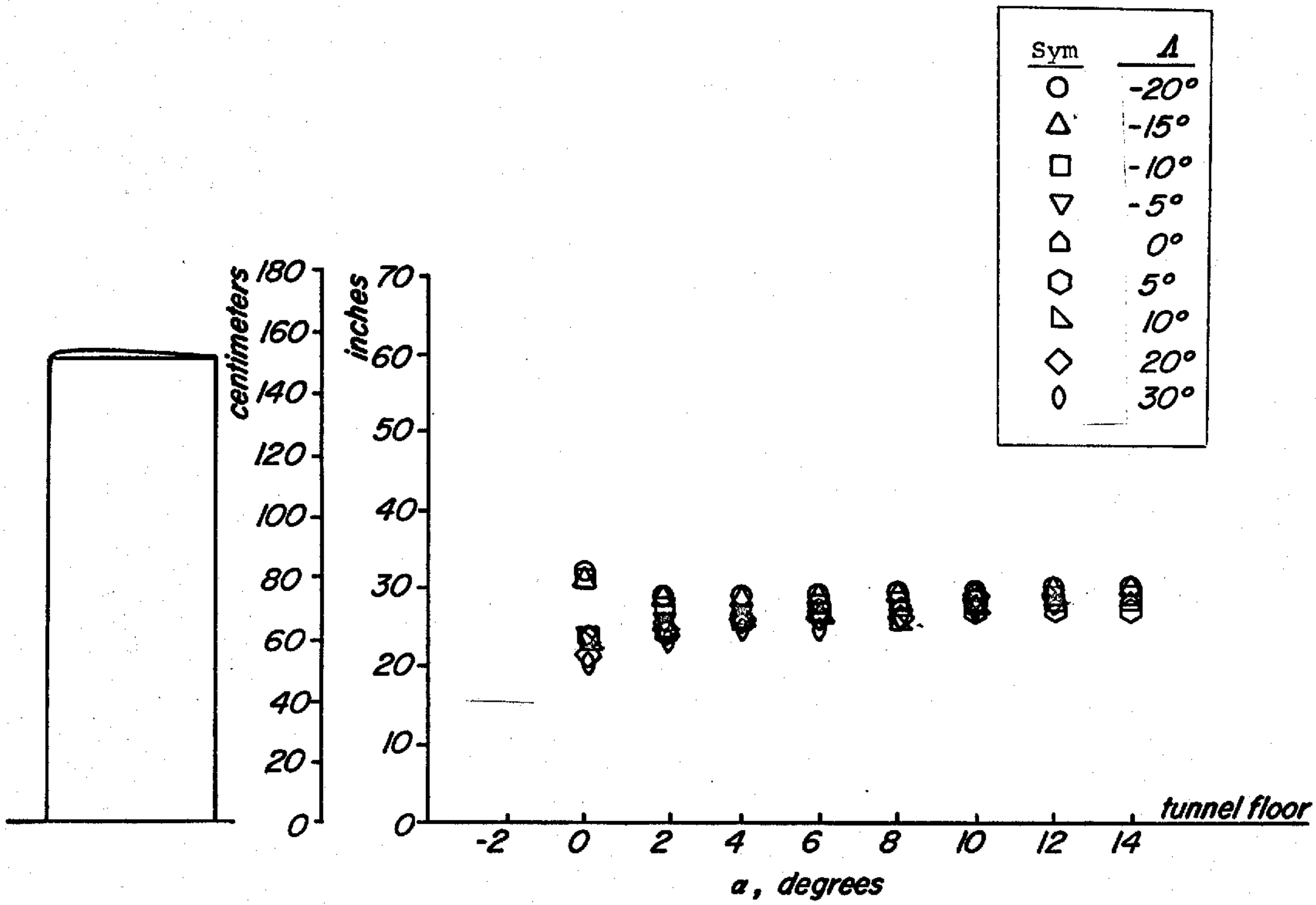

Spanwise Lift Center vs. Angle of Attack

Figure 13. Spanwise lift center vs. angle of attack for sweep variation of the conventional-tip model

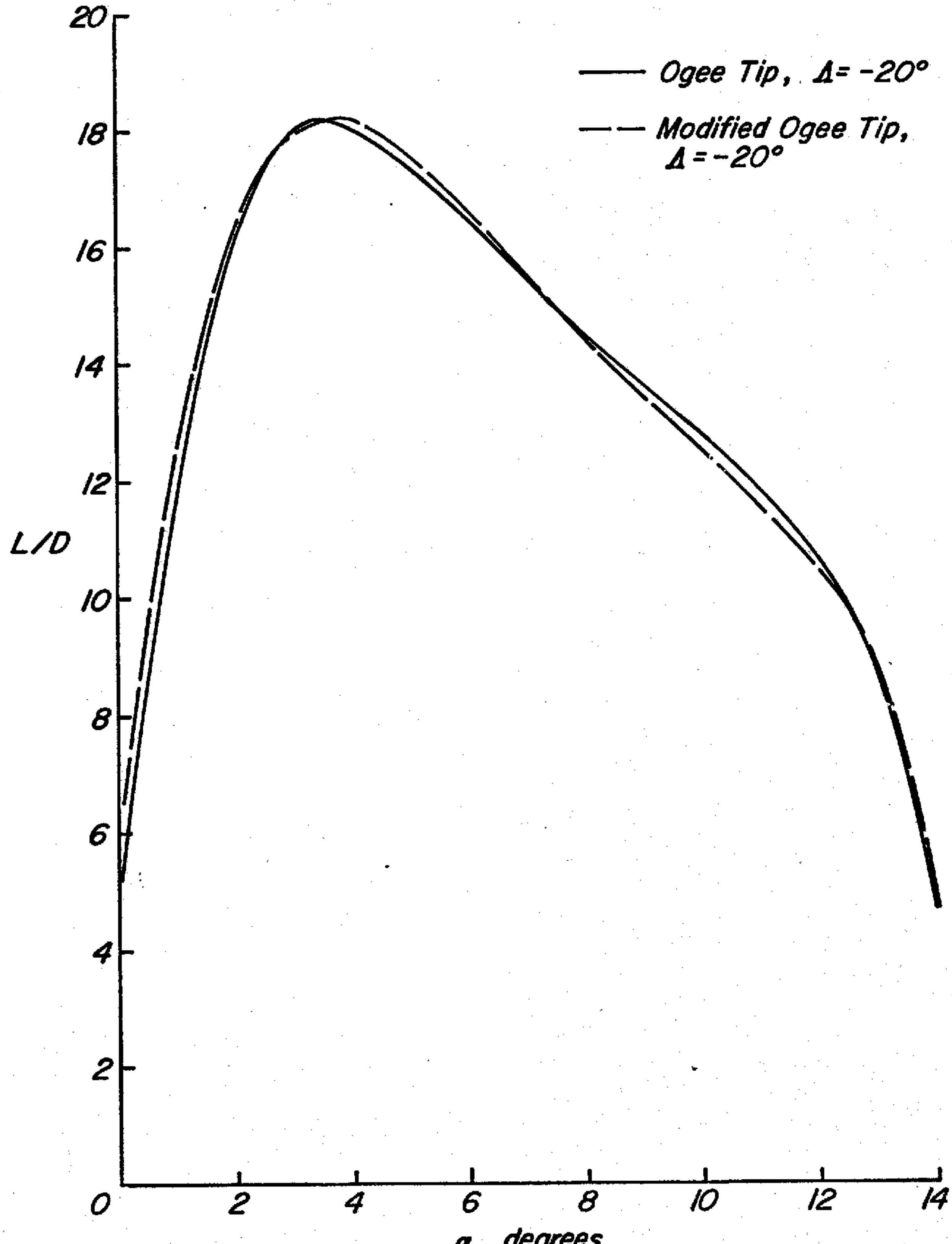

Figure 14. Effect of the modified ogee-tip on the L/D performance of the ogee model at Λ=-20°

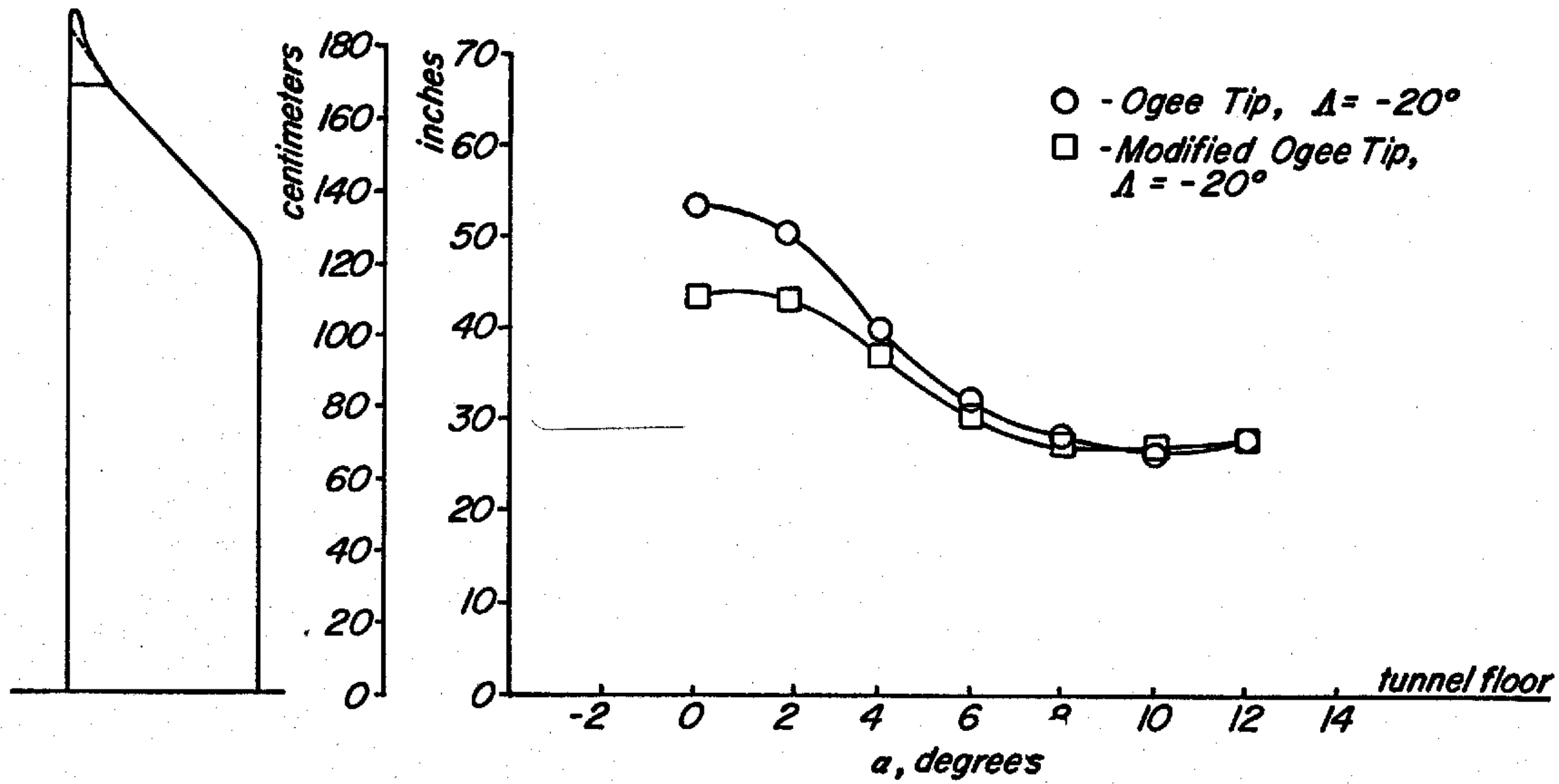

Effect of Modified Ogee Tip on Spanwise Drag Center

Figure 15. Effect of the modified ogee-tip on the spanwise drag center of the ogee model at Λ=-20°

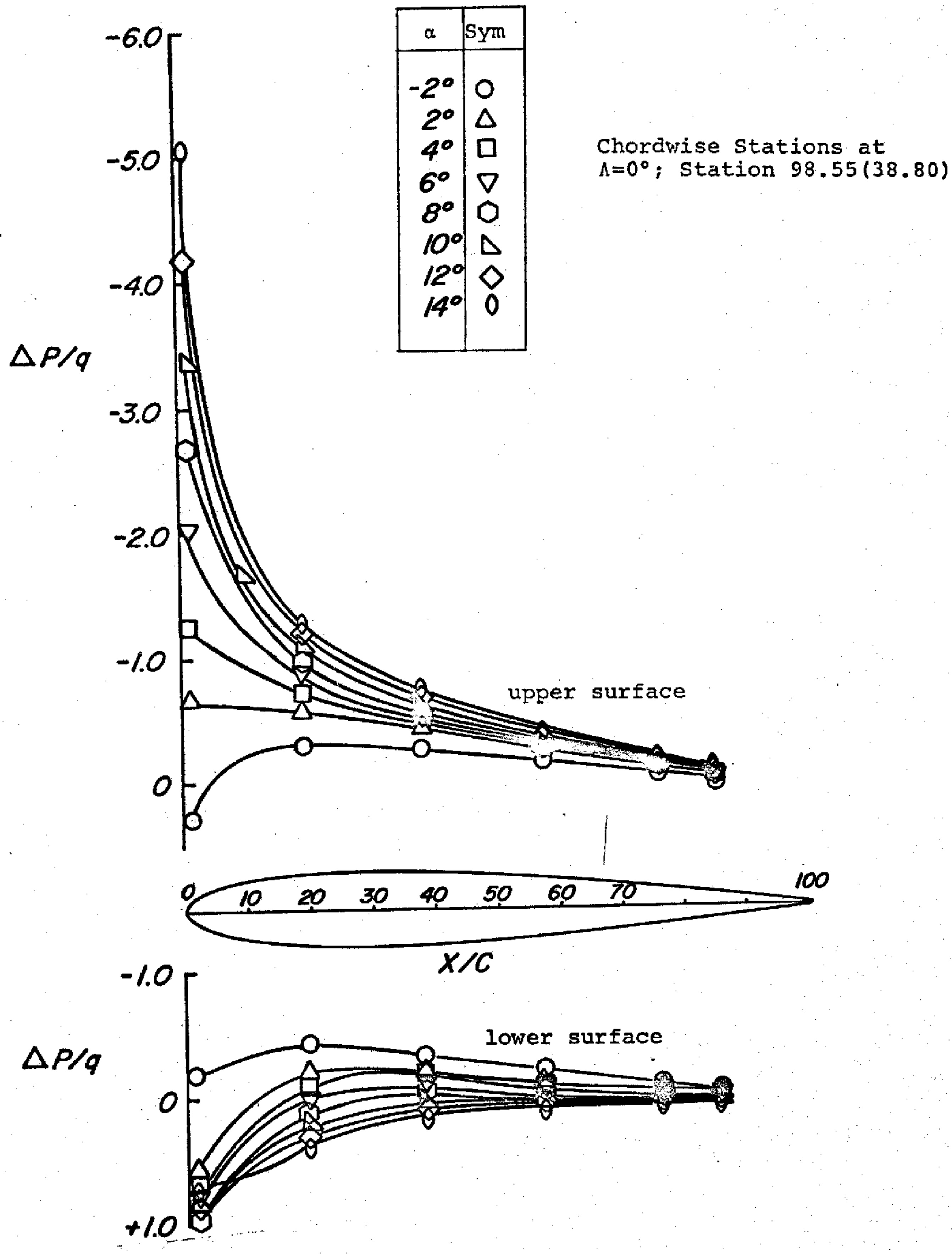

Figure 16. Chordwise pressure distributions of the ogee for $\Lambda=0°$

Chordwise Stations at Λ=0°; Station 117.86(46.40)

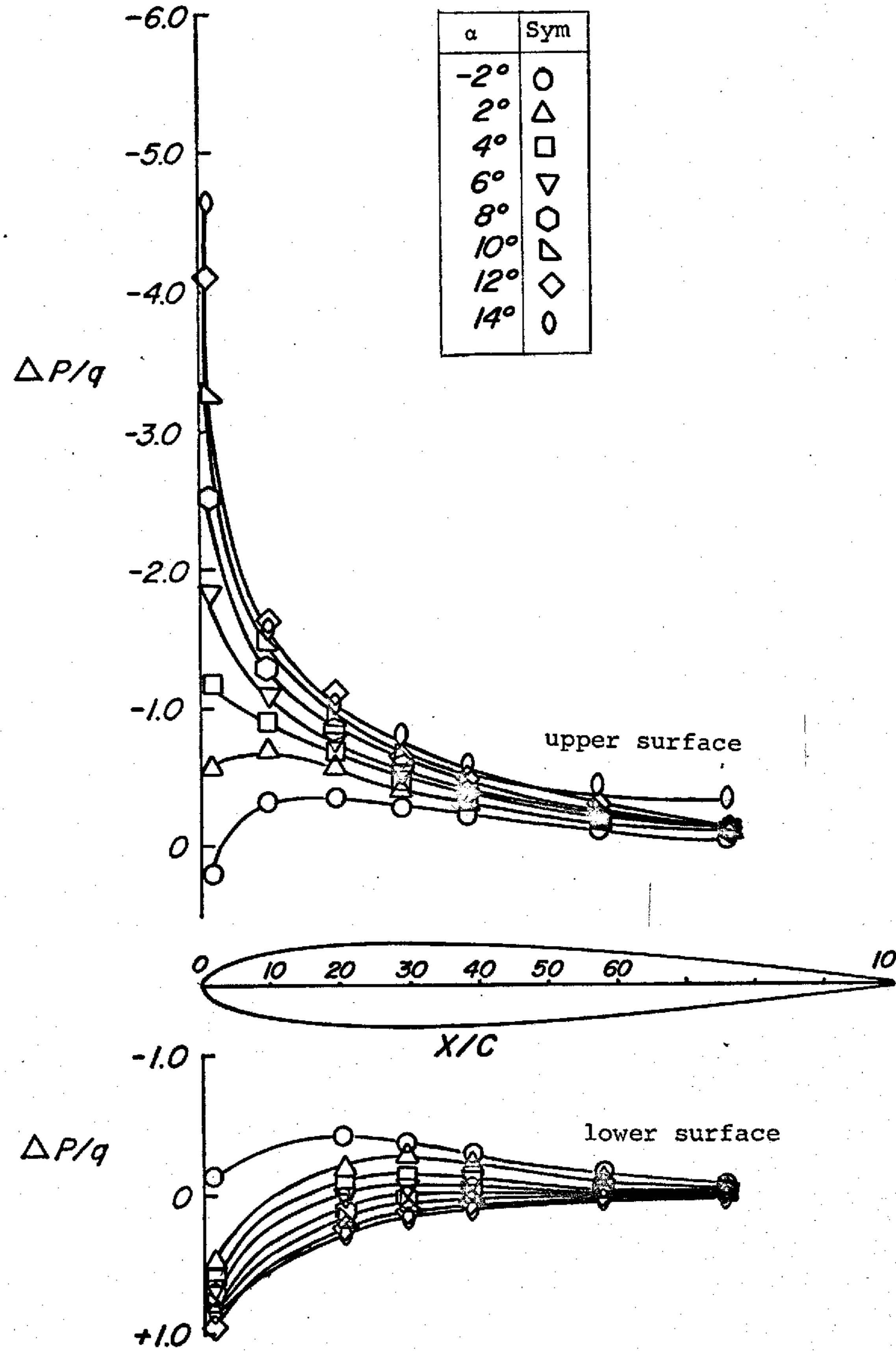

Figure 16. Chordwise pressure distributions of the ogee for Λ=0° - Continued

Chordwise Stations at $\Lambda=0°$; Station 136.14(53.60)

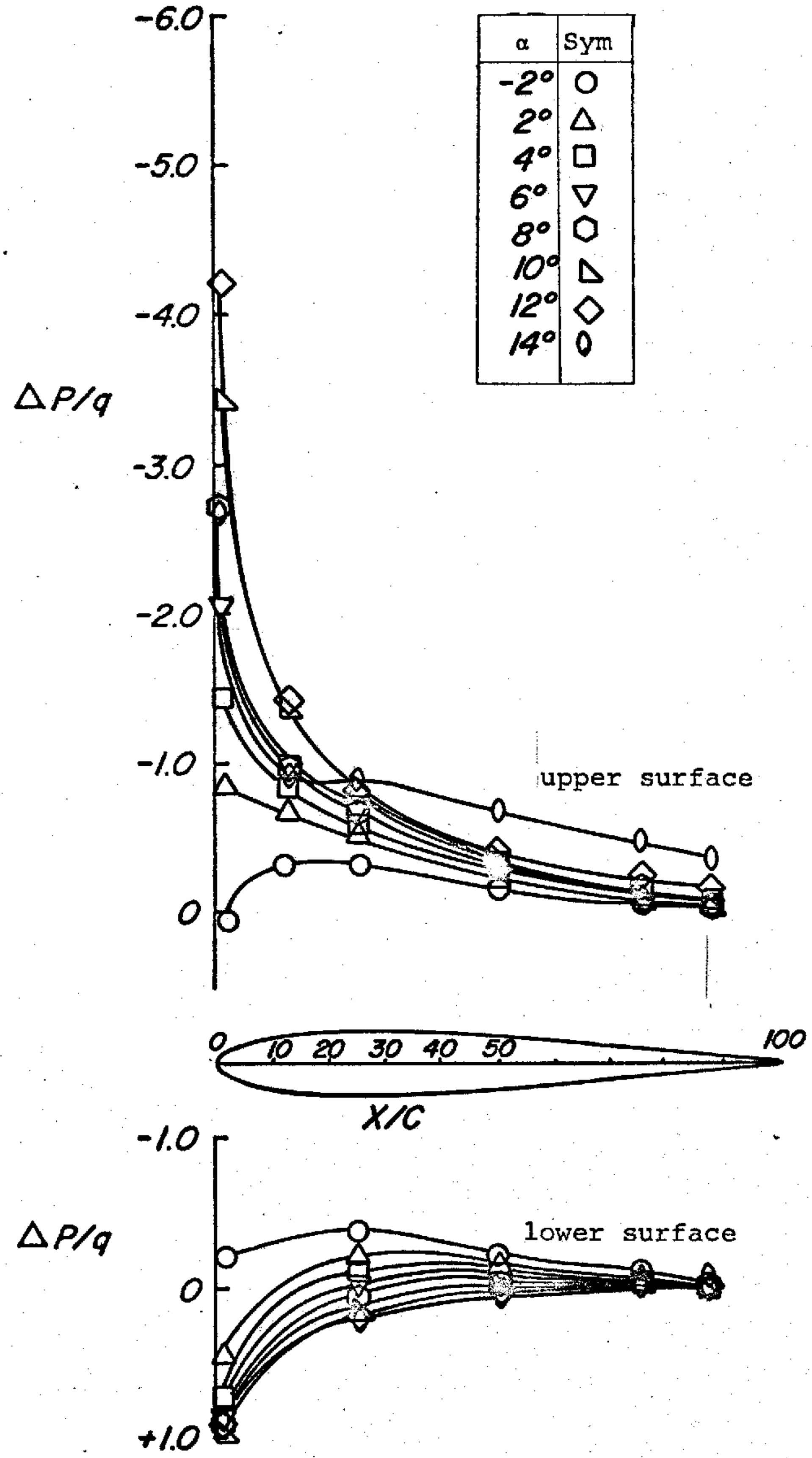

Figure 16. Chordwise pressure distributions of the ogee for $\Lambda=0°$ - Continued

Chordwise Stations at Λ=0°; Station 149.86(59.00)

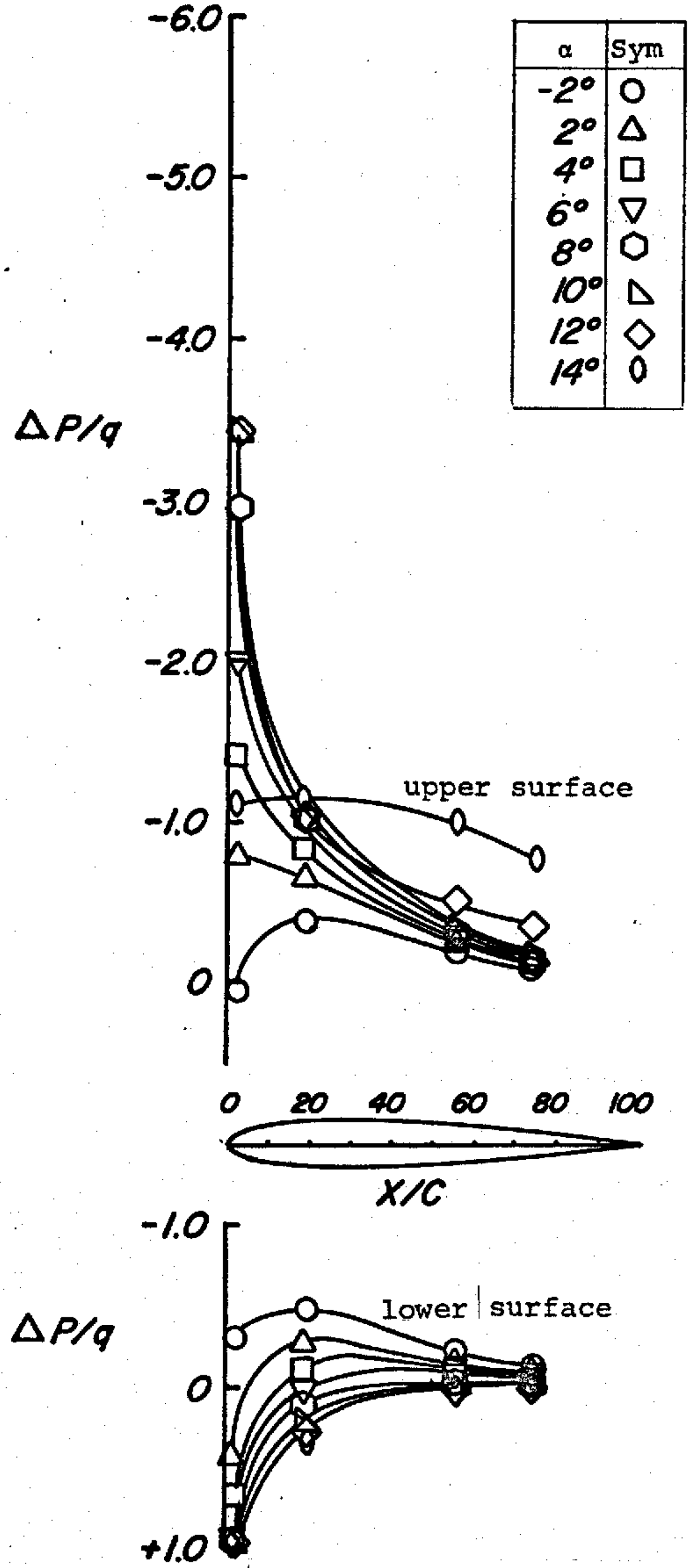

Figure 16. Chordwise pressure distributions of the ogee for Λ=0° - continued

Chordwise Stations at
Λ=0°; Station 159.51(62.80

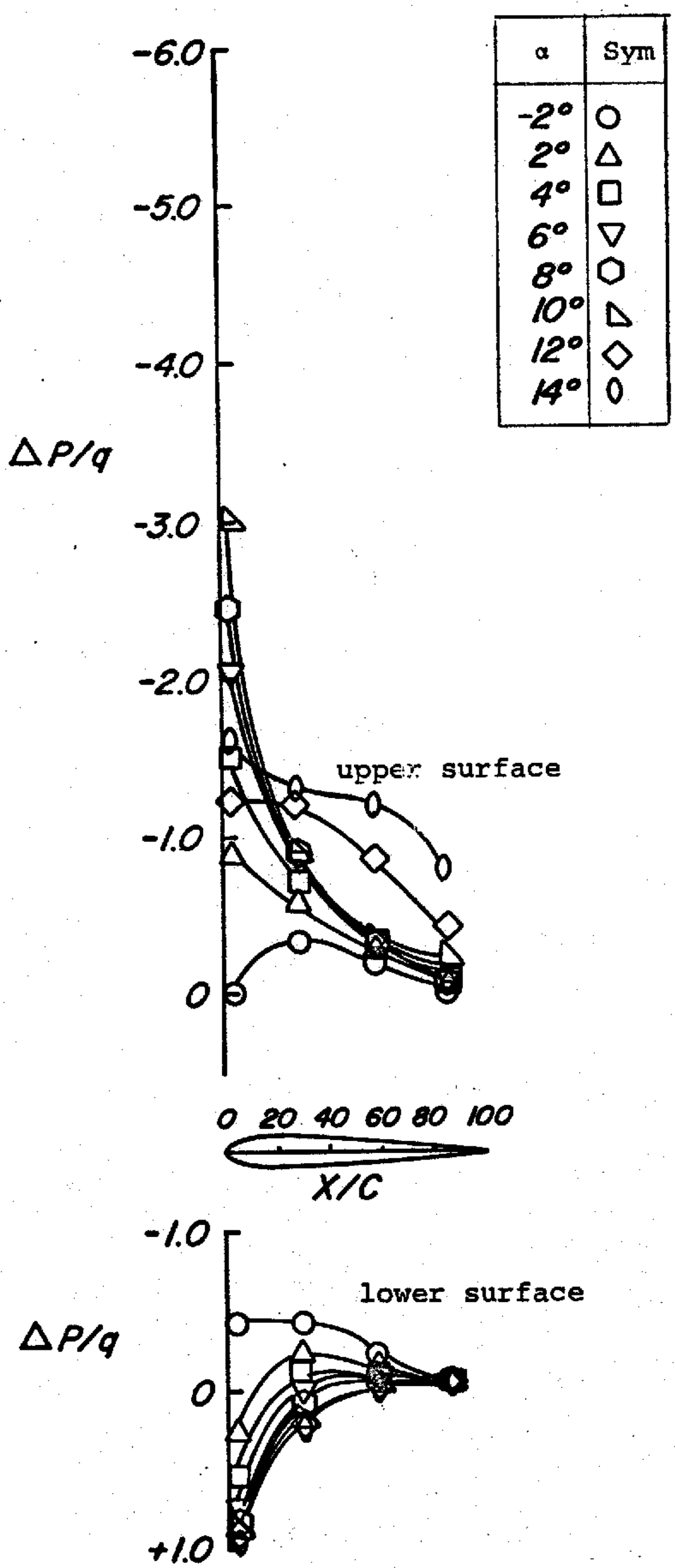

Figure 16. Chordwise pressure distributions of the ogee for Λ=0° - Continued

Chordwise Stations at $\Lambda=0°$; Station 168.15(66.20)

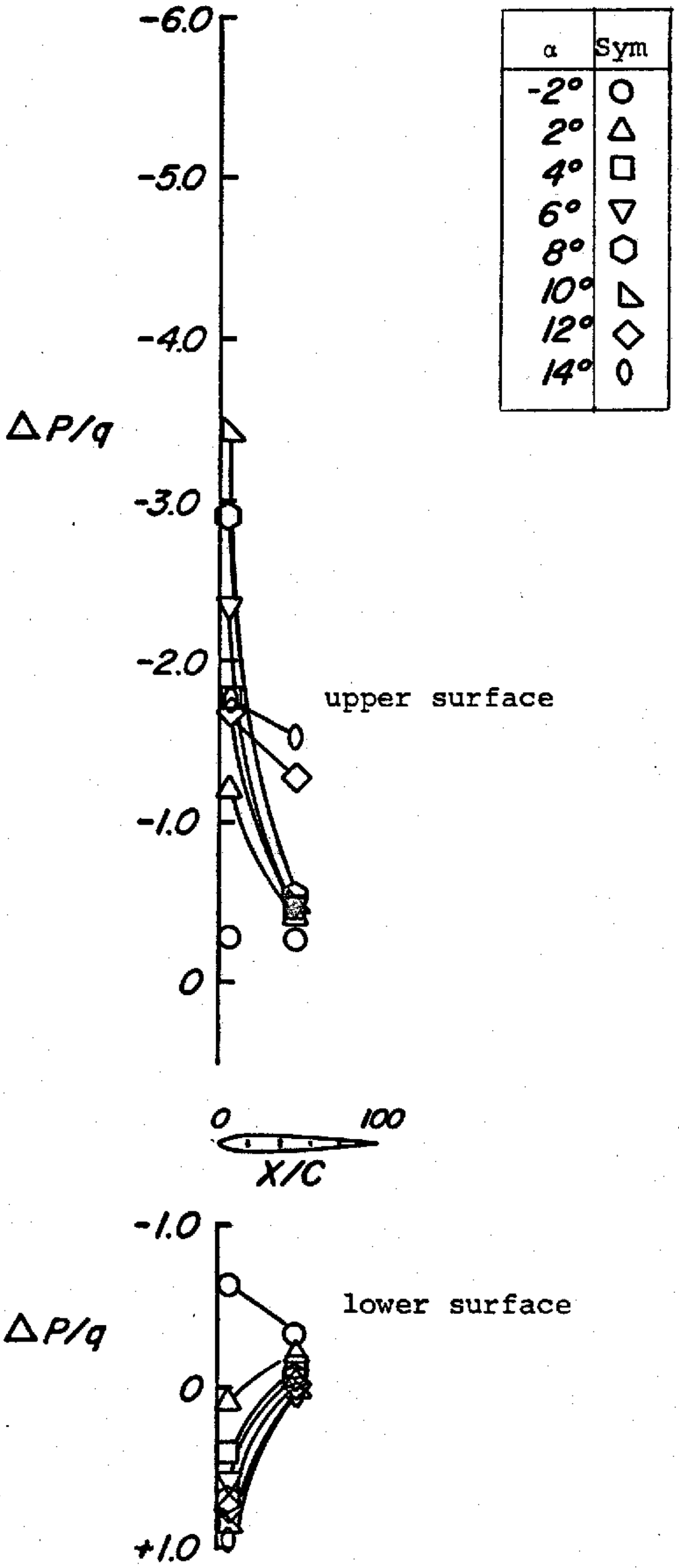

Figure 16. Chordwise pressure distributions of the ogee for $\Lambda=0°$ - Concluded

Chordwise Stations at Λ=-20°; Station 117.86(46.40)

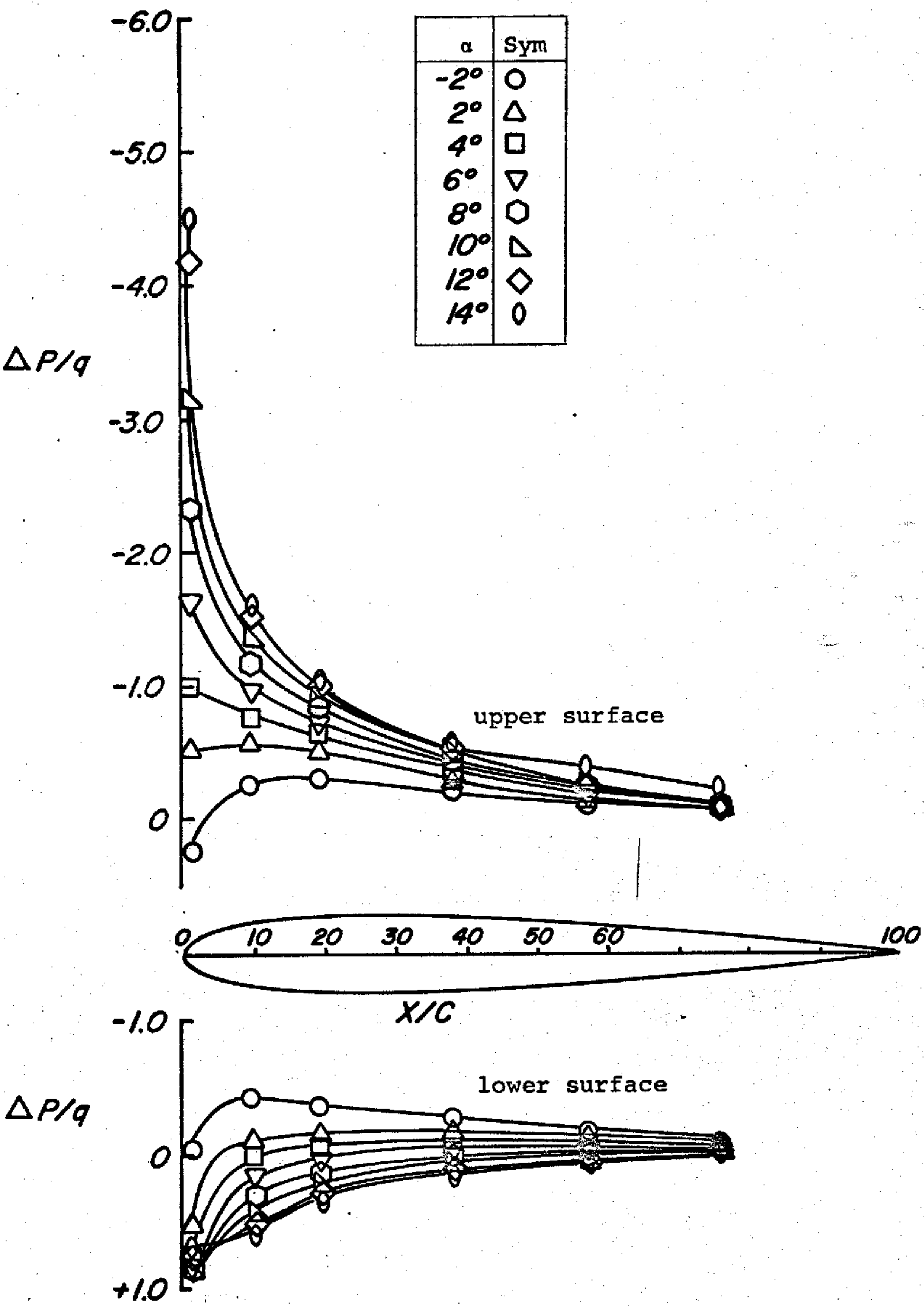

Figure 17. Chordwise pressure distributions of the ogee for Λ=-20°

Chordwise Stations at Λ=-20°; Station 132.33(52.10)

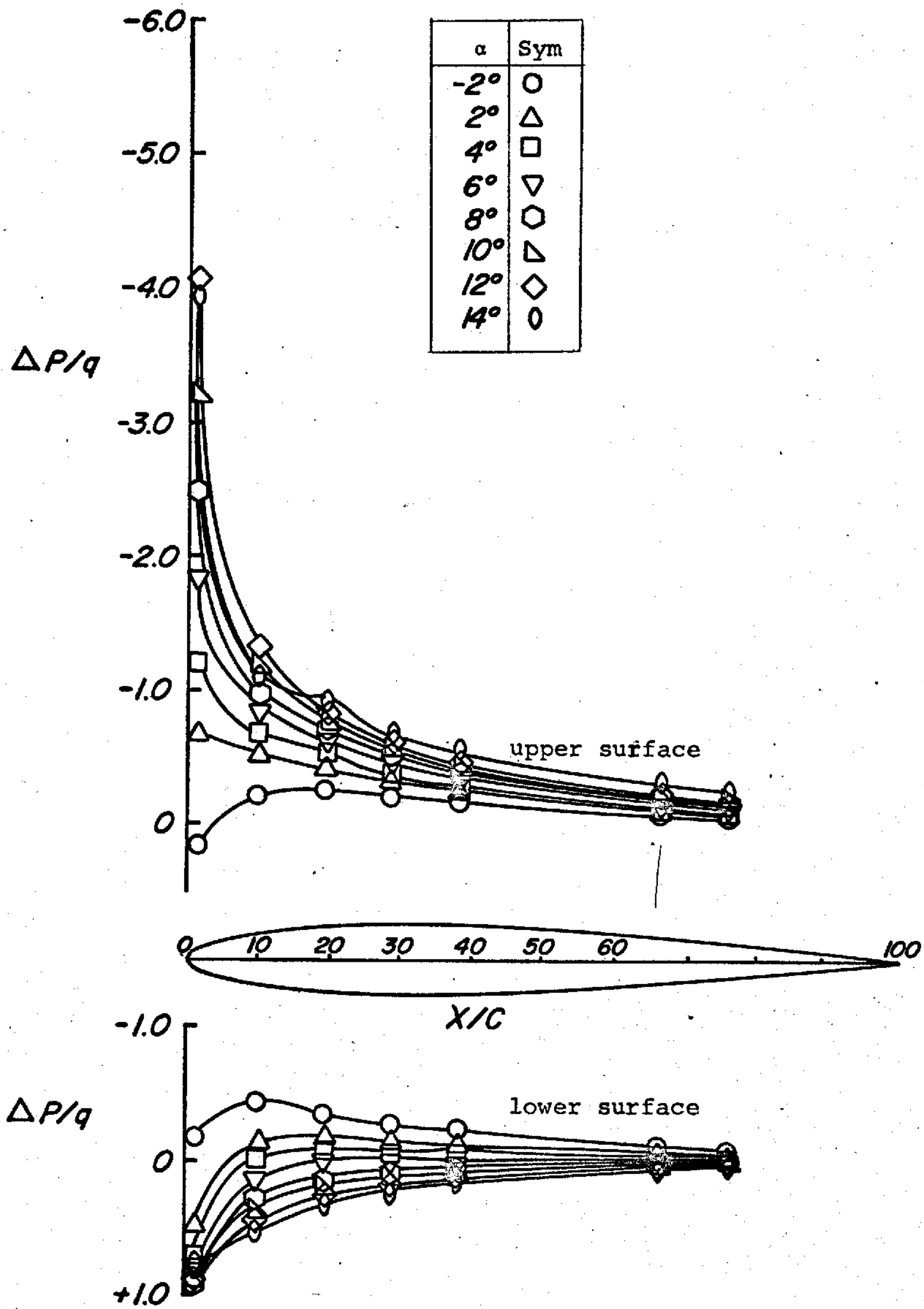

Figure 17. Chordwise pressure distributions of the ogee for Λ=-20° - Continued

Chordwise Stations at Λ=-20°; 146.94(57.85)

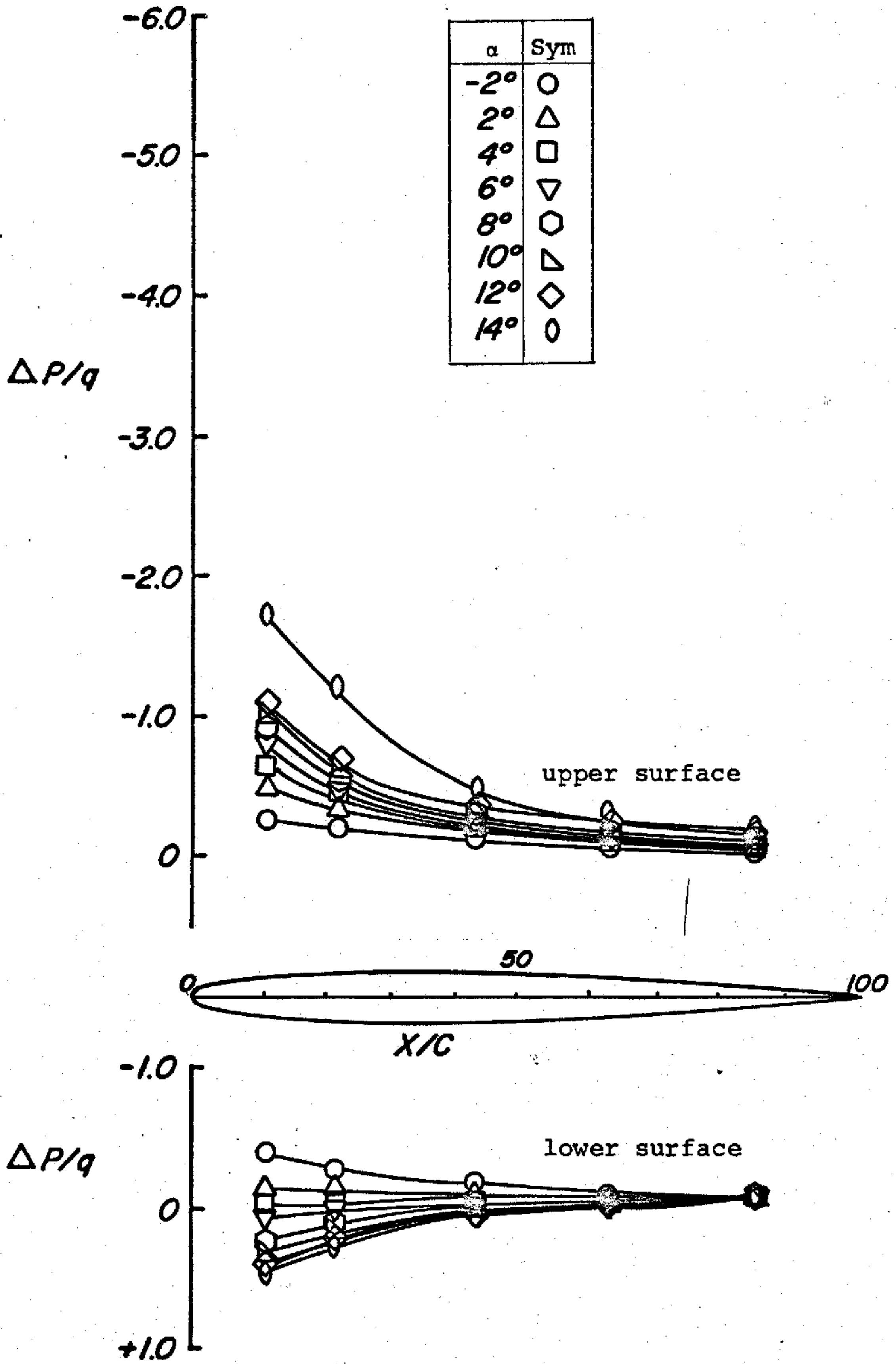

Figure 17. Chordwise pressure distributions of the ogee for Λ=-20° - Continued

Chordwise Stations at Λ=-20°; Station 155.19(61.10)

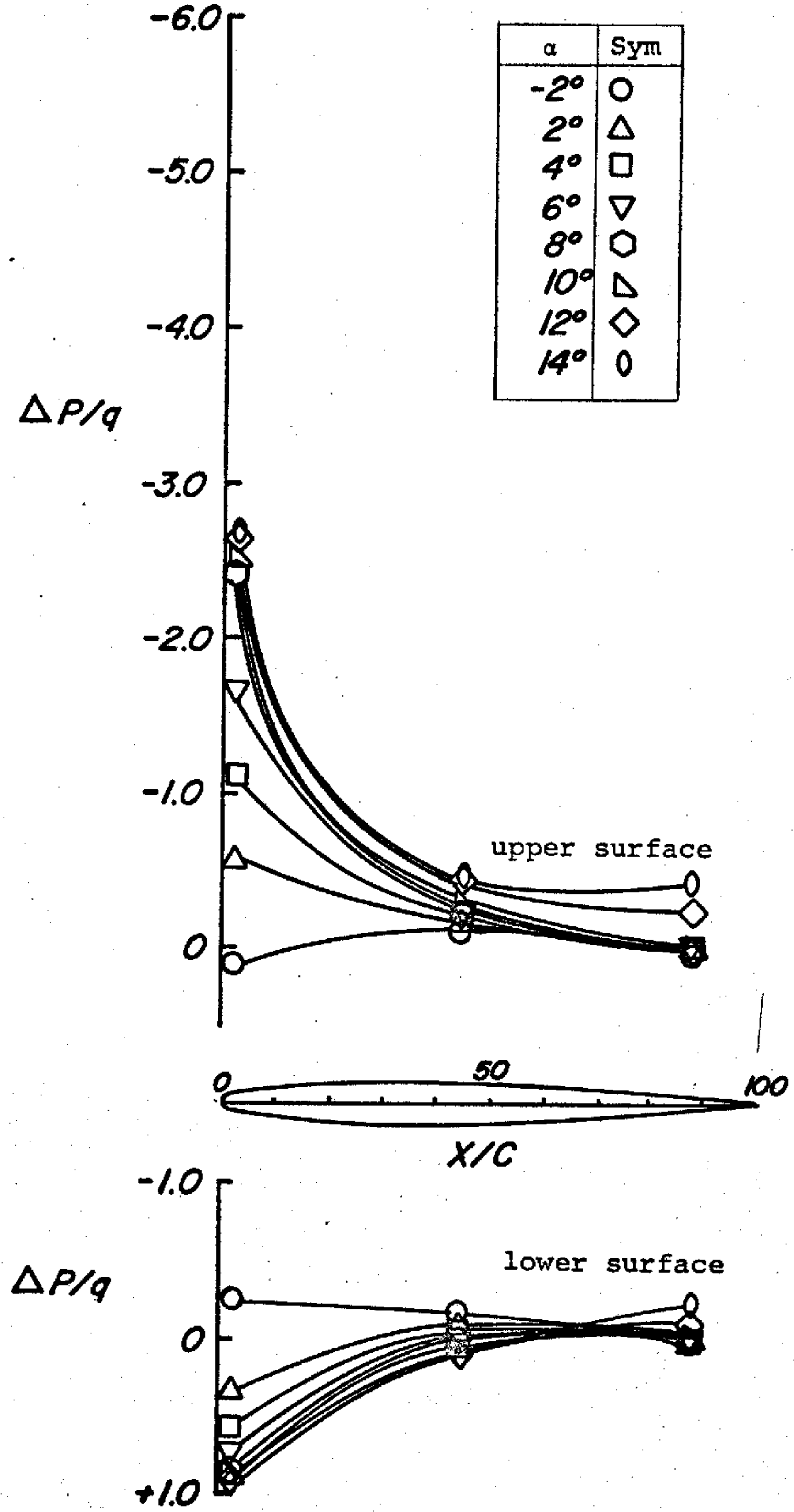

Figure 17. Chordwise pressure distributions of the ogee for Λ=-20° - Continued

Chordwise Stations at Λ=-20°; Station 164.85(64.90)

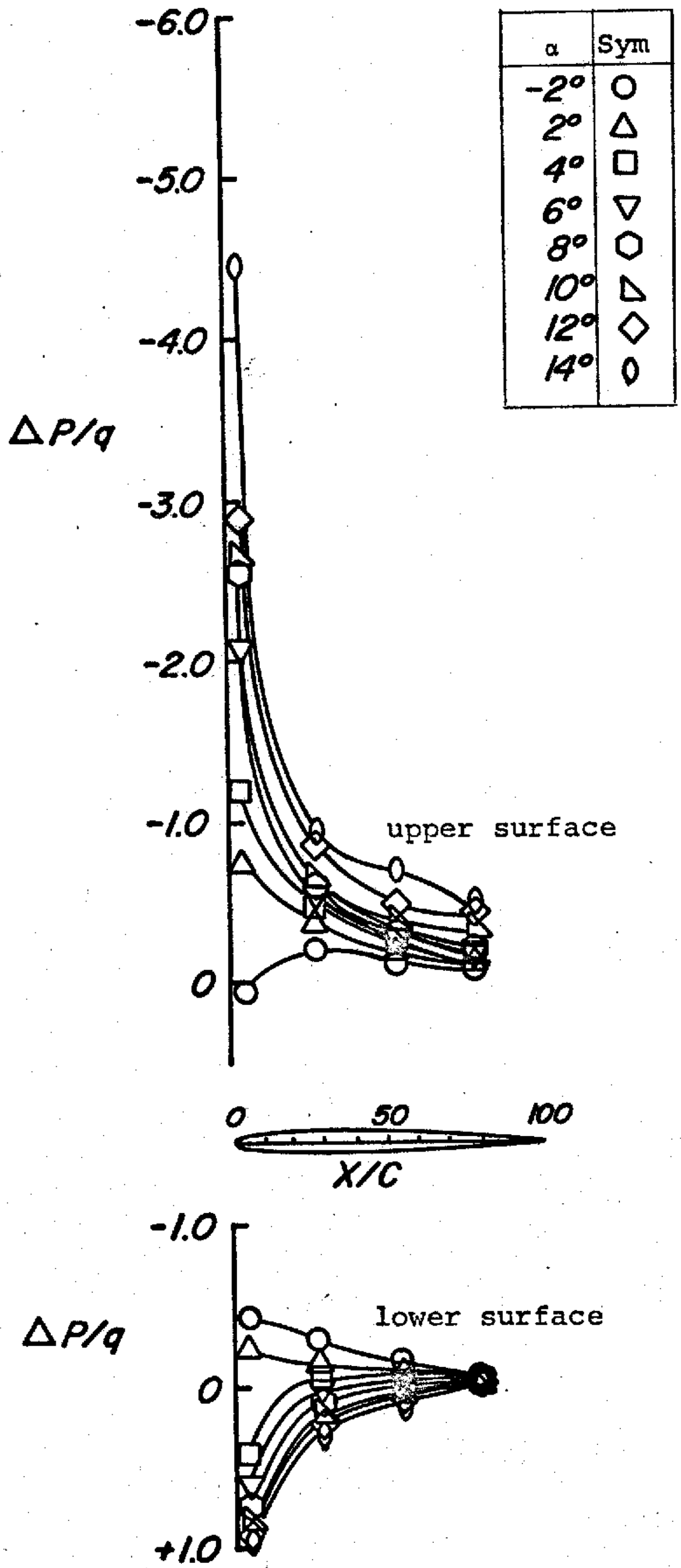

Figure 17. Chordwise pressure distributions of the ogee for Λ=-20° - Continued

Chordwise Stations at Λ=-20°; Station 175.01(68.90)

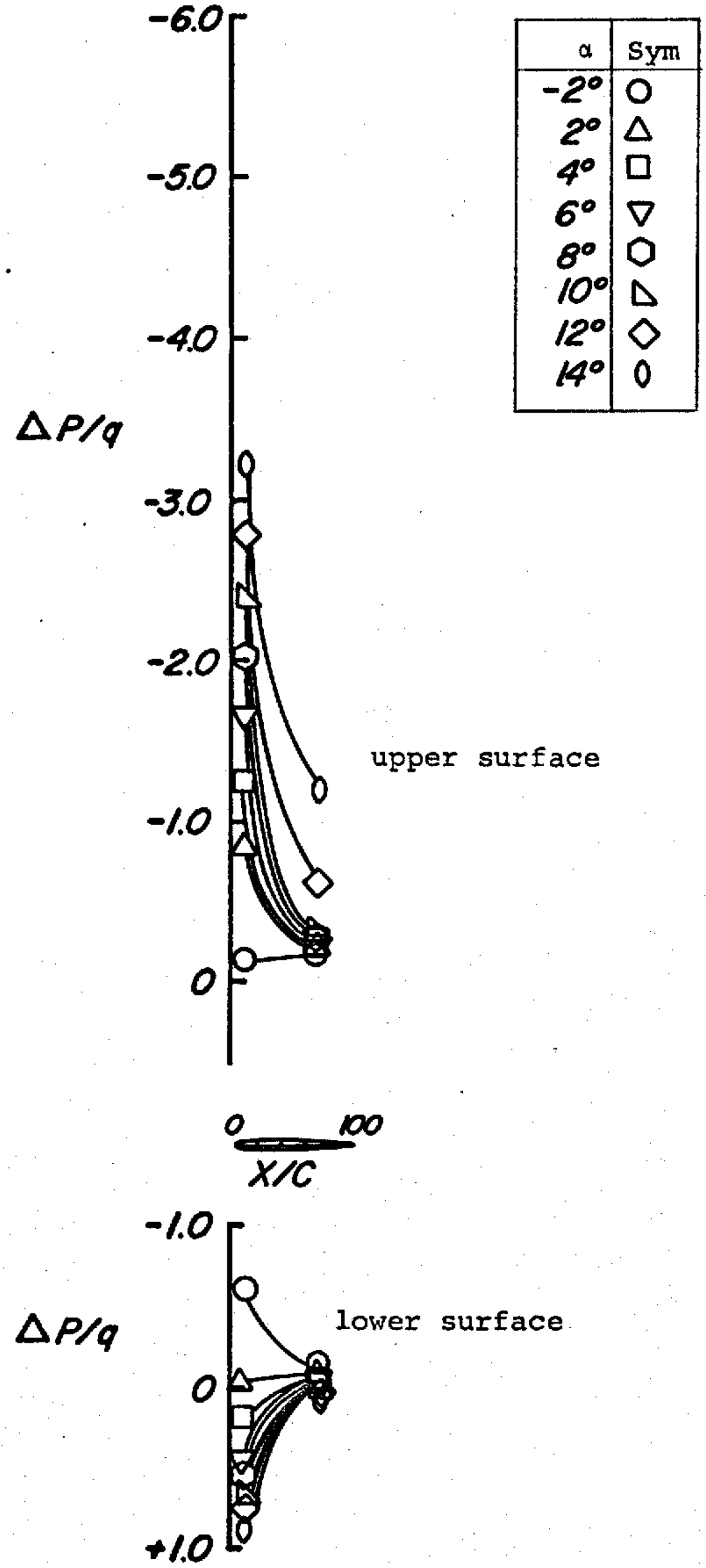

Figure 17. Chordwise pressure distributions of the ogee for Λ=-20° - Concluded

Chordwise Stations at Λ=+20°; Station 98.55(38.80)

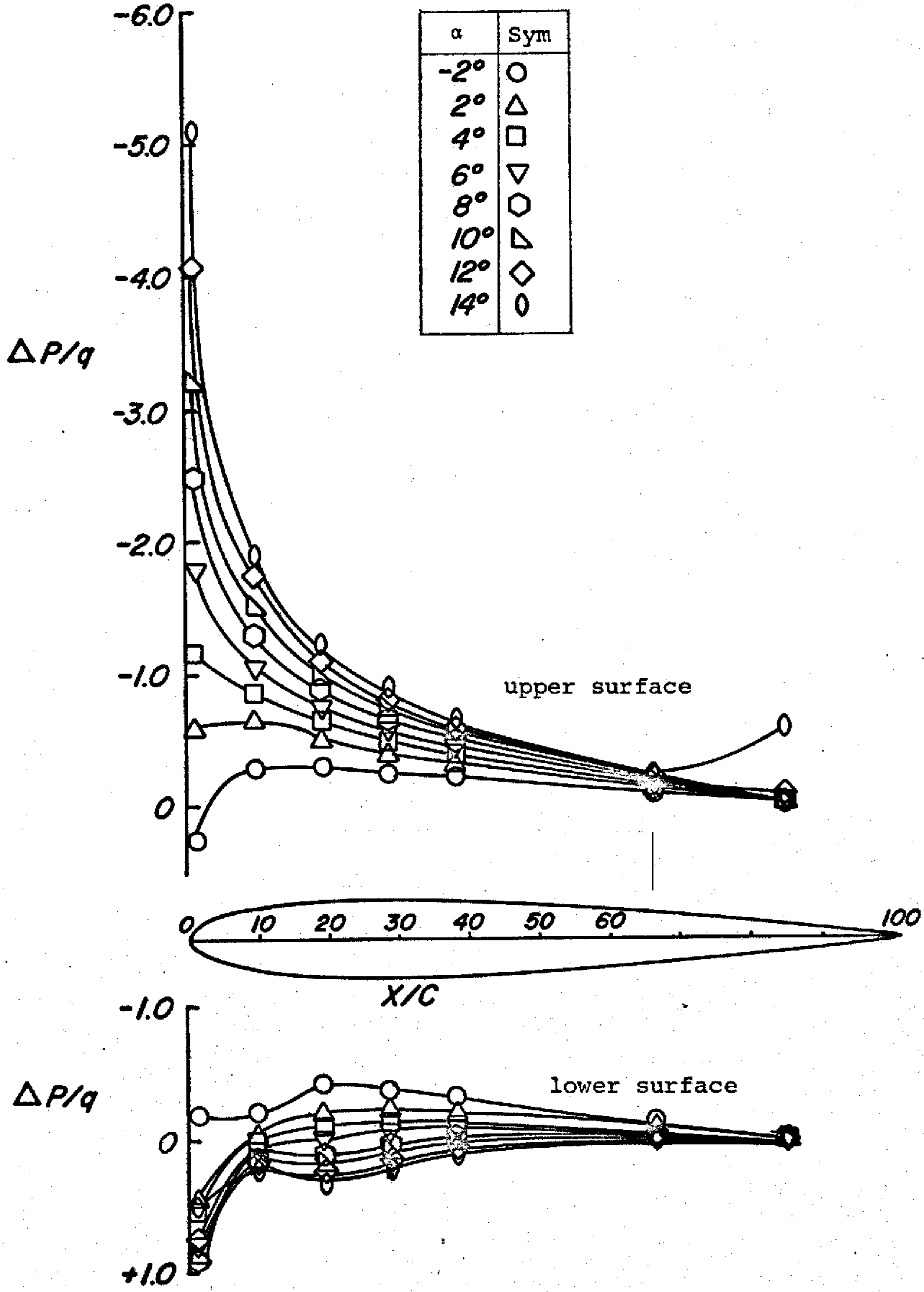

Figure 18. Chordwise pressure distributions of the ogee for Λ=+20°

Chordwise Stations at Λ=+20°; Station 117.86(46.40)

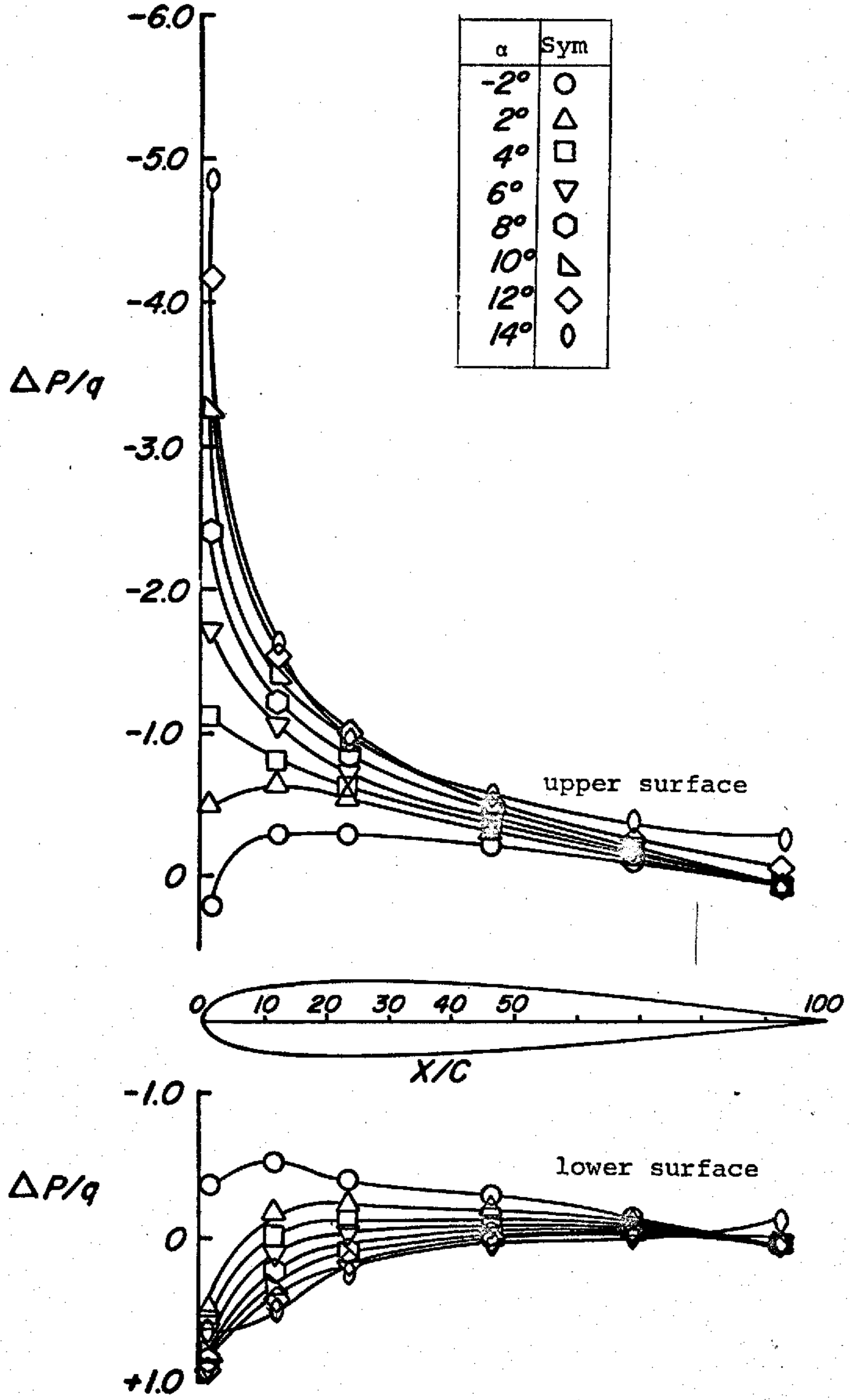

Figure 18. Chordwise pressure distributions of the ogee for Λ=+20° - Continued

Chordwise Stations at Λ=+20°; Station 132.33(52.10)

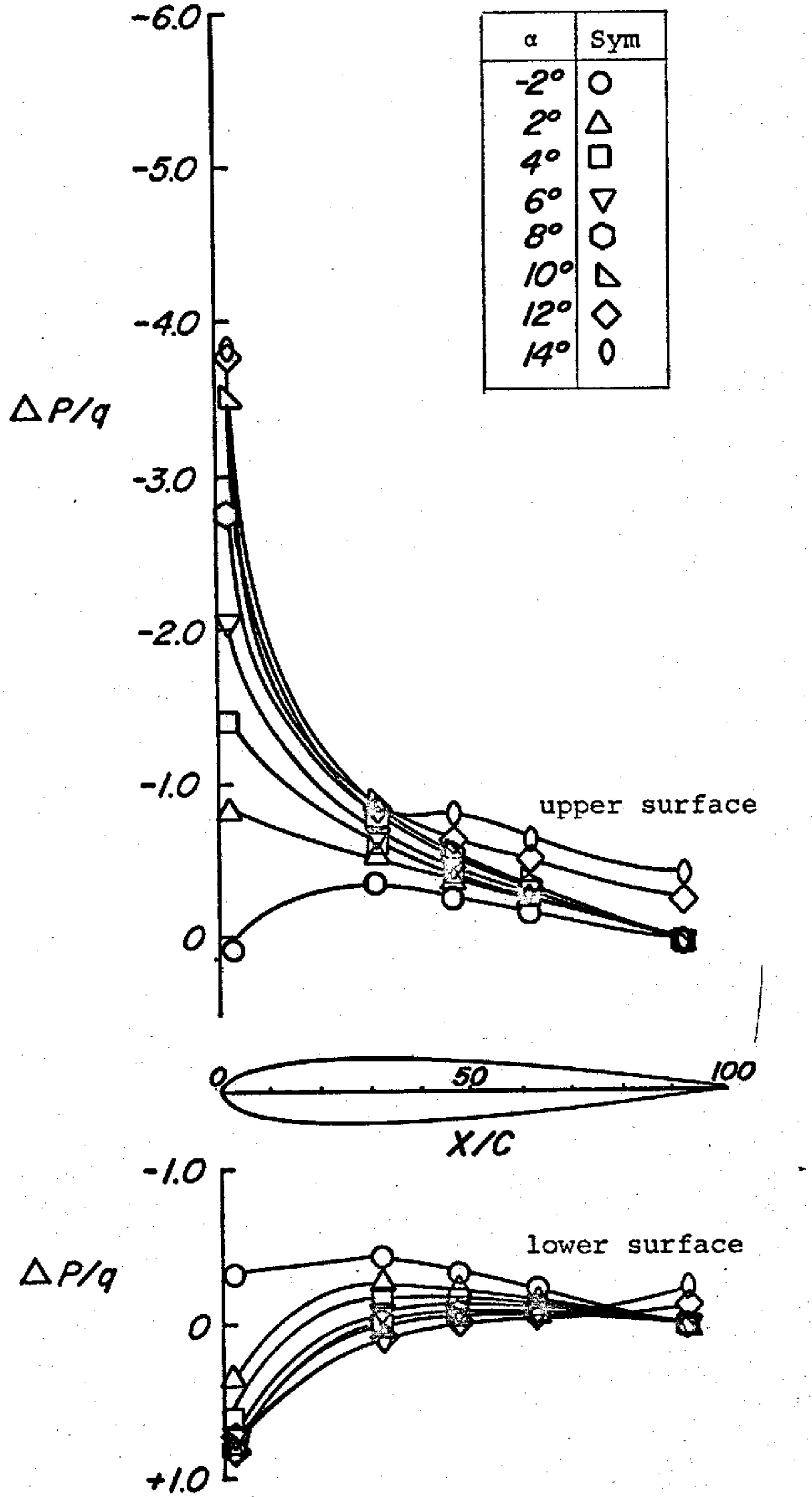

Figure 18. Chordwise pressure distributions of the ogee for Λ=+20° - Continued

Chordwise Stations at Λ=+20°; Station 144.78(57.00)

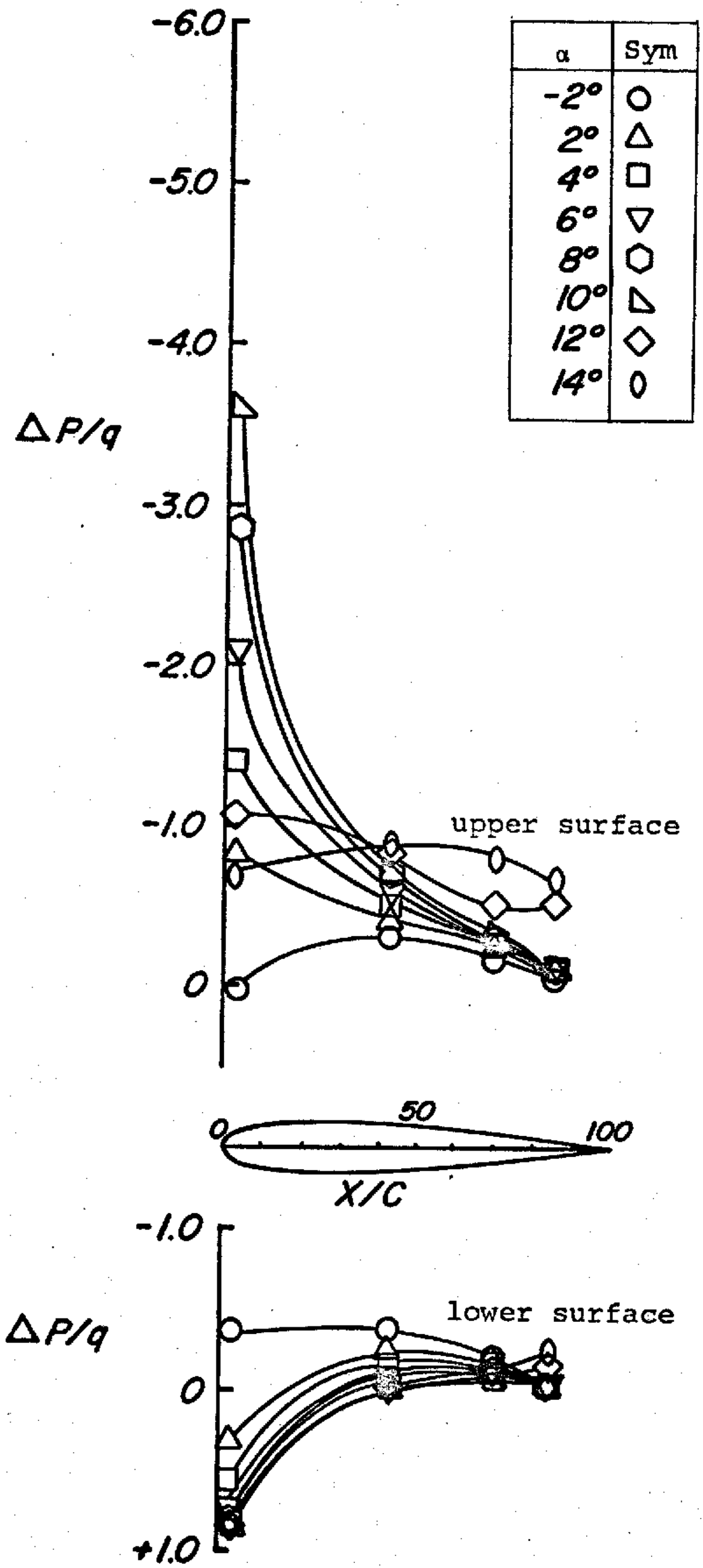

Figure 18. Chordwise pressure distributions of the ogee for Λ=+20° - Continued

Chordwise Stations at Λ=+20°; Station 157.73(62.10)

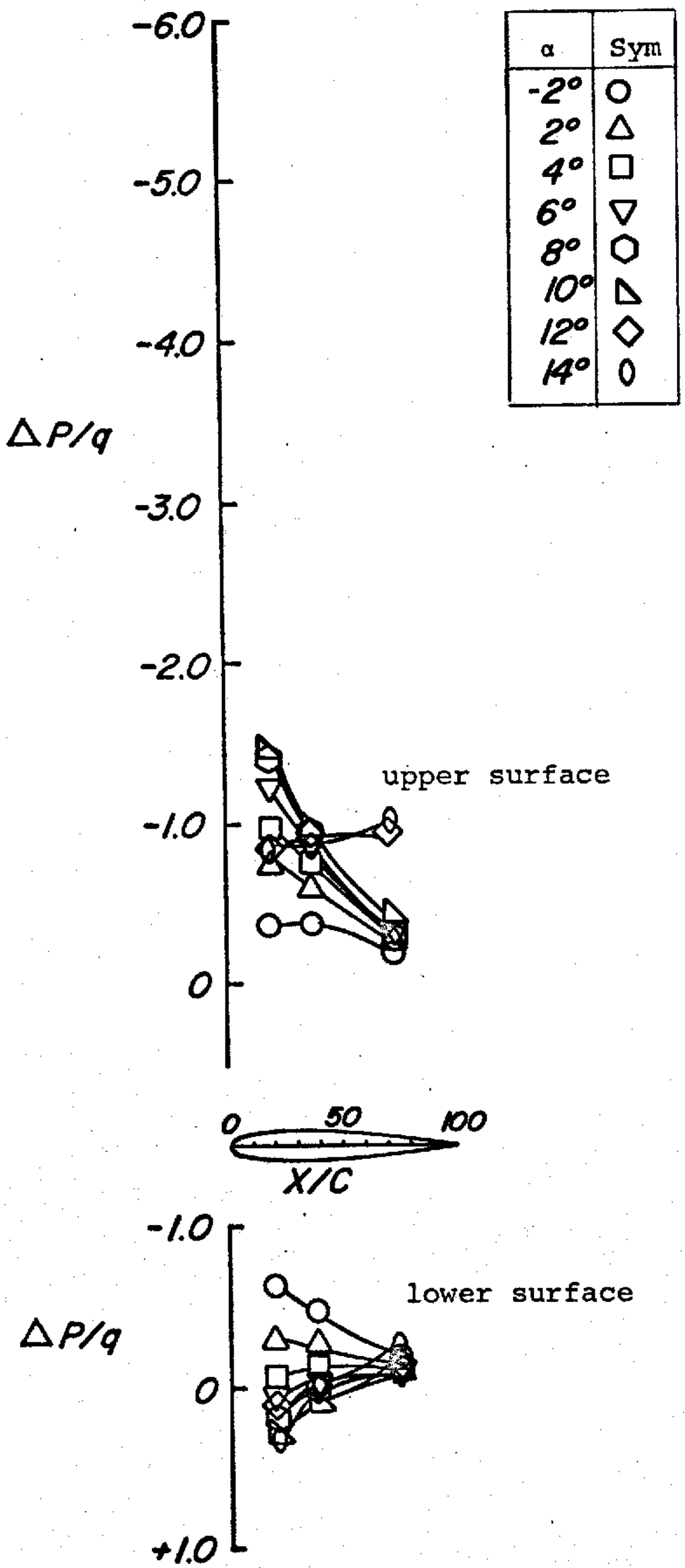

Figure 18. Chordwise pressure distributions of the ogee for Λ=+20° - Continued

Chordwise Stations at Λ=+20°; Station 171.45(67.50)

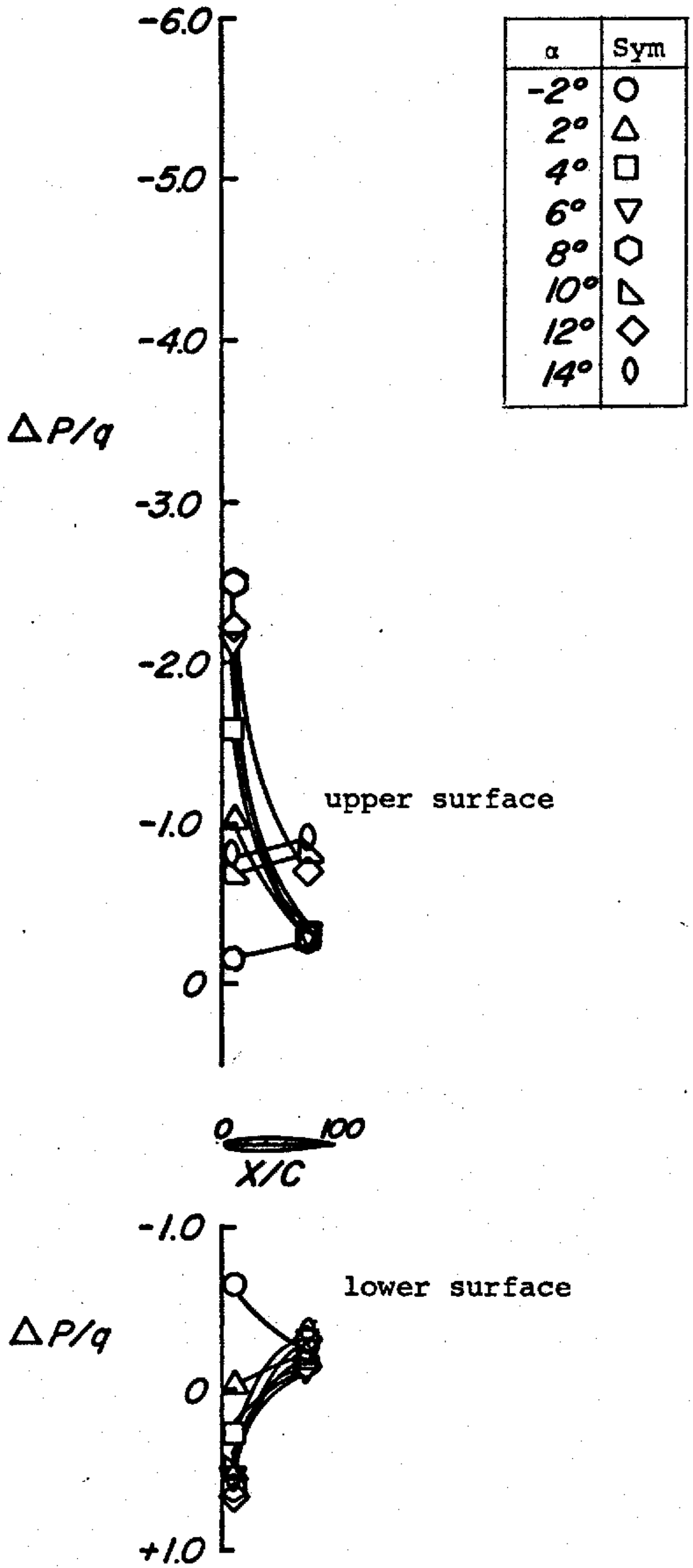

Figure 18. Chordwise pressure distributions of the ogee for Λ=+20° - Concluded

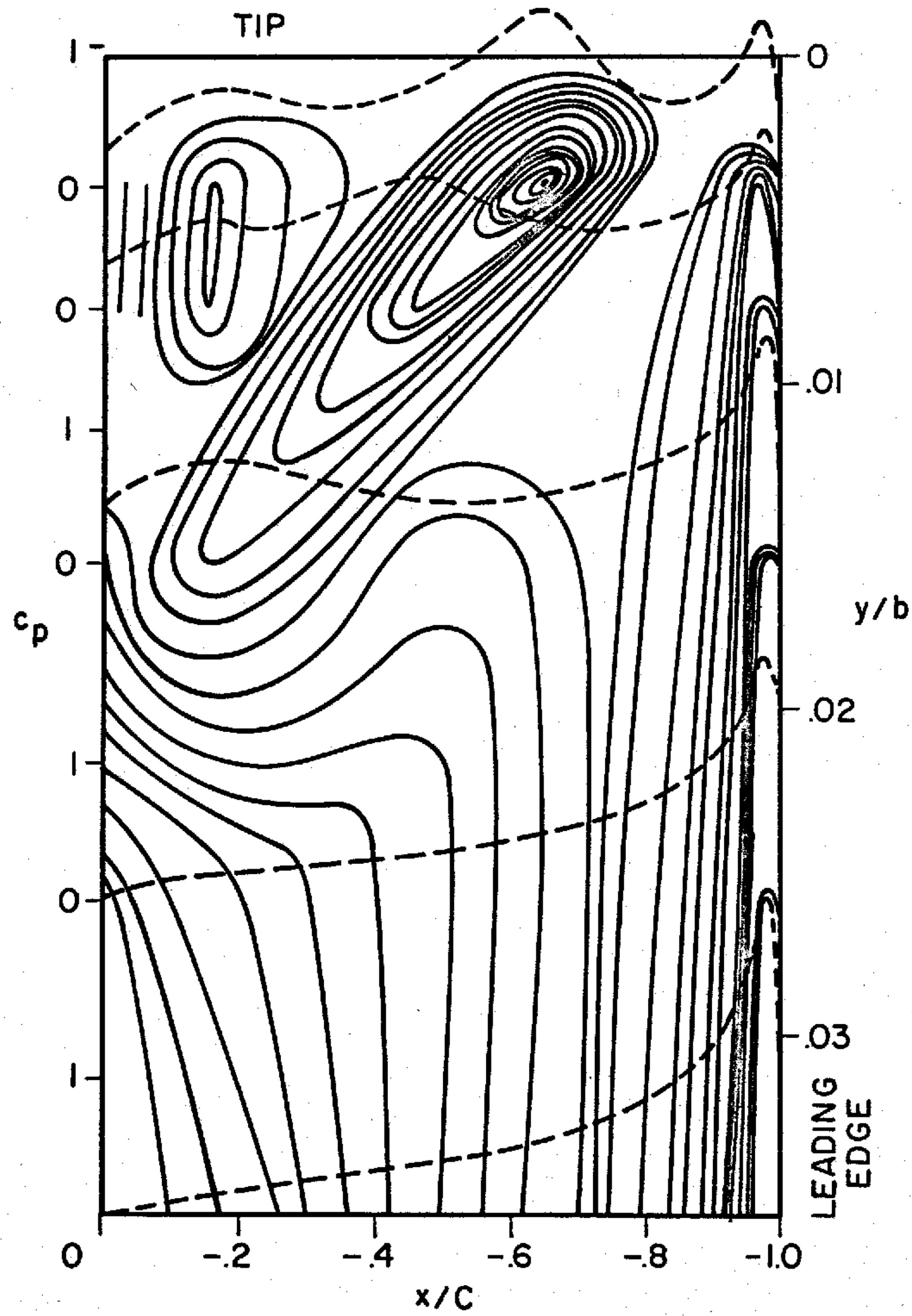

Figure 19. Isobars on top surface of wing (tip region), $\lambda = 0$, $\alpha = 12°$. (Figure 3 of Reference 4).

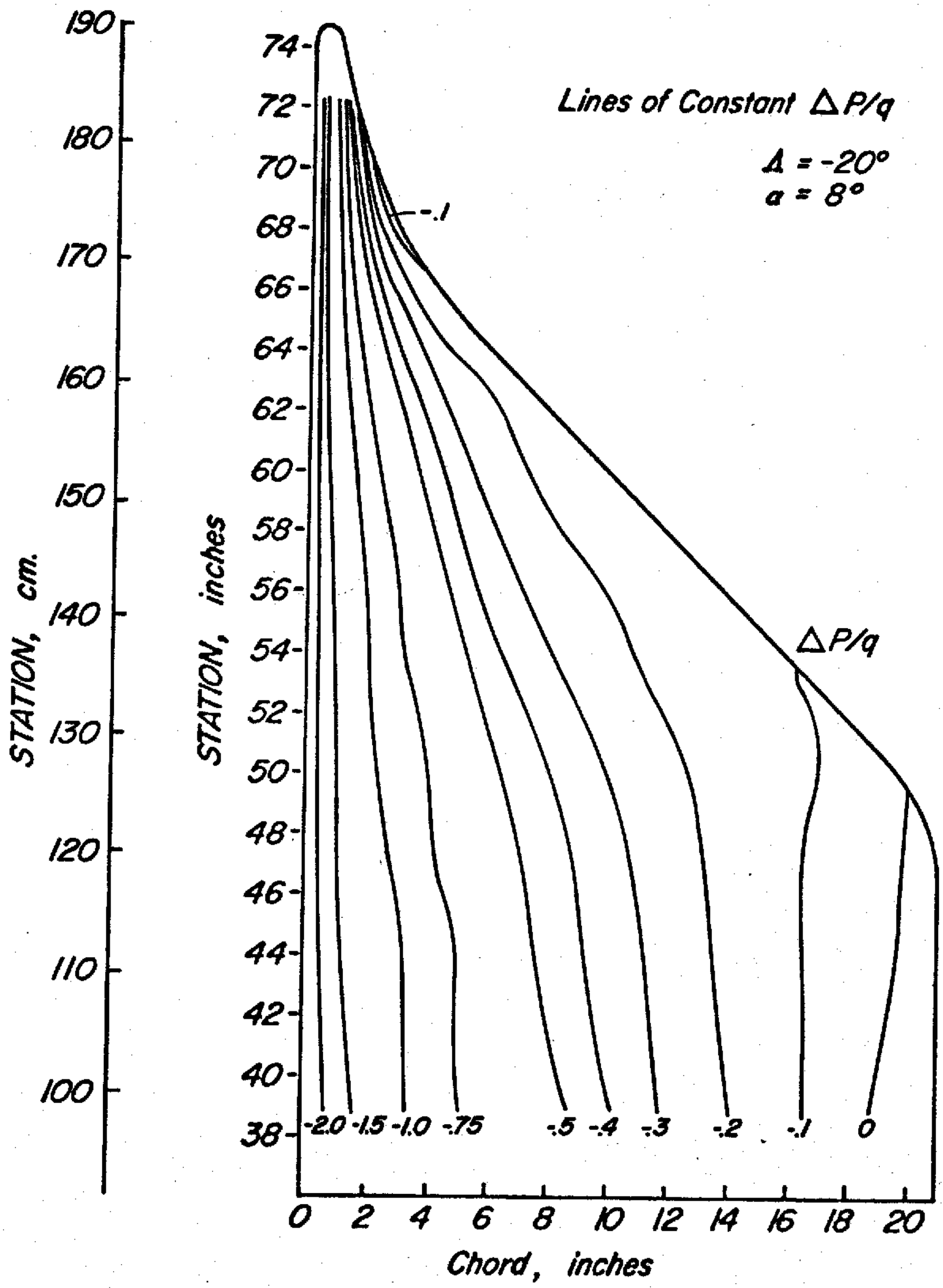

Figure 20. Contour pressure plot of the ogee-tip section at α=8° and Λ=-20°

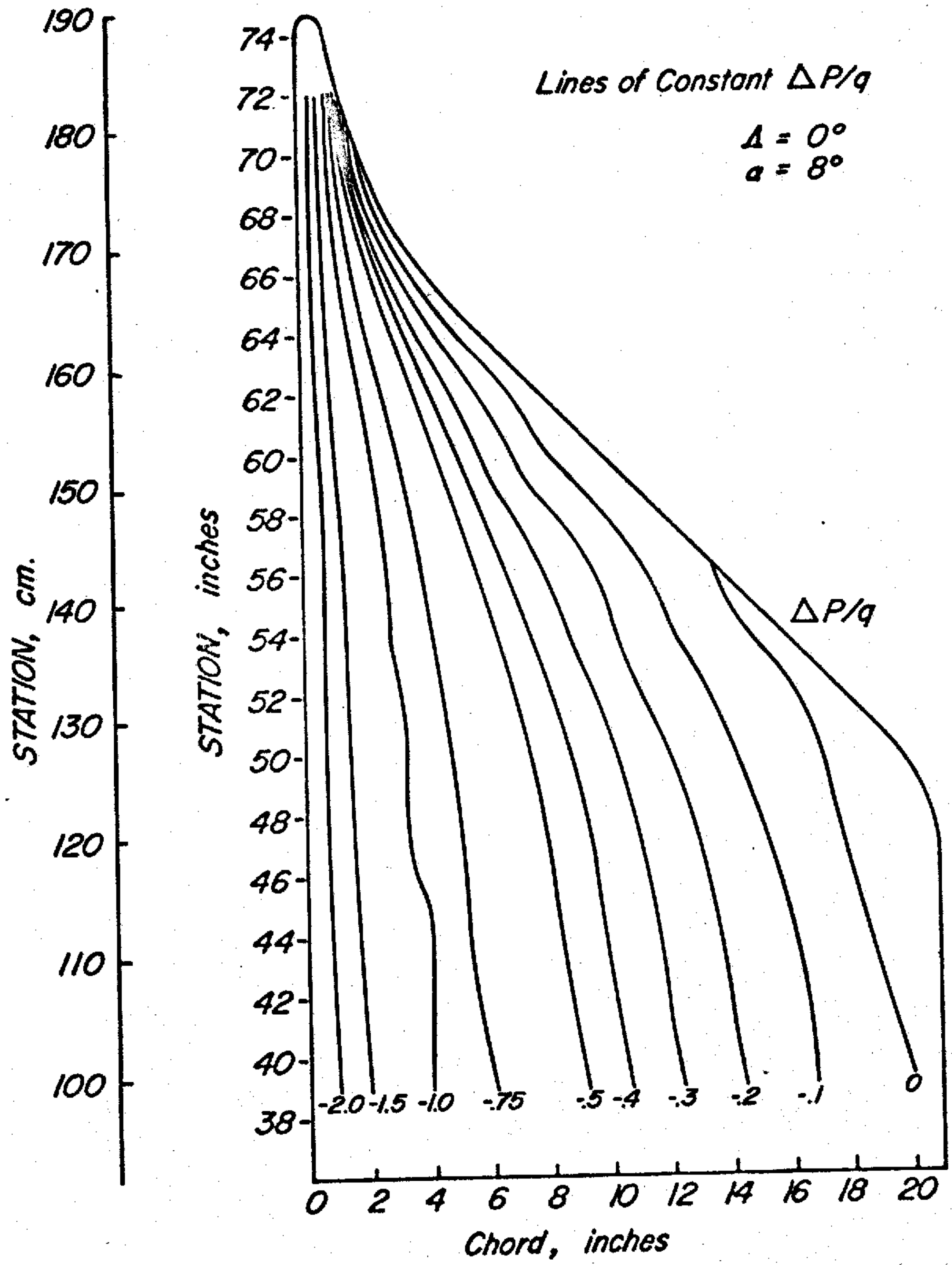

Figure 21. Contour pressure plot of the ogee-tip section at $\alpha=8°$ and $\Lambda=0°$

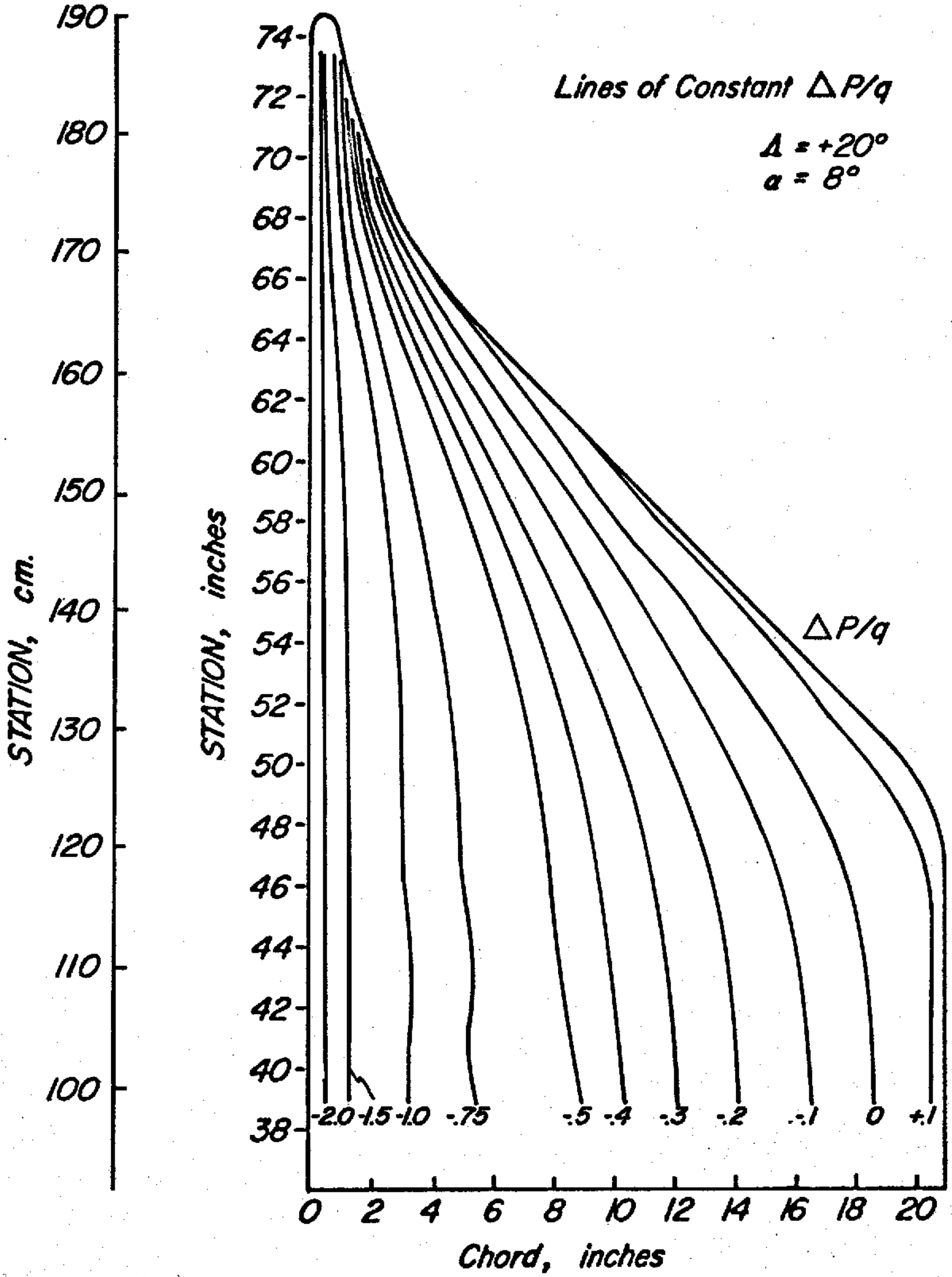

Figure 22. Contour pressure plot of the ogee-tip section at $\alpha=8°$ and $\Lambda=+20°$

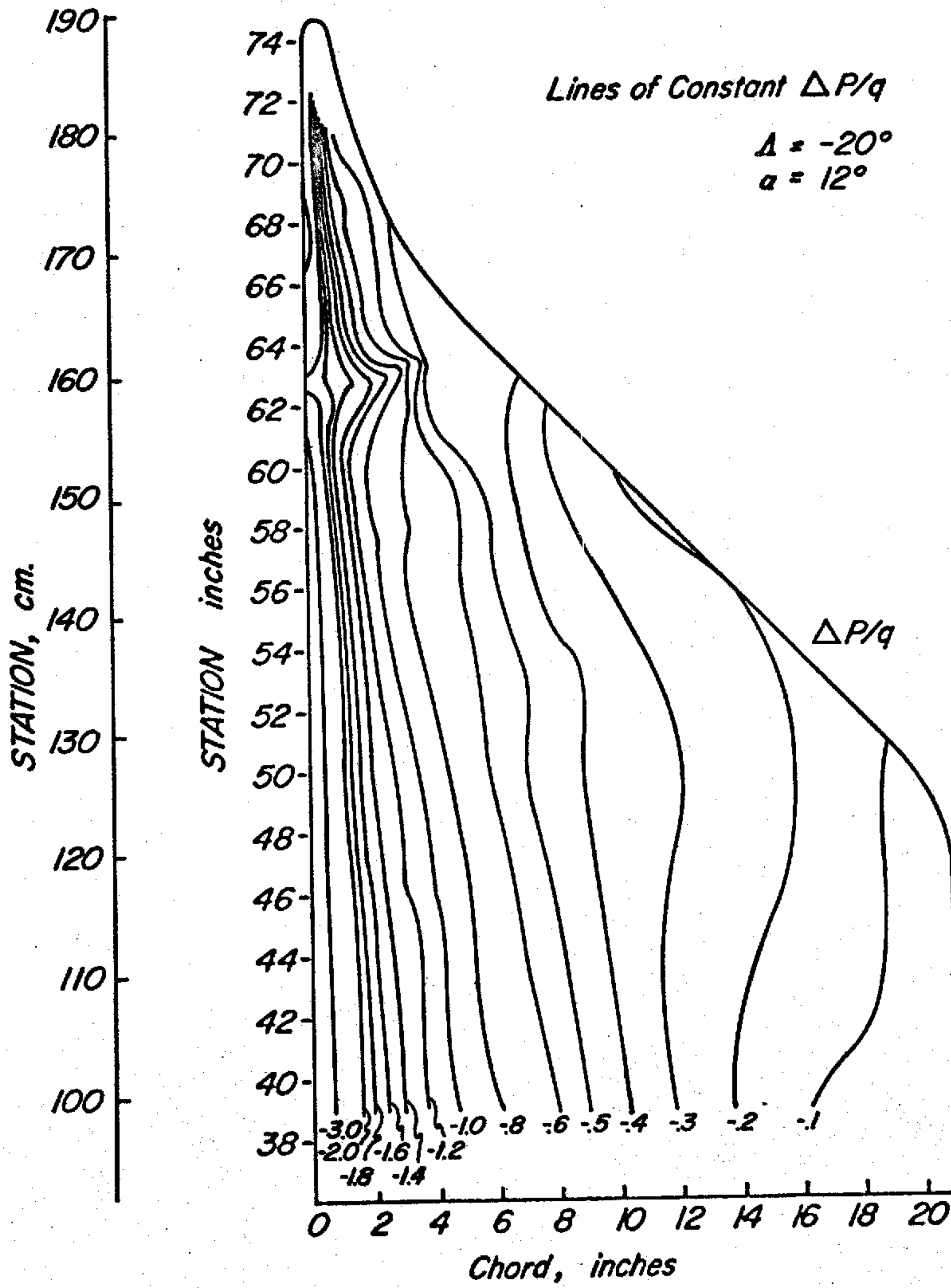

Figure 23. Contour pressure plot of the ogee-tip section at $\alpha=12°$ and $\Lambda=-20°$

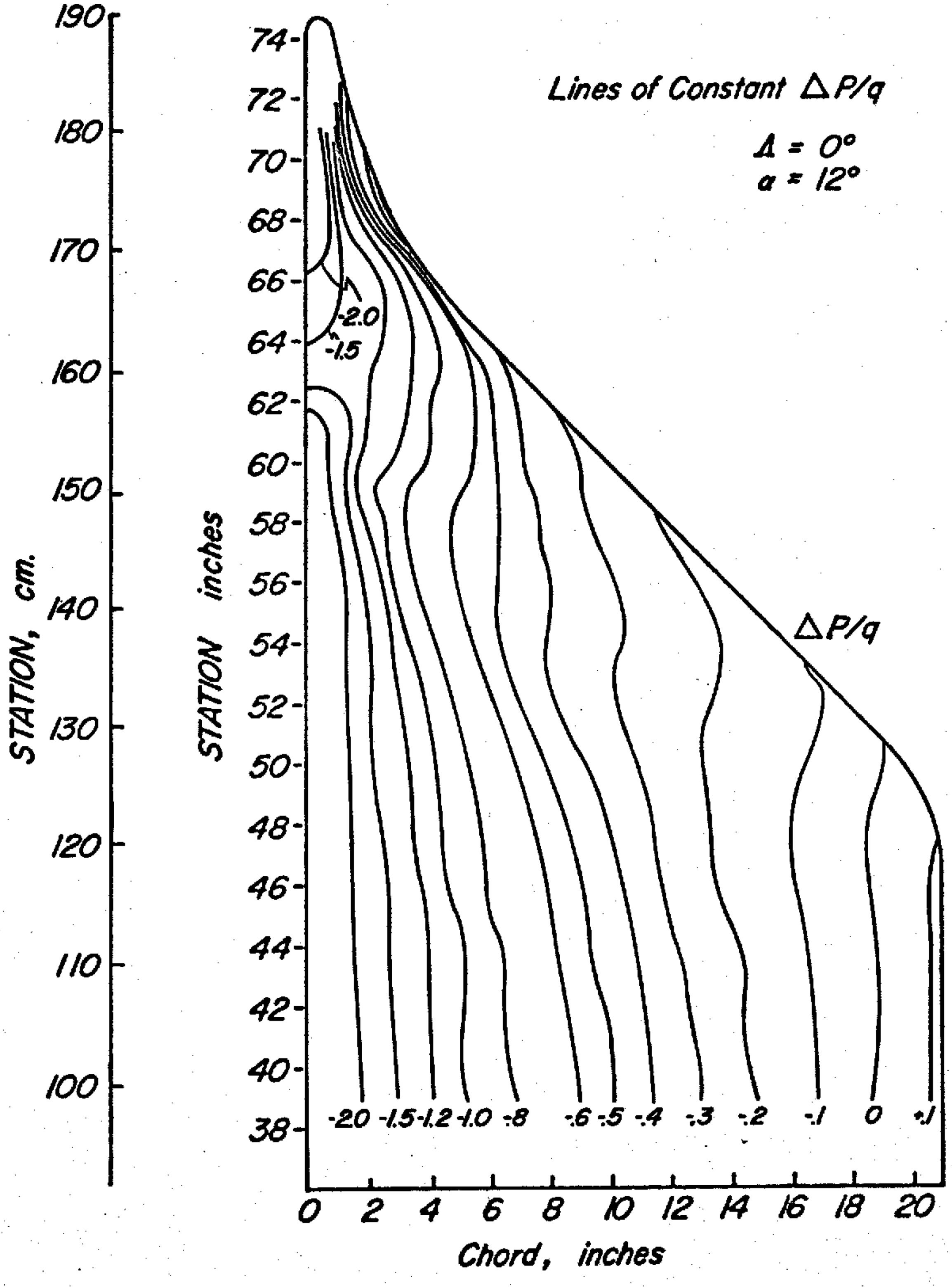

Figure 24. Contour pressure plot of the ogee-tip section at α=12° and Λ=0°

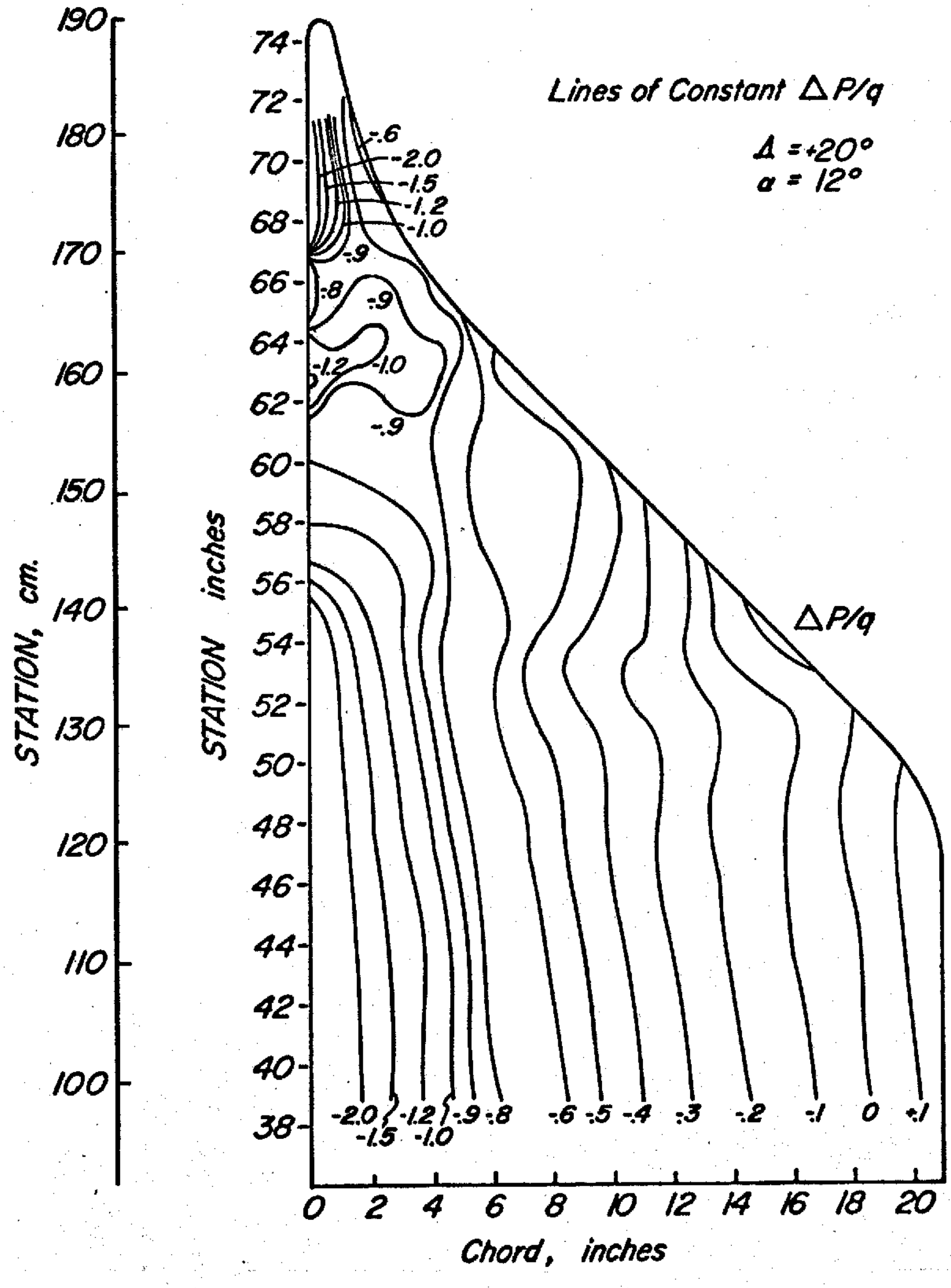

Figure 25. Contour pressure plot of the ogee-tip section at $\alpha=12°$ and $\Lambda=+20°$

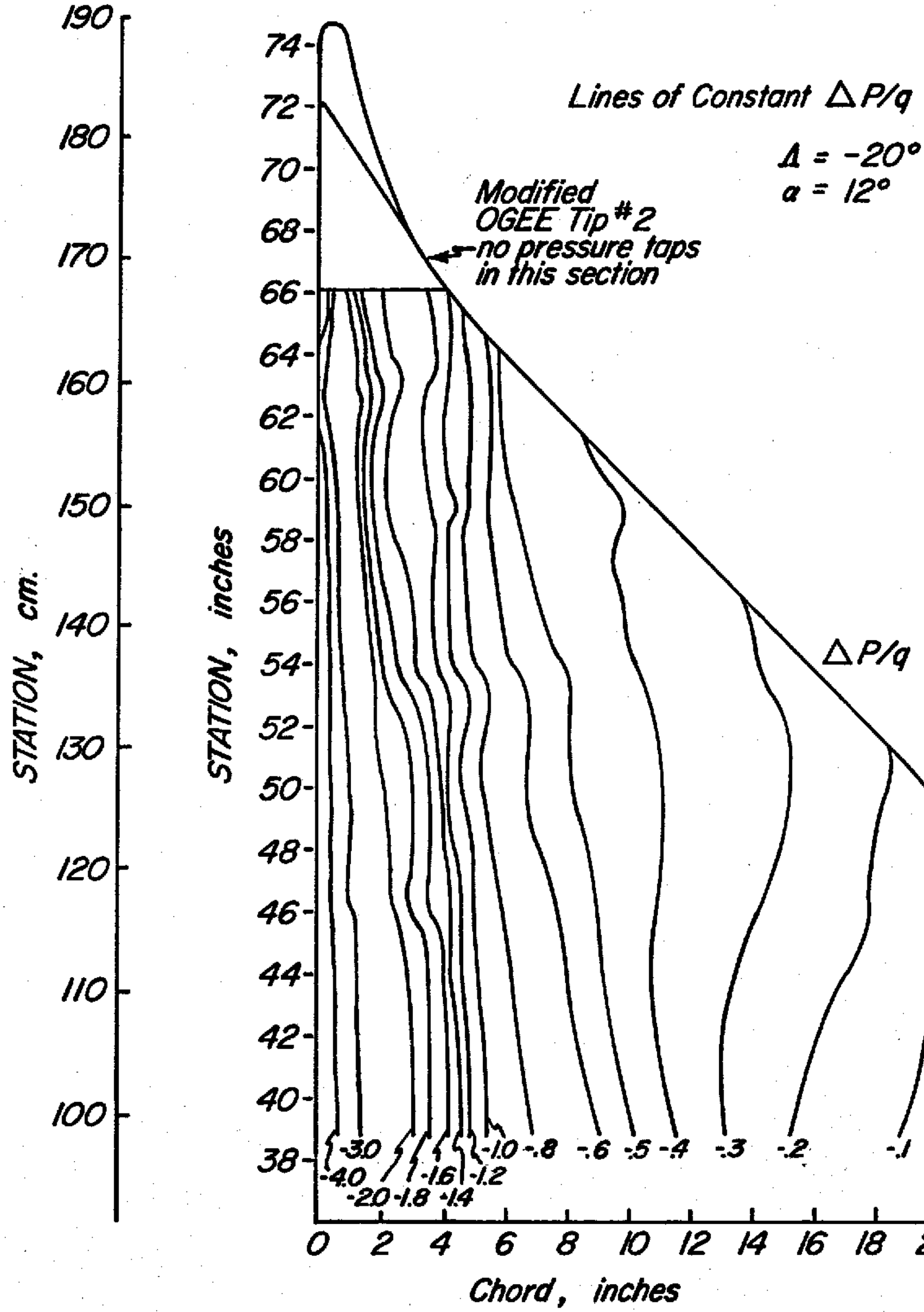

Figure 26. Contour pressure plot of the ogee-tip section with a modified tip at α=12° and Λ=-20°

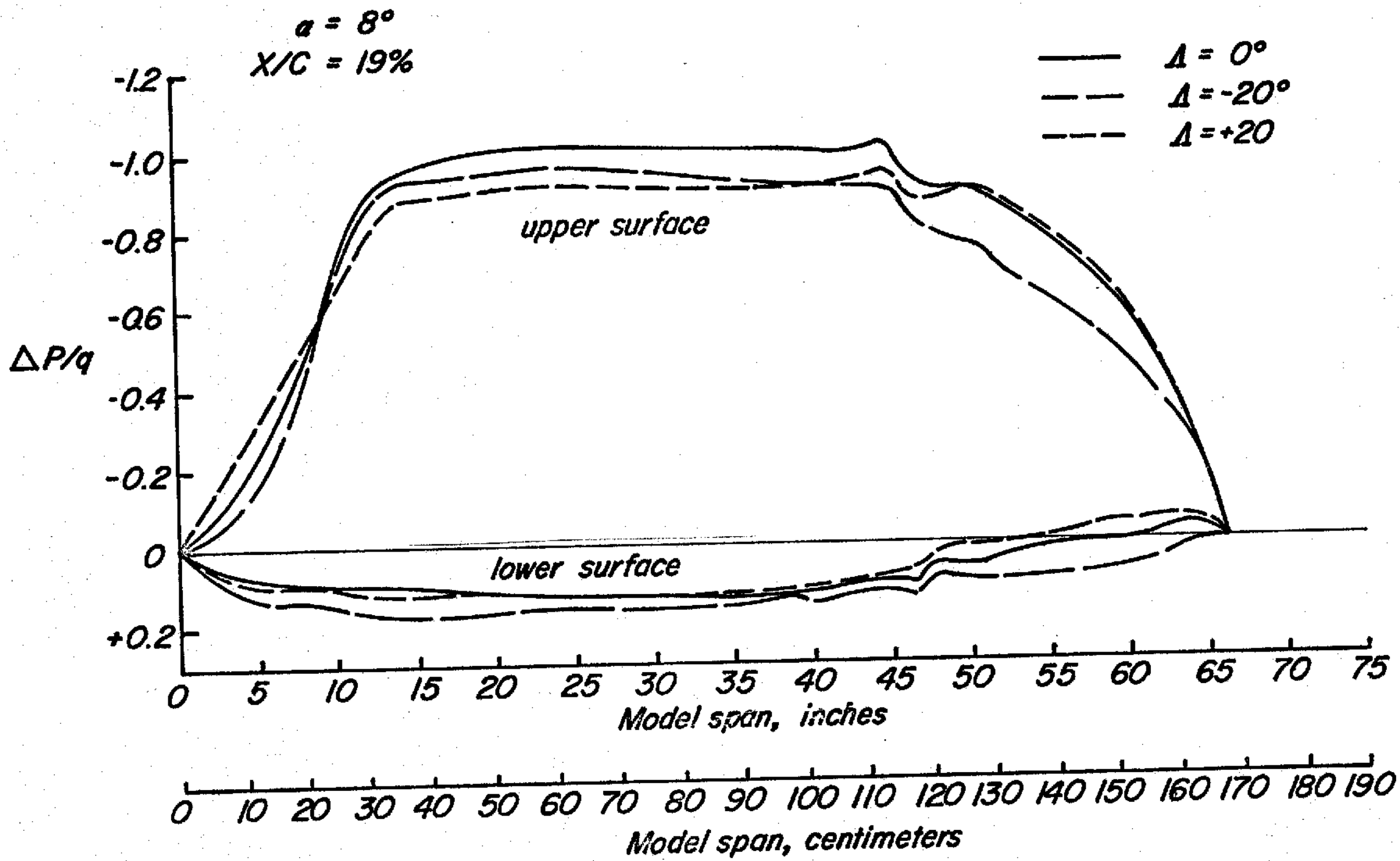

Figure 27. Spanwise pressure distributions of the ogee model at $\alpha=8°$ and $\Lambda=-20°$, 0°, and +20°

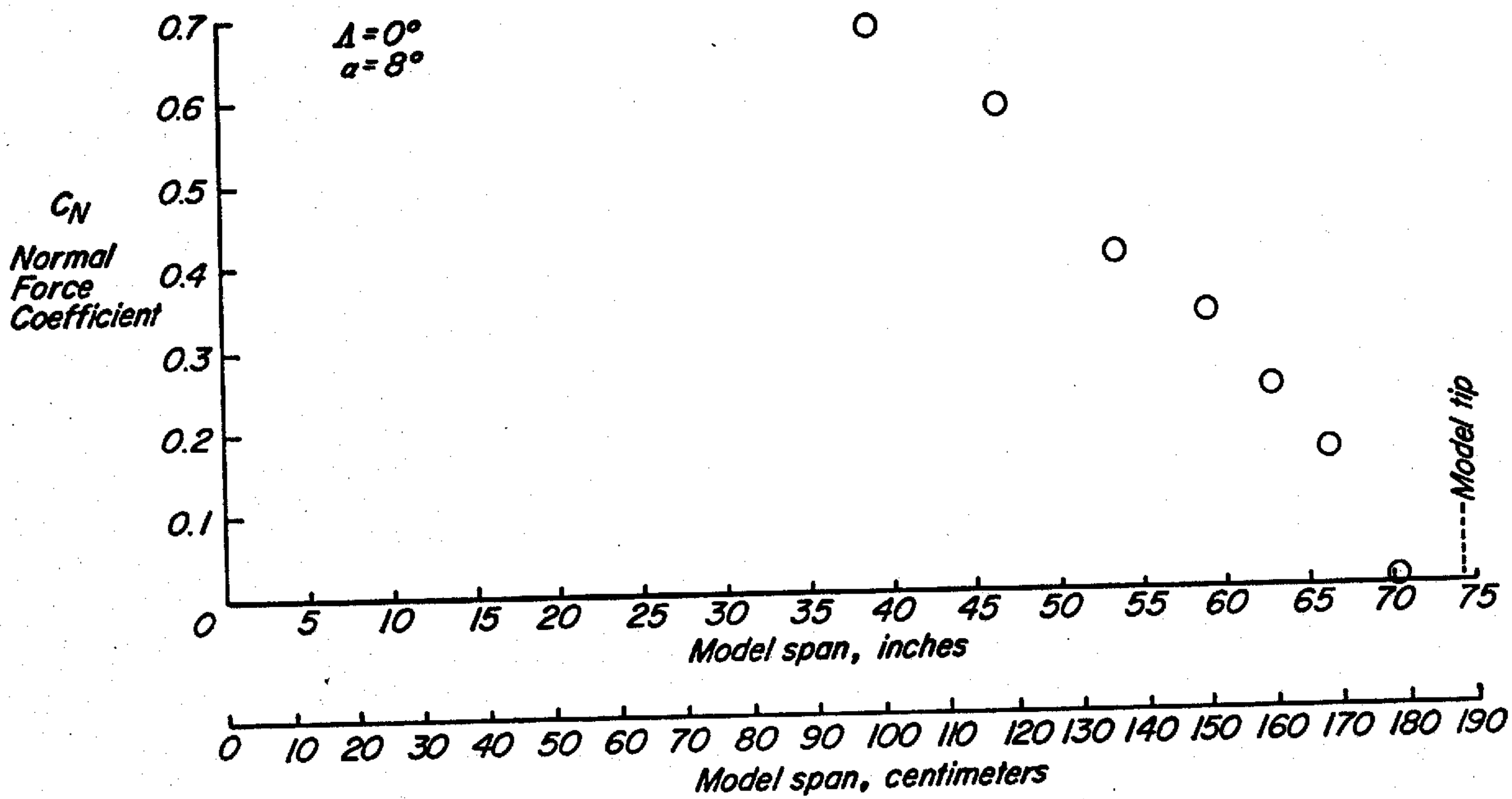

Figure 28. Spanwise loading distribution for the ogee-tip section at α=8° and Λ=0°

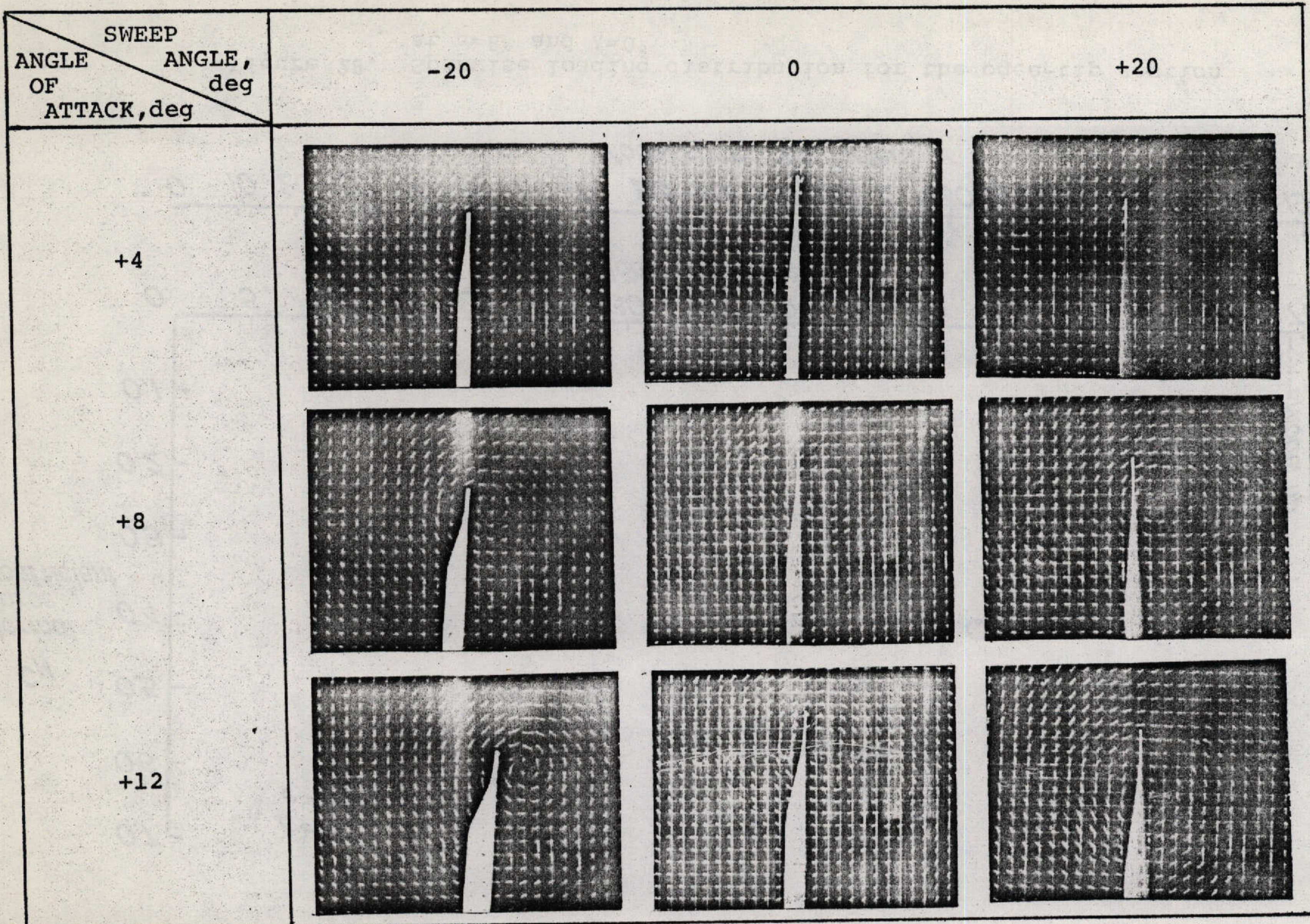

Figure 29. Tuft-grid visualization for the Ogee model with sweep and angle-of-attack variation

Model Configuration / Angle of Attack, deg	Conventional-Tip Model $\Lambda=-20°$	Ogee-Tip Model $\Lambda=-20°$
+4	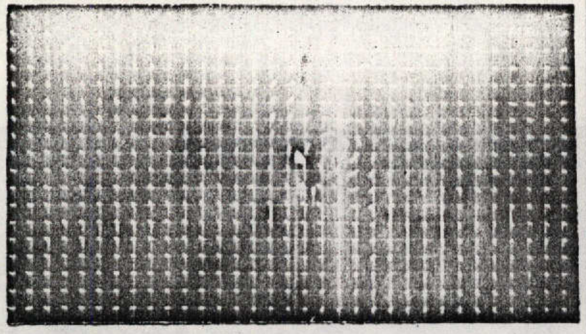	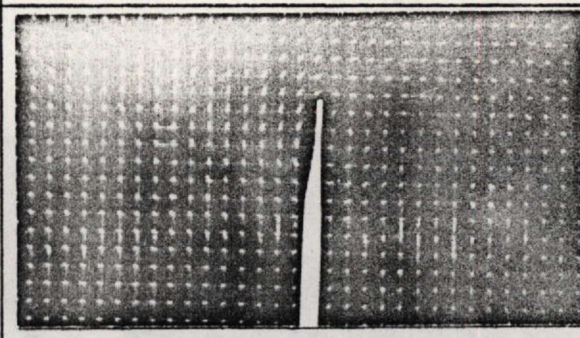
+8	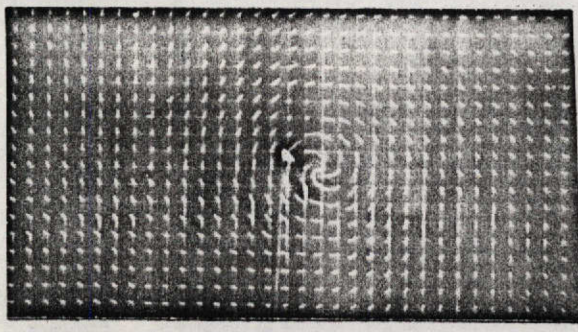	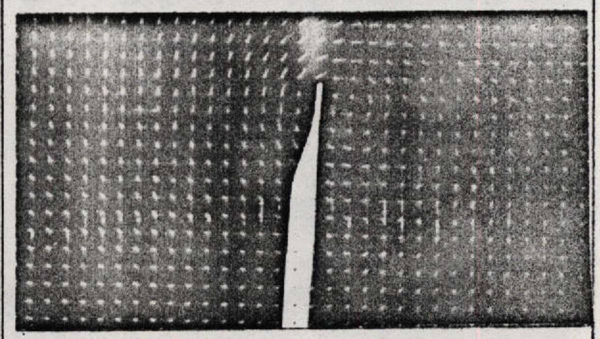
+12	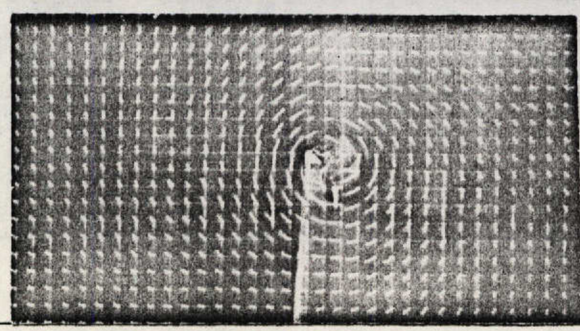	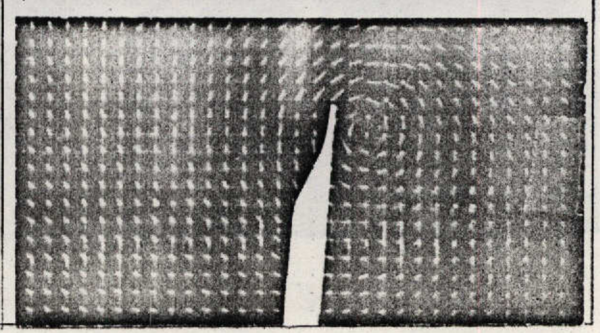

Figure 30. Tuft grid comparison of conventional and Ogee tip model at $\Lambda=-20°$

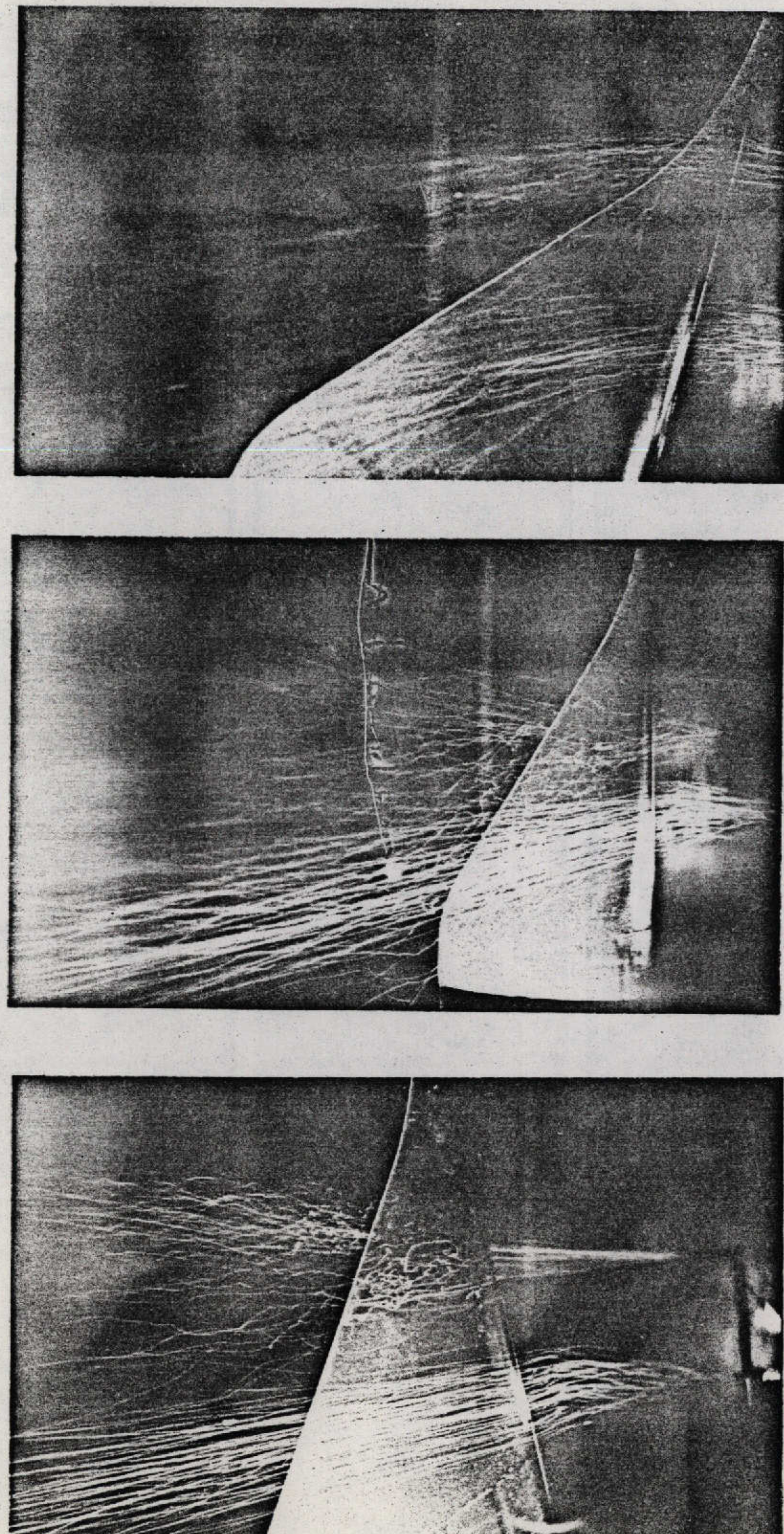

$\Lambda = -20°$
$\alpha = 8°$

$\Lambda = 0°$
$\alpha = 8°$

$\Lambda = +20°$
$\alpha = 8°$

Figure 31. Influence of sweep angle on the flow field of the ogee-tip at $\alpha=8°$

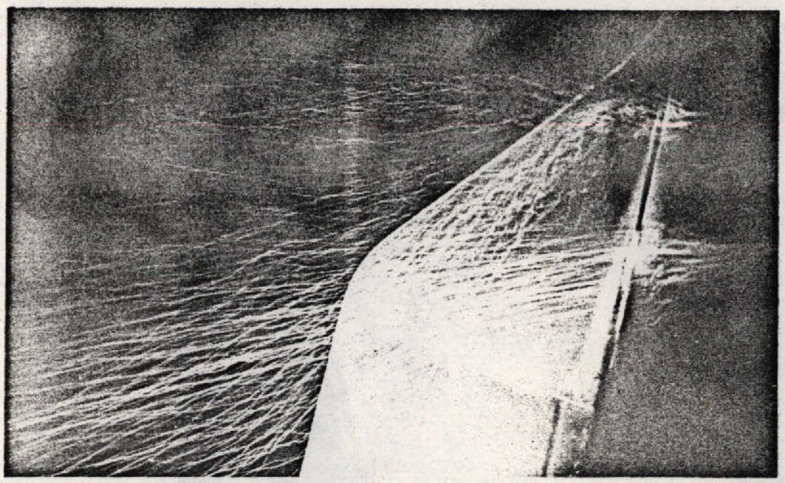

Λ = -20°
α = 10°

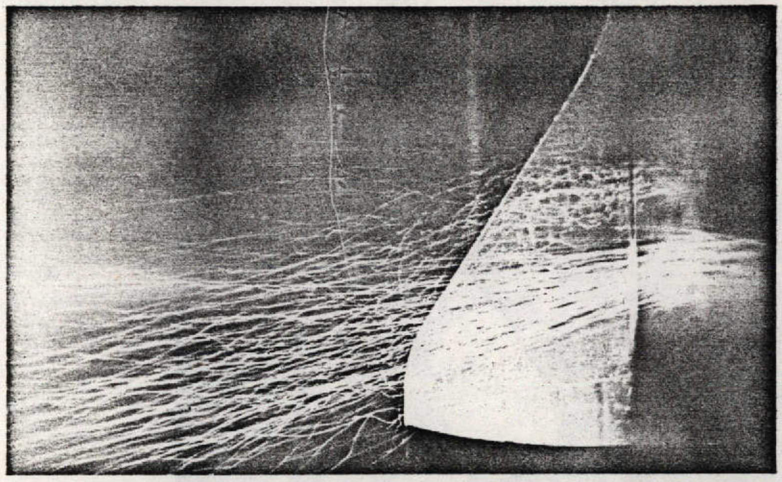

Λ = 0°
α = 10°

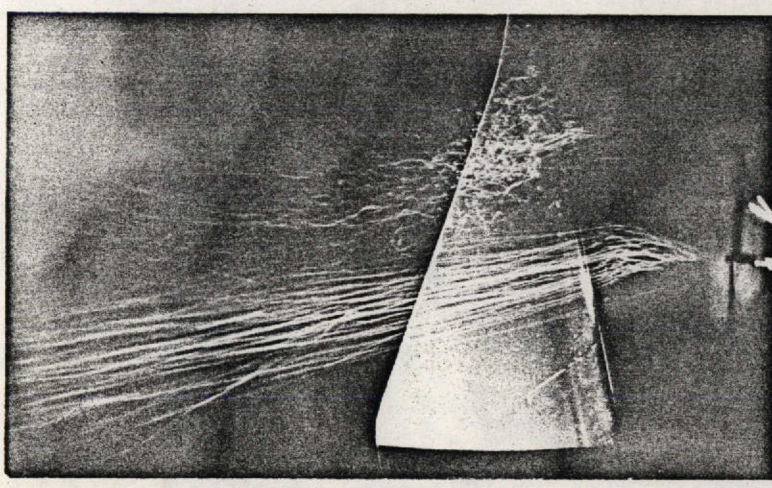

Λ = +20°
α = 10°

Figure 32. Influence of sweep angle on the flow field of the ogee-tip at $\alpha=10°$

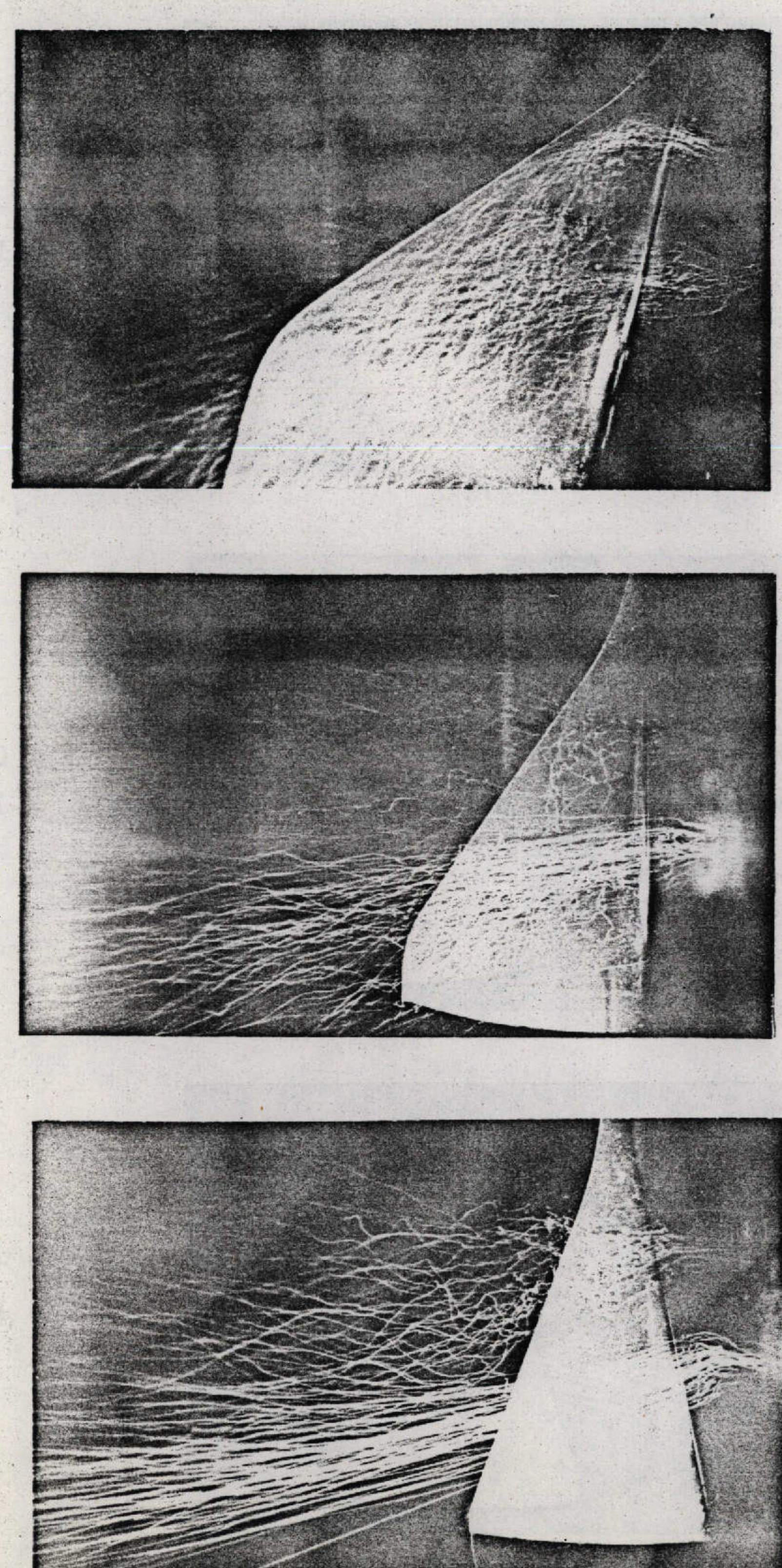

$\Lambda = -20°$

$\alpha = 12°$

$\Lambda = 0°$

$\alpha = 12°$

$\Lambda = +20°$

$\alpha = 12°$

Figure 33. Influence of sweep angle on the flow field of the ogee-tip at α=12°

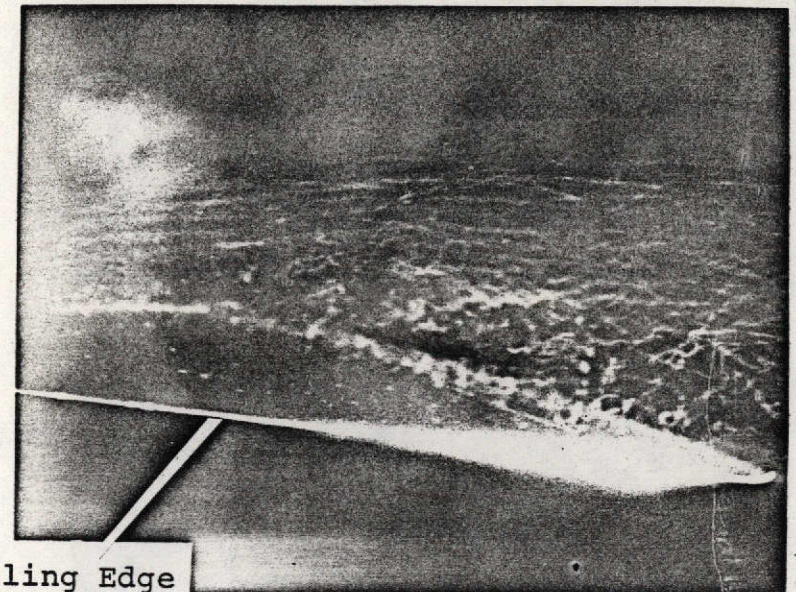

View looking forward
and inboard

Figure 34. Spanwise view of the flow field;
$\Lambda=0°$, $\alpha=10°$

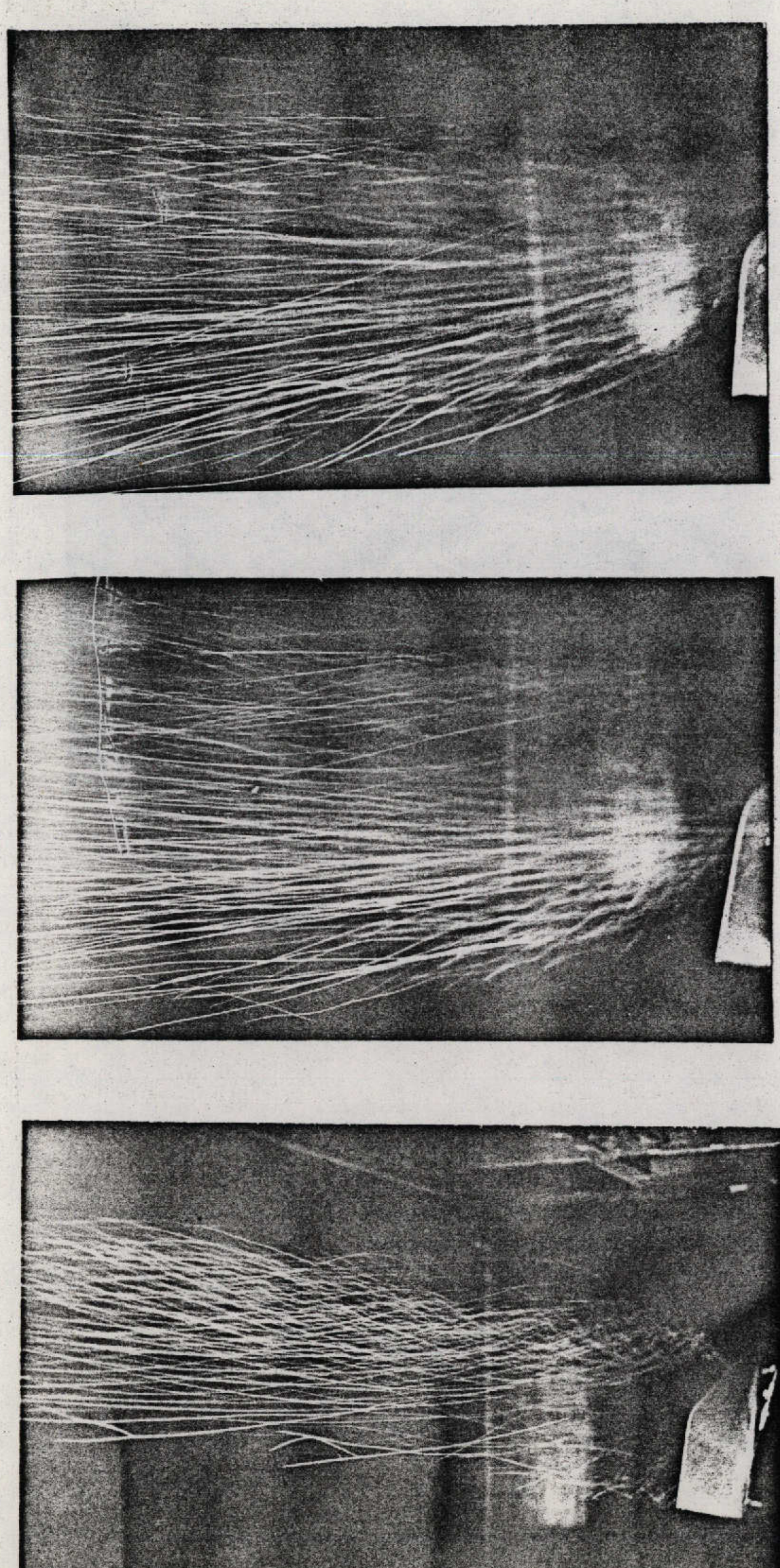

$\Lambda = -20°$
$\alpha = 8°$

$\Lambda = -20°$
$\alpha = 10°$

$\Lambda = -20°$
$\alpha = +12°$

Figure 35. Downstream flow-visualization of the ogee-tip at Λ=-20°

Model Configuration / Angle of Attack, degrees	Conventional-Tip Model $\Lambda=-15°$	Ogee-Tip Model $\Lambda=-15°$
+8	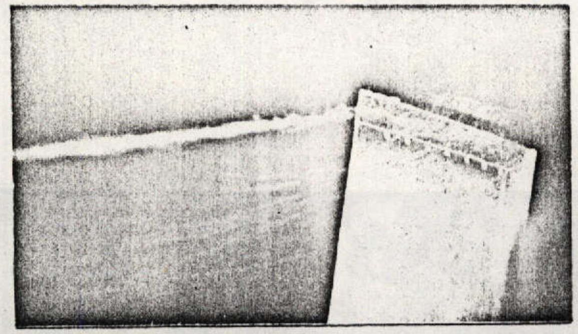	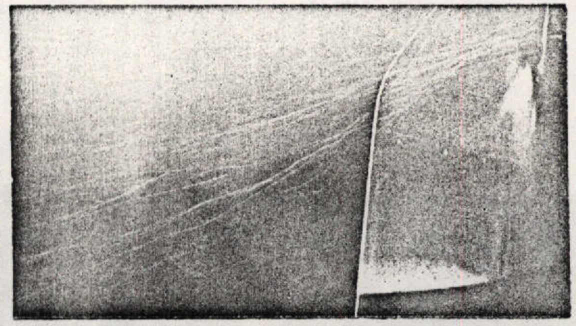
+10	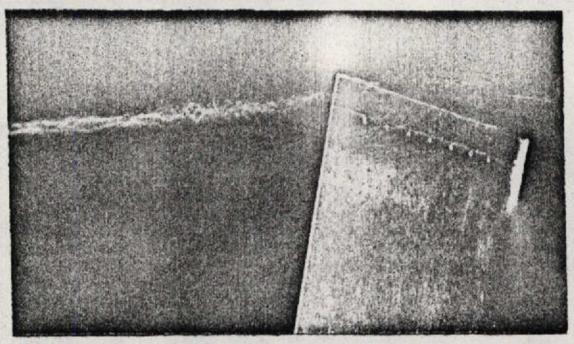	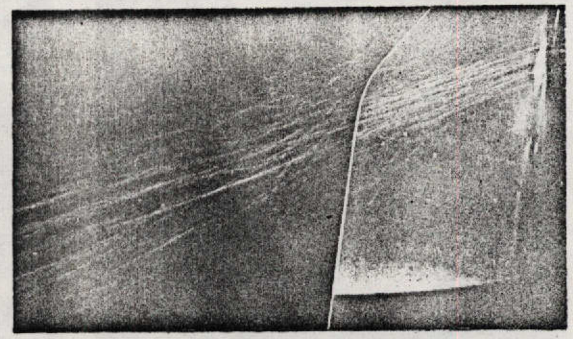
+12	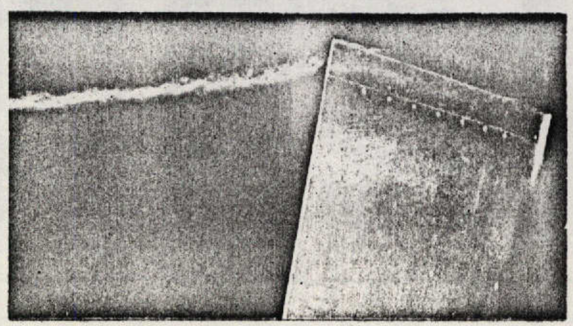	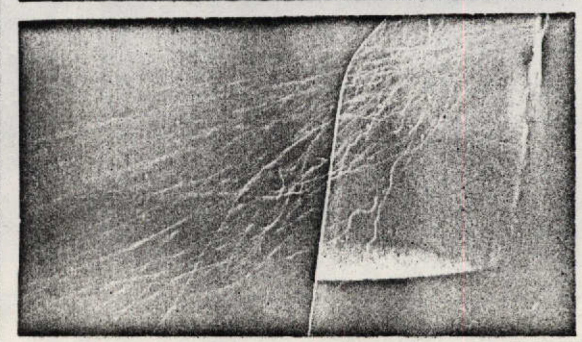

Figure 36. Flow field comparison of the conventional and Ogee-tip models at $\Lambda=-15°$

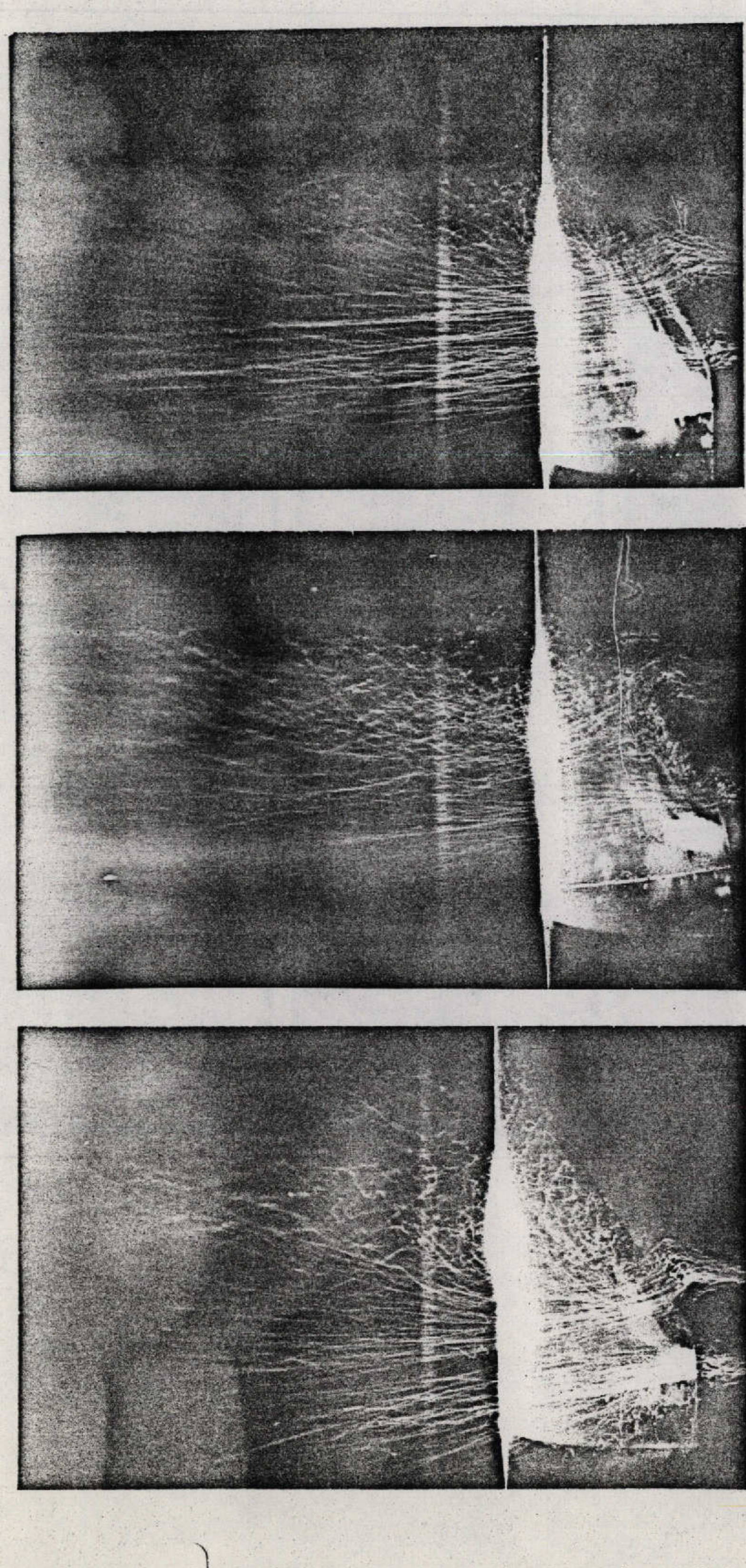

$\Lambda = 0°$
$\alpha = 8°$

$\Lambda = 0°$
$\alpha = 10°$

$\Lambda = 0°$
$\alpha = 12°$

Figure 37. Flow field visualization for the "reverse" ogee-tip configuration at $\Lambda=0°$

APPENDIX A

WIND AXES BALANCE DATA

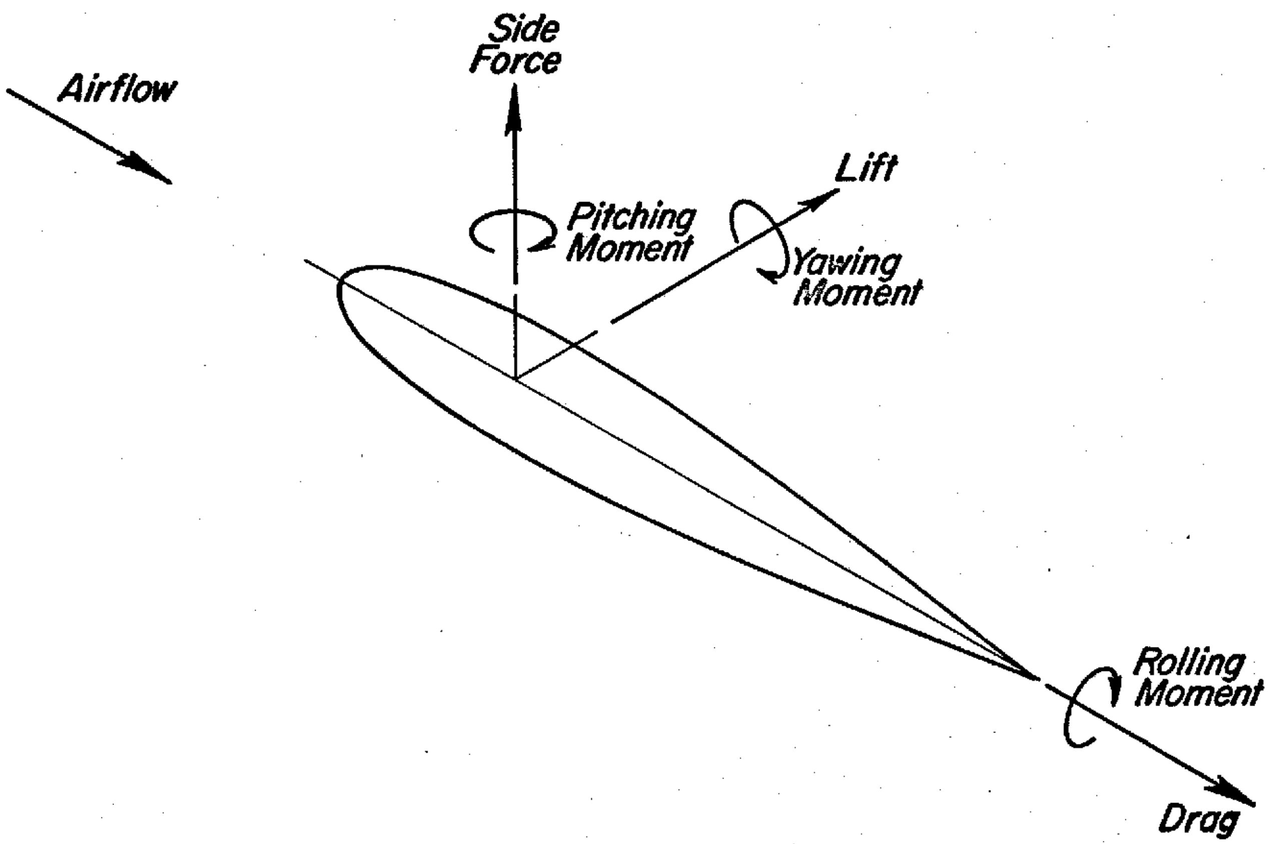

Wind-axes Coordinate System

UNIVERSITY OF MARYLAND

WIND TUNNEL OPERATIONS DEPT.

RUN NO TEST NO   WIND AXES   05/07/73

1 656   5 31 01 00 00 00 00

AA	AY	L	D	PM	YM	RM	SF	C CP	L/D	S CP	Q
-002.0	-000.0	-0034.1	003.24	-0002.5	-0005.5	-00078.9	-0001.4	-00.073	-10.524	00.230	038.53
-000.0	-000.0	0015.6	003.33	0000.6	-0008.5	00047.6	-0001.3	-00.038	04.684	00.305	038.53
002.0	-000.0	0068.3	004.21	0003.5	-0011.3	00181.8	-0002.0	-00.051	16.223	00.266	038.53
004.0	-000.0	0122.9	005.86	0007.8	-0016.0	00323.3	-0001.0	-00.063	20.972	00.263	038.53
006.0	-000.0	0173.7	008.59	0010.3	-0026.6	00441.0	0000.9	-00.059	20.221	00.254	038.53
008.0	-000.0	0218.3	012.66	0012.5	-0035.2	00562.2	0001.7	-00.057	17.243	00.257	038.53
010.0	-000.0	0258.0	017.93	0013.2	-0044.0	00680.1	0002.2	-00.051	14.389	00.263	038.53
012.0	-000.0	0296.7	025.98	0013.9	-0069.3	00781.6	0002.1	-00.047	11.420	00.263	038.53
014.0	-000.0	0320.8	039.75	0010.9	-0119.2	00843.2	0000.7	-00.033	08.070	00.263	038.53

UNIVERSITY OF MARYLAND
WIND TUNNEL OPERATIONS DEPT.

RUN NO TEST NO
2 656

WIND AXES 05/07/73
9 31 01 00 00 00 00

AA	AY	L	D	PM	YM	RM	SF	C CP	L/D	S CP	Q
-002.0	-000.0	-0034.0	004.05	0037.0	0000.2	-00078.7	-0000.8	01.085	-08.395	00.230	056.64
000.0	-000.0	0015.8	002.21	-0021.8	-0002.8	00034.2	-0001.5	01.379	07.149	00.216	032.48
002.0	-000.0	0068.1	003.62	-0084.6	-0005.0	00154.4	-0001.6	01.240	18.812	00.226	040.42
004.0	-000.0	0123.4	005.08	-0151.7	-0005.8	00283.7	-0003.4	01.229	24.291	00.229	043.25
006.0	-000.0	0174.0	007.17	-0212.7	-0007.1	00396.2	-0009.0	01.223	24.267	00.227	044.33
008.0	-000.0	0218.3	010.40	-0264.8	-0008.6	00500.1	-0014.0	01.216	20.990	00.228	044.50
010.0	-000.0	0258.4	016.28	-0305.9	-0020.0	00528.2	-0016.2	01.189	15.872	00.203	044.50
012.0	-000.0	0296.9	022.96	-0345.5	-0034.9	00654.6	-0020.3	01.170	12.931	00.219	044.50
014.0	-000.0	0321.5	032.32	-0369.5	-0059.1	00688.6	-0025.0	01.155	09.947	00.213	043.77

UNIVERSITY OF MARYLAND

WIND TUNNEL OPERATIONS DEPT.

RUN NO TEST NO WIND AXES 05/07/73

3 656 8 31 01 00 00 00 00

AA	AY	L	D	PM	YM	RM	SF	C CP	L/D	S CP	Q
-002.0	-000.0	-0033.8	003.85	0024.5	-0003.3	-00086.2	-0000.6	00.722	-08.779	00.254	047.20
000.0	-000.0	0015.6	002.75	-0015.0	-0005.4	00093.5	0000.6	00.961	05.672	00.599	031.75
002.0	-000.0	0068.4	003.81	-0057.4	-0008.2	00287.1	-0001.7	00.837	17.952	00.419	038.45
004.0	-000.0	0122.9	005.16	-0102.7	-0009.6	00487.4	0001.1	00.835	23.817	00.396	040.34
006.0	-000.0	0174.3	008.01	-0145.3	-0016.6	00434.0	-0004.6	00.834	21.760	00.248	041.88
008.0	-000.0	0217.8	010.60	-0180.4	-0019.7	00540.1	-0005.8	00.830	20.547	00.247	040.85
010.0	-000.0	0258.4	014.82	-0207.8	-0028.7	00629.0	-0007.7	00.808	17.435	00.242	039.94
012.0	-000.0	0297.8	021.45	-0237.4	-0046.4	00711.9	-0010.6	00.802	13.883	00.238	040.46
014.0	-000.0	0320.8	032.30	-0252.4	-0081.6	00746.3	-0012.5	00.791	09.931	00.233	039.91
-002.0	-000.0	-0033.7	003.75	0027.2	-0004.3	-00089.1	-0000.7	00.804	-08.986	00.263	047.20
000.0	-000.0	0016.0	002.35	-0014.5	-0005.3	00034.7	-0000.4	00.906	06.808	00.216	028.32
002.0	-000.0	0068.1	003.66	-0056.5	-0008.1	00162.5	0000.4	00.828	18.606	00.238	037.33
004.0	-000.0	0123.5	005.16	-0102.9	-0010.7	00302.1	-0001.3	00.833	23.934	00.244	040.12

UNIVERSITY OF MARYLAND
WIND TUNNEL OPERATIONS DEPT.

RUN NO TEST NO WIND AXES 05/07/73

5 656 7 31 01 00 00 00 00

AA	AY	L	D	PM	YM	RM	SF	C CP	L/D	S CP	Q
-002.0	-000.0	-0033.4	003.19	0011.3	-0006.0	-00078.5	-0001.4	00.337	-10.470	00.234	036.90
000.0	-000.0	0015.9	003.50	-0006.5	-0009.2	00046.2	-0001.5	00.408	04.542	00.290	043.34
002.0	-000.0	0068.0	003.81	-0026.4	-0011.4	00175.6	-0001.3	00.387	17.847	00.258	038.02
004.0	-000.0	0123.2	005.13	-0047.5	-0015.2	00315.6	-0001.5	00.385	24.015	00.256	038.36
006.0	-000.0	0174.4	006.98	-0066.1	-0019.9	00444.1	-0002.8	00.379	24.985	00.254	037.98
008.0	-000.0	0218.4	009.37	-0080.6	-0025.4	00554.0	-0003.8	00.370	23.308	00.253	037.16
010.0	-000.0	0257.7	013.05	-0094.3	-0035.3	00644.1	-0003.8	00.368	19.747	00.250	036.47
012.0	-000.0	0297.2	019.48	-0108.2	-0057.8	00737.3	-0007.0	00.367	15.256	00.248	036.30
014.0	-000.0	0321.2	029.77	-0119.6	-0094.4	00780.0	-0007.4	00.375	10.789	00.244	036.30

UNIVERSITY OF MARYLAND
WIND TUNNEL OPERATIONS DEPT.

RUN NO TEST NO
7 656

WIND AXES 05/07/73
6 31 01 00 00 00 00

AA	AY	L	D	PM	YM	RM	SF	C CP	L/D	S CP	Q
-002.0	-000.0	-0034.1	002.99	0003.8	-0004.4	-00081.2	0002.1	00.111	-11.404	00.237	035.40
000.0	-000.0	0015.4	003.51	-0002.4	-0008.7	00043.4	-0000.6	00.155	04.387	00.281	043.12
002.0	-000.0	0068.0	003.75	-0010.6	-0010.9	00174.9	-0001.0	00.155	18.133	00.257	037.76
004.0	-000.0	0123.1	005.09	-0019.8	-0015.3	00317.1	-0000.3	00.160	24.184	00.257	038.18
006.0	-000.0	0174.0	006.91	-0026.1	-0020.1	00445.7	-0001.4	00.150	25.180	00.256	037.46
008.0	-000.0	0218.0	009.59	-0032.6	-0027.6	00553.1	-0001.6	00.150	22.732	00.253	036.47
010.0	-000.0	0257.8	012.63	-0037.9	-0034.9	00650.6	0000.2	00.148	20.411	00.252	035.48
012.0	-000.0	0297.2	019.98	-0044.6	-0060.1	00745.0	-0000.4	00.151	14.874	00.251	035.61
014.0	-000.0	0321.0	032.08	-0053.2	-0101.5	00790.0	-0001.6	00.166	10.006	00.247	035.74

UNIVERSITY OF MARYLAND
WIND TUNNEL OPERATIONS DEPT.

RUN NO TEST NO
12 656

WIND AXES 05/07/73
4 31 01 00 00 00 00

AA	AY	L	D	PM	YM	RM	SF	C CP	L/D	S CP	Q
-002.0	-000.0	-0033.8	003.74	-0008.2	-0007.9	-00078.4	0000.3	-00.241	-09.037	00.231	040.97
000.0	-000.0	0015.9	002.98	0005.7	-0008.8	00045.1	-0002.0	-00.358	05.335	00.283	031.84
002.0	-000.0	0068.2	003.92	0021.1	-0012.4	00180.7	-0001.0	-00.308	17.397	00.265	035.14
004.0	-000.0	0123.2	005.87	0036.1	-0017.4	00318.0	-0000.9	-00.292	20.988	00.258	036.64
006.0	-000.0	0174.4	008.34	0050.6	-0023.3	00449.4	-0000.3	-00.290	20.911	00.257	036.64
008.0	-000.0	0218.3	013.13	0061.4	-0032.8	00567.4	0001.8	-00.281	16.626	00.259	037.12
010.0	-000.0	0258.5	018.10	0071.3	-0043.6	00670.8	0003.0	-00.276	14.281	00.259	036.69
012.0	-000.0	0297.5	027.49	0083.1	-0074.0	00777.1	0004.6	-00.280	10.822	00.261	037.33
014.0	-000.0	0321.1	041.14	0083.2	-0122.3	00844.1	0004.0	-00.258	07.805	00.263	037.03

UNIVERSITY OF MARYLAND

WIND TUNNEL OPERATIONS DEPT.

RUN NO TEST NO WIND AXES 05/07/73

13 656 3 31 01 00 00 00 00

AA	AY	L	D	PM	YM	RM	SF	C CP	L/D	S CP	Q
-002.0	-000.0	-0034.1	003.71	-0014.5	-0010.1	-00076.5	-0000.7	-00.423	-09.191	00.224	039.52
000.0	-000.0	0015.7	003.09	0010.4	-0011.3	00043.8	-0001.0	-00.662	05.080	00.278	033.08
002.0	-000.0	0068.4	003.95	0036.2	-0014.2	00174.2	0001.1	-00.528	17.316	00.254	034.97
004.0	-000.0	0122.8	005.84	0063.3	-0019.4	00311.6	0000.6	-00.515	21.027	00.254	036.34
006.0	-000.0	0174.5	008.88	0089.4	-0025.7	00442.4	0002.4	-00.512	19.650	00.253	037.07
008.0	-000.0	0218.3	013.45	0111.0	-0034.6	00557.0	0004.6	-00.509	16.230	00.255	037.07
010.0	-000.0	0258.3	018.42	0130.4	-0045.3	00662.9	0006.4	-00.506	14.022	00.256	036.64
012.0	-000.0	0297.3	026.01	0149.3	-0068.6	00769.5	0007.7	-00.504	11.430	00.258	036.64
014.0	-000.0	0321.2	037.67	0159.0	-0107.8	00833.1	0009.7	-00.495	08.526	00.260	035.98

UNIVERSITY OF MARYLAND
WIND TUNNEL OPERATIONS DEPT.

RUN NO TEST NO
14 656

WIND AXES 05/07/73
1 32 01 00 00 00 00

AA	AY	L	D	PM	YM	RM	SF	C CP	L/D	S CP	Q
-002.0	-000.0	-0034.0	003.38	-0026.3	-0011.2	-00072.5	-0001.2	-00.771	-10.059	00.213	038.40
000.0	-000.0	0015.5	003.47	0019.6	-0014.5	00043.9	-0001.2	-01.264	04.466	00.283	037.07
002.0	-000.0	0067.8	004.23	0065.2	-0016.7	00164.0	-0000.8	-00.960	16.028	00.242	037.63
004.0	-000.0	0122.6	006.79	0114.7	-0021.3	00294.6	0001.5	-00.934	18.055	00.240	039.21
006.0	-000.0	0173.9	010.53	0161.5	-0026.6	00423.9	0003.3	-00.928	16.514	00.243	039.65
008.0	-000.0	0217.8	014.99	0201.8	-0033.3	00536.0	0006.9	-00.926	14.529	00.245	038.06
010.0	-000.0	0257.6	020.11	0239.4	-0041.9	00639.4	0011.1	-00.931	12.809	00.247	037.68
012.0	-000.0	0297.8	027.76	0280.2	-0060.9	00748.9	0015.2	-00.943	10.727	00.250	037.89
014.0	-000.0	0320.6	067.73	0299.1	-0155.8	00857.8	0008.2	-00.913	04.733	00.265	042.00
013.0	-000.0	0312.1	043.74	0293.2	-0091.3	00782.8	0013.4	-00.934	07.135	00.249	040.24
013.0	-000.0	0327.4	040.09	0301.5	-0084.4	00834.2	0010.9	-00.919	08.166	00.253	040.24
013.0	-000.0	0320.8	042.69	0295.3	-0093.0	00806.9	0009.8	-00.916	07.514	00.250	040.24

UNIVERSITY OF MARYLAND

WIND TUNNEL OPERATIONS DEPT.

RUN NO TEST NO WIND AXES 05/07/73

18 656 1 32 01 00 00 00 00

AA	AY	L	D	PM	YM	RM	SF	C CP	L/D	S CP	Q
-002.0	-000.0	-0033.5	004.55	-0019.5	-0011.9	-00058.5	-0001.6	-00.580	-07.362	00.175	054.18
000.0	-000.0	0016.1	002.44	0016.9	-0007.6	00040.8	-0001.3	-01.049	06.598	00.253	028.06
002.0	-000.0	0068.7	004.43	0059.7	-0014.6	00155.7	-0001.7	-00.867	15.507	00.226	038.70
004.0	-000.0	0123.6	007.33	0104.1	-0022.3	00281.1	-0001.5	-00.840	16.862	00.227	041.88
006.0	-000.0	0174.5	011.83	0147.6	-0032.7	00399.1	-0000.8	-00.844	14.750	00.229	043.33
008.0	-000.0	0217.9	016.87	0181.8	-0043.3	00502.8	0000.5	-00.833	12.916	00.230	042.05
010.0	-000.0	0257.9	023.21	0213.6	-0059.1	00602.7	0002.2	-00.828	11.111	00.234	041.40
012.0	-000.0	0298.8	030.50	0249.7	-0076.4	00703.9	0004.4	-00.836	09.796	00.235	041.66
013.0	-000.0	0309.6	033.90	0259.9	-0084.4	00730.7	0005.4	-00.840	09.132	00.236	040.85
014.0	-000.0	0320.5	038.41	0266.9	-0057.6	00762.6	0003.9	-00.833	08.344	00.235	040.85
015.0	-000.0	0278.9	071.95	0226.2	-0180.3	00736.4	-0009.0	-00.785	03.876	00.263	040.85
016.0	-000.0	0278.2	079.46	0223.0	-0204.4	00714.0	-0011.8	-00.770	03.501	00.256	040.85
017.0	-000.0	0273.4	088.96	0218.9	-0238.6	00728.8	-0014.0	-00.761	03.073	00.266	040.85
018.0	-000.0	0272.6	095.47	0219.5	-0259.9	00735.4	-0016.5	-00.760	02.855	00.270	040.85

UNIVERSITY OF MARYLAND
WIND TUNNEL OPERATIONS DEPT.

RUN NO TEST NO
19 656

WIND AXES 05/07/73
2 32 01 00 00 00 00

AA	AY	L	D	PM	YM	RM	SF	C CP	L/D	S CP	Q
-002.0	-000.0	-0033.3	005.17	-0015.6	-0014.1	-00064.1	-0002.2	-00.467	-06.441	00.193	063.42
000.0	-000.0	0015.6	002.10	0011.9	-0007.5	00038.5	-0001.0	-00.762	07.428	00.246	023.42
002.0	-000.0	0067.9	004.45	0044.9	-0015.3	00156.5	-0001.8	-00.660	15.258	00.230	036.00
004.0	-000.0	0123.1	007.91	0078.3	-0024.0	00284.7	-0001.9	-00.635	15.562	00.231	040.72
006.0	-000.0	0173.3	012.40	0108.8	-0033.9	00401.3	-0001.7	-00.626	13.975	00.231	042.18
008.0	-000.0	0218.1	017.72	0136.0	-0045.9	00512.1	-0001.1	-00.622	12.308	00.235	042.48
010.0	-000.0	0257.4	023.85	0160.9	-0061.4	00611.5	-0000.1	-00.624	10.792	00.237	041.40
012.0	-000.0	0297.7	031.31	0187.8	-0080.0	00715.0	0001.0	-00.630	09.508	00.240	041.40
013.0	-000.0	0309.2	034.62	0194.4	-0088.4	00744.6	0001.6	-00.629	08.931	00.241	040.97
014.0	-000.0	0321.5	038.10	0202.6	-0097.0	00777.1	0001.9	-00.630	08.438	00.242	040.97
015.0	-000.0	0266.6	071.78	0150.2	-0181.8	00705.2	-0010.9	-00.544	03.714	00.263	040.97
016.0	-000.0	0262.5	077.53	0145.4	-0200.0	00681.7	-0012.3	-00.531	03.385	00.259	040.97
017.0	-000.0	0257.4	085.30	0144.5	-0228.3	00695.9	-0014.5	-00.533	03.017	00.270	040.97

UNIVERSITY OF MARYLAND
WIND TUNNEL OPERATIONS DEPT.

WIND AXES 05/07/73

RUN NO TEST NO
32 656

5 31 01 00 00 00 00

AA	AY	L	D	PM	YM	RM	SF	C CP	L/D	S CP	Q
182.0	-000.0	0046.9	006.65	0042.4	-0017.8	00121.5	-0001.0	00.900	07.052	00.259	038.53
180.0	-000.0	0007.5	005.88	0006.4	-0015.8	00017.0	-0001.2	00.853	01.275	00.226	038.53
178.0	-000.0	-0031.6	006.56	-0034.0	-0016.7	-00092.3	-0001.6	01.069	-04.817	00.291	038.53
176.0	-000.0	-0085.0	009.42	-0079.6	-0021.2	-00232.0	-0002.4	00.932	-09.023	00.272	038.53
174.0	-000.0	-0144.7	015.80	-0134.1	-0036.2	-00381.5	-0002.8	00.921	-09.158	00.263	038.53
172.0	-000.0	-0186.2	025.20	-0175.2	-0061.6	-00476.1	-0003.0	00.932	-07.388	00.255	038.53
170.0	-000.0	-0215.5	039.12	-0194.3	-0096.2	-00544.5	-0002.8	00.887	-05.508	00.252	038.53
168.0	-000.0	-0224.8	053.44	-0194.6	-0127.5	-00572.6	-0002.5	00.842	-04.206	00.253	038.53
180.0	-000.0	0000.3	-000.17	-0000.0	-0000.6	-00000.4	-0000.1	-00.000	-01.764	-00.133	038.53

UNIVERSITY OF MARYLAND
WIND TUNNEL OPERATIONS DEPT.

RUN NO TEST NO
33 656

WIND AXES 05/07/73
2 32 01 00 00 00 00

AA	AY	L	D	PM	YM	RM	SF	C CP	L/D	S CP	Q
-002.0	-000.0	-0033.6	003.37	-0021.8	-0009.6	-00076.5	-0000.6	-00.646	-09.970	00.227	035.65
000.0	-000.0	0015.7	003.33	0014.3	-0011.2	00044.9	-0001.4	-00.910	04.714	00.285	035.65
002.0	-000.0	0068.3	004.31	0052.1	-0015.2	00169.2	-0000.9	-00.761	15.846	00.247	037.11
004.0	-000.0	0123.2	006.84	0089.6	-0021.1	00308.2	-0000.0	-00.726	18.011	00.250	038.66
006.0	-000.0	0174.4	010.44	0127.8	-0026.1	00439.1	0002.3	-00.732	16.704	00.251	038.66
008.0	-000.0	0217.3	014.60	0160.6	-0033.7	00549.8	0004.8	-00.739	14.883	00.252	038.18
010.0	-000.0	0258.2	019.65	0190.2	-0044.9	00659.7	0008.0	-00.738	13.139	00.255	037.37
012.0	-000.0	0299.0	027.71	0222.8	-0067.3	00771.2	0011.4	-00.747	10.790	00.257	037.50
013.0	-000.0	0308.8	032.86	0229.7	-0084.0	00799.7	0011.4	-00.745	09.397	00.258	036.94
014.0	-000.0	0321.2	038.40	0237.0	-0101.6	00836.7	0013.6	-00.738	08.364	00.260	036.60
015.0	-000.0	0337.9	043.79	0248.6	-0118.1	00884.5	0014.7	-00.736	07.716	00.262	036.60
016.0	-000.0	0278.1	077.66	0194.8	-0203.0	00795.3	0001.7	-00.674	03.580	00.284	036.60

UNIVERSITY OF MARYLAND
WIND TUNNEL OPERATIONS DEPT.

RUN NO TEST NO WIND AXES 05/07/73
34 656 1 32 01 00 00 00 00

AA	AY	L	D	PM	YM	RM	SF	C CP	L/D	S CP	Q
-002.0	-000.0	-0033.6	003.69	-0024.7	-0010.2	-00069.1	-0001.0	-00.732	-09.105	00.205	041.62
000.0	-000.0	0015.8	002.93	0017.1	-0010.0	00043.0	-0001.4	-01.082	05.392	00.272	032.18
002.0	-000.0	0068.6	004.24	0064.4	-0014.4	00162.9	-0001.0	-00.937	16.179	00.237	036.94
004.0	-000.0	0123.1	006.75	0113.3	-0019.6	00291.5	0000.5	-00.918	18.237	00.236	038.87
006.0	-000.0	0174.9	010.49	0161.4	-0024.8	00420.4	0003.0	-00.922	16.673	00.240	039.99
008.0	-000.0	0218.6	015.13	0200.7	-0032.4	00530.2	0006.5	-00.918	14.448	00.242	039.64
010.0	-000.0	0259.2	020.73	0242.1	-0044.8	00638.7	0010.4	-00.935	12.503	00.245	038.61
012.0	-000.0	0297.8	028.24	0278.7	-0061.8	00740.1	0015.1	-00.938	10.545	00.247	038.18
013.0	-000.0	0310.7	034.93	0284.9	-0075.3	00779.1	0009.8	-00.917	08.894	00.249	038.18
014.0	-000.0	0290.0	060.40	0263.1	-0138.9	00743.4	0006.0	-00.889	04.801	00.255	038.18

UNIVERSITY OF MARYLAND

WIND TUNNEL OPERATIONS DEPT.

RUN NO TEST NO

035 666

WIND AXES 07/09/73

00 5 31 01 00 00 00 00

AA	AY	L	D	PM	YM	RM	SF	C CP	V	RN	Q
-002.0	-146.0	-0033.8	004.89	0008.8	-0009.9	-00080.2	-0000.0	-01.550	229.08	02.148	062.41
-000.0	-007.0	0016.2	002.81	0001.2	-0006.8	00031.9	-0000.0	-00.308	161.30	01.512	030.94
002.0	-000.0	0068.0	004.53	0004.5	-0011.2	00142.8	-0000.0	-00.066	182.20	01.708	039.48
004.0	-000.0	0123.2	007.22	0007.0	-0018.3	00267.0	-0000.0	-00.056	189.90	01.781	042.89
006.0	-000.0	0173.7	010.95	0008.1	-0027.6	00382.9	-0000.0	-00.046	192.71	01.807	044.16
008.0	-000.0	0217.9	017.55	0008.1	-0040.0	00491.6	-0000.0	-00.037	191.78	01.798	043.74
010.0	-000.0	0258.2	023.60	0006.9	-0053.7	00590.0	-0000.0	-00.026	191.78	01.798	043.74
012.0	-000.0	0296.6	030.76	0005.0	-0069.5	00692.1	-0000.0	-00.016	191.78	01.798	043.74
014.0	-000.0	0321.3	038.68	0006.5	-0088.9	00755.8	-0000.0	-00.020	188.01	01.763	042.04

UNIVERSITY OF MARYLAND
WIND TUNNEL OPERATIONS DEPT.

RUN NO TEST NO
36 666

WIND AXES 07/09/73
6 31 01 00 00 00 00

AA	AY	L	D	PM	YM	RM	SF	C CP	V	RN	Q
-002.0	-000.0	-0033.9	005.66	0003.7	-0008.3	-00064.9	-0000.0	00.108	256.13	02.402	078.01
-000.0	-000.0	0016.2	002.32	-0002.6	-0005.3	00032.1	-0000.0	00.160	152.12	01.427	027.52
002.0	-000.0	0067.6	003.98	-0008.5	-0008.9	00130.8	-0000.0	00.125	180.22	01.690	038.62
004.0	-000.0	0122.7	006.40	-0015.8	-0015.3	00260.7	-0000.0	00.128	188.01	01.763	042.04
006.0	-000.0	0172.9	009.39	-0022.0	-0022.7	00369.8	-0000.0	00.127	188.01	01.763	042.04
008.0	-000.0	0217.4	012.86	-0028.0	-0030.6	00468.4	-0000.0	00.129	186.09	01.745	041.18
010.0	-000.0	0259.1	017.46	-0036.8	-0042.7	00569.1	-0000.0	00.142	181.21	01.699	039.05
012.0	-000.0	0295.5	022.74	-0041.0	-0053.2	00649.6	-0000.0	00.139	181.21	01.699	039.05
014.0	-000.0	0320.4	027.38	-0044.4	-0063.8	00714.4	-0000.0	00.139	177.21	01.662	037.35

UNIVERSITY OF MARYLAND
WIND TUNNEL OPERATIONS DEPT.

RUN NO TEST NO — 37 666 — WIND AXES 07/09/73

7 31 01 00 00 00 00

AA	AY	L	D	PM	YM	RM	SF	C CP	V	RN	Q
-002.0	-000.0	-0034.2	006.08	0009.2	-0006.7	-00075.1	-0000.0	00.267	267.61	02.510	085.16
-000.0	-000.0	0016.4	001.84	-0004.8	-0002.7	00031.2	-0000.0	00.292	148.53	01.393	026.23
002.0	-000.0	0068.9	003.51	-0020.7	-0006.6	00138.0	-0000.0	00.300	180.21	01.690	038.62
004.0	-000.0	0123.5	005.93	-0036.3	-0012.6	00255.4	-0000.0	00.293	188.96	01.772	042.46
006.0	-000.0	0174.7	008.76	-0051.8	-0018.3	00365.1	-0000.0	00.296	190.84	01.790	043.31
008.0	-000.0	0217.8	012.25	-0066.4	-0024.5	00453.0	-0000.0	00.305	188.01	01.763	042.04
010.0	-000.0	0257.3	024.86	-0080.4	-0033.0	00552.2	-0000.0	00.312	186.09	01.745	041.18
012.0	-000.0	0297.6	043.44	-0080.5	-0055.1	00779.9	-0000.0	00.268	200.89	01.884	047.99
012.0	-000.0	0296.7	045.07	-0097.7	-0036.3	00687.0	-0000.0	00.326	189.90	01.781	042.89

UNIVERSITY OF MARYLAND
WIND TUNNEL OPERATIONS DEPT.

RUN NO TEST NO
38 666

WIND AXES 07/09/73
8 31 01 00 00 00 00

AA	AY	L	D	PM	YM	RM	SF	C CP	V	RN	Q
-002.0	-000.0	-0032.2	006.58	0019.3	-0002.6	-00065.8	-0000.0	00.595	272.18	02.552	088.10
-000.0	-000.0	0016.6	002.33	-0011.7	-0002.3	00027.7	-0000.0	00.704	154.46	01.448	028.37
002.0	-000.0	0068.7	004.27	-0046.7	-0004.9	00131.8	-0000.0	00.678	188.01	01.763	042.03
004.0	-000.0	0123.5	006.68	-0082.1	-0009.2	00245.4	-0000.0	00.663	196.38	01.841	045.87
006.0	-000.0	0174.4	009.62	-0120.8	-0012.8	00349.7	-0000.0	00.692	199.10	01.867	047.14
008.0	-000.0	0218.5	013.06	-0144.2	-0014.2	00446.4	-0000.0	00.661	197.29	01.850	046.29
010.0	-000.0	0258.5	034.25	-0213.1	-0020.0	00600.6	-0000.0	00.818	207.88	01.949	051.39
012.0	-000.0	0254.8	060.41	-0262.7	-0027.7	00702.5	-0000.0	01.003	207.88	01.949	051.39
014.0	-000.0	0232.7	088.04	-0316.3	-0040.3	00801.0	-0000.0	01.280	207.88	01.949	051.39

UNIVERSITY OF MARYLAND
WIND TUNNEL OPERATIONS DEPT.

RUN NO TEST NO
39 666

WIND AXES 07/09/73
9 31 01 00 00 00 00

AA	AY	L	D	PM	YM	RM	SF	C CP	V	RN	Q
-002.0	-000.0	-0030.5	006.47	0027.8	0003.4	-00060.5	-0000.0	00.905	274.12	02.570	089.36
-000.0	-000.0	0017.1	001.87	-0016.7	0000.9	00024.8	-0000.0	00.976	160.18	01.502	030.51
002.0	-000.0	0067.9	003.85	-0068.9	0000.0	00114.3	-0000.0	01.013	193.63	01.815	044.59
004.0	-000.0	0122.8	006.30	-0120.0	-0001.4	00219.7	-0000.0	00.976	205.28	01.925	050.12
006.0	-000.0	0173.6	009.04	-0174.8	-0000.8	00304.9	-0000.0	01.006	207.02	01.941	050.97
008.0	-000.0	0223.1	013.08	-0224.5	0002.5	00408.8	-0000.0	01.008	208.73	01.957	051.81
010.0	-000.0	0258.1	023.25	-0268.2	0006.9	00503.4	-0000.0	01.038	208.73	01.957	051.81
012.0	-000.0	0205.3	039.92	-0304.3	0008.4	00598.6	-0000.0	01.455	208.73	01.957	051.81
014.0	-000.0	0202.4	078.99	-0360.9	0004.4	00676.7	-0000.0	01.675	208.73	01.957	051.81

UNIVERSITY OF MARYLAND
WIND TUNNEL OPERATIONS DEPT.

RUN NO 40 TEST NO 666

WIND AXES 07/09/73

3 31 01 00 00 00 00

AA	AY	L	D	PM	YM	RM	SF	C CP	V	RN	Q
-002.0	-000.0	-0034.2	004.86	-0012.3	-0012.0	-00082.6	-0000.0	-00.358	222.78	02.089	059.02
-000.0	-000.0	0017.0	002.38	0008.0	-0007.5	00042.8	-0000.0	-00.470	153.30	01.437	027.95
002.0	-000.0	0067.9	004.15	0029.9	-0013.5	00153.8	-0000.0	-00.439	175.17	01.643	036.49
004.0	-000.0	0123.6	006.66	0052.1	-0020.2	00274.3	-0000.0	-00.420	184.15	01.726	040.33
006.0	-000.0	0173.9	011.39	0071.6	-0031.3	00400.9	-0000.0	-00.411	187.05	01.754	041.61
008.0	-000.0	0220.1	016.93	0091.0	-0044.8	00511.2	-0000.0	-00.413	188.01	01.763	042.04
010.0	-000.0	0257.5	022.89	0105.3	-0060.4	00605.0	-0000.0	-00.408	185.13	01.736	040.76
012.0	-000.0	0298.5	029.98	0123.2	-0077.1	00712.6	-0000.0	-00.413	184.15	01.726	040.33
014.0	-000.0	0321.2	037.07	0132.0	-0097.4	00774.5	-0000.0	-00.411	180.22	01.690	038.63

UNIVERSITY OF MARYLAND
WIND TUNNEL OPERATIONS DEPT.

RUN NO TEST NO
41 666

WIND AXES 07/09/73
4 31 01 00 00 00 00

AA	AY	L	D	PM	YM	RM	SF	C CP	V	RN	Q
-002.0	-000.0	-0033.3	006.38	-0005.8	-0013.1	-00072.1	-0000.0	-00.173	253.36	02.376	076.34
-000.0	-000.0	0016.7	002.29	0004.5	-0006.5	00033.1	-0000.0	-00.269	146.08	01.370	025.38
002.0	-000.0	0068.4	004.07	0016.2	-0011.8	00151.2	-0000.0	-00.236	174.15	01.633	036.07
004.0	-000.0	0122.5	006.63	0028.6	-0019.6	00271.2	-0000.0	-00.233	183.18	01.717	039.91
008.0	-000.0	0217.3	014.24	0048.7	-0040.0	00481.7	-0000.0	-00.224	184.15	01.726	040.33
010.0	-000.0	0257.6	022.61	0052.7	-0056.8	00597.4	-0000.0	-00.204	185.13	01.736	040.76
012.0	-000.0	0297.3	030.28	0059.6	-0075.1	00701.6	-0000.0	-00.200	185.13	01.736	040.76
014.0	-000.0	0321.4	038.61	0063.3	-0096.4	00771.4	-0000.0	-00.197	184.15	01.726	040.33

UNIVERSITY OF MARYLAND

WIND TUNNEL OPERATIONS DEPT.

RUN NO TEST NO WIND AXES 07/09/73

042 666 00 1 32 01 00 00 00 00

AA	AY	L	D	PM	YM	RM	SF	C CP	V	RN	Q
-002.0	-000.0	-0033.3	004.17	-0027.4	-0011.6	-00082.7	-0000.0	-00.820	212.97	01.997	053.94
-000.0	-000.0	0017.0	003.27	0015.5	-0010.7	00036.2	-0000.0	-00.911	171.03	01.604	034.79
002.0	-000.0	0069.3	004.72	0059.1	-0016.3	00153.5	-0000.0	-00.851	182.20	01.708	039.48
004.0	-000.0	0124.0	007.46	0100.8	-0024.2	00275.9	-0000.0	-00.811	184.15	01.726	040.33
006.0	-000.0	0175.3	011.55	0142.2	-0033.4	00394.6	-0000.0	-00.810	184.15	01.726	040.33
008.0	-000.0	0218.7	017.16	0179.8	-0046.0	00496.7	-0000.0	-00.821	184.15	01.726	040.33
010.0	-000.0	0258.8	023.03	0213.3	-0059.8	00595.4	-0000.0	-00.824	182.20	01.708	039.48
012.0	-000.0	0297.8	030.37	0248.2	-0076.5	00693.8	-0000.0	-00.834	182.20	01.708	039.48
014.0	-000.0	0300.5	058.06	0244.1	-0130.9	00738.1	-0000.0	-00.799	182.20	01.708	039.48
015.0	-000.0	0300.4	065.20	0243.9	-0152.1	00757.7	-0000.0	-00.794	182.20	01.708	039.48

APPENDIX B

PRESSURE DATA

NASA OGEE TIP
UNIVERSITY OF MARYLAND
WIND TUNNEL OPERATIONS DEPT.
RUN NO. TEST NO. 02/27/73
1 656

AA = -2.0 AY = 0.0 Q = 38.53 PSF V = 122.73 MPH

TUBE NO	PRESS COEFF	TUBE NO	PRESS COEFF	TUBE NO	PRESS COEFF	TUBE NO	PRESS COEFF	TUBE NO	PRESS COEFF
1	-.153	31	-.345	61	-.138	117	-.318	146	-.338
2	-.214	32	-.328	62	-.147	118	-.388	147	-.366
3	-.223	33	-.341	63	-.157	119	-.418	148	-.398
4	-.284	34	-.354	64	-.014	120	-.497	149	-.091
5	-.030	35	-.332	65	-.090	121	-.522	150	-.123
6	-.021	36	-.336	66	-.114	122	-.512	151	-.215
7	.056	37	-.336	67	.014	123	-.502	152	-.219
8	.052	38	-.328	68	-.047	124	-.497	153	-.265
9	.083	39	-.323	69	-.071	125	-.204	154	-.297
10	.056	40	-.315	70	-.080	126	-.194	155	-.302
11	.083	41	-.196	71	.057	127	-.219	156	-.316
12	.214	42	-.043	72	.023	128	-.328	157	-.338
13	.258	43	-.047	73	-.009	129	-.358	158	-.018
14	-.468	44	-.190	74	-.009	130	-.383	159	-.091
15	-.354	45	-.252	101	-.861	131	-.423	160	-.142
16	-.262	46	-.280	102	-.726	132	-.388	161	-.174
17	-.271	47	-.285	103	-.666	133	-.413	162	-.187
18	-.332	48	-.290	104	-.622	134	-.413	163	-.187
19	-.345	49	-.061	105	-.532	135	-.423	164	-.009
20	-.385	50	-.095	106	-.418	136	-.418	165	-.100
21	-.376	51	-.180	107	-.398	137	-.457	166	-.128
22	-.332	52	-.185	108	-.303	138	-.467	167	.013
23	-.319	53	-.233	109	-.223	139	-.472	168	-.059
24	-.310	54	-.247	110	-.214	140	-.482	169	-.082
25	-.328	55	-.247	111	-.233	141	-.492	170	-.082
26	-.179	56	-.257	112	-.064	142	-.487	171	.050
27	-.201	57	-.271	113	-.174	143	-.036	172	.018
28	-.293	58	-.009	114	-.662	144	-.215	173	0.000
29	-.301	59	-.076	115	-.557	145	-.297	174	-.022
30	-.332	60	-.109	116	-.214				

NASA OGEE TIP
UNIVERSITY OF MARYLAND
WIND TUNNEL OPERATIONS DEPT.
RUN NO. TEST NO. 02/27/73
1 656

AA = 2.0 AY = 0.0 Q = 38.53 PSF V = 122.73 MPH

TUBE NO	PRESS COEFF	TUBE NO	PRESS COEFF	TUBE NO	PRESS COEFF	TUBE NO	PRESS COEFF	TUBE NO	PRESS COEFF
1	-.957	31	-.562	61	-.180	117	-.191	146	-.209
2	-1.110	32	-.562	62	-.204	118	-.216	147	-.223
3	-1.079	33	-.584	63	-.223	119	-.206	148	-.227
4	-1.209	34	-.598	64	-.014	120	-.261	149	-.069
5	-.899	35	-.593	65	-.118	121	-.266	150	-.092
6	-.899	36	-.598	66	-.147	122	-.211	151	-.153
7	-.827	37	-.611	67	.014	123	-.171	152	-.157
8	-.813	38	-.620	68	-.066	124	-.165	153	-.176
9	-.831	39	-.607	69	-.099	125	-.050	154	-.195
10	-.867	40	-.593	70	-.104	126	-.125	155	-.199
11	-.863	41	-.400	71	.066	127	-.145	156	-.199
12	-.575	42	-.116	72	.019	128	-.191	157	-.199
13	-.696	43	-.061	73	-.009	129	-.206	158	-.027
14	-.768	44	-.247	74	-.023	130	-.216	159	-.069
15	-.719	45	-.352	101	-.206	131	-.226	160	-.097
16	-.269	46	-.395	102	-.065	132	-.201	161	-.116
17	-.422	47	-.409	103	.035	133	-.196	162	-.125
18	-.535	48	-.437	104	.115	134	-.201	163	-.116
19	-.566	49	-.085	105	.150	135	-.196	164	-.018
20	-.669	50	-.123	106	.296	136	-.196	165	-.069
21	-.674	51	-.247	107	.326	137	-.216	166	-.088
22	-.674	52	-.257	108	.417	138	-.226	167	.004
23	-.692	53	-.337	109	.457	139	-.231	168	-.041
24	-.683	54	-.356	110	.472	140	-.231	169	-.051
25	-.719	55	-.361	111	.497	141	-.231	170	-.046
26	-.265	56	-.376	112	.593	142	-.226	171	.037
27	-.292	57	-.423	113	.558	143	-.027	172	.027
28	-.436	58	-.009	114	-.452	144	-.153	173	.009
29	-.467	59	-.095	115	-.221	145	-.195	174	-.013
30	-.526	60	-.142	116	-.150				

NASA OGEE TIP
UNIVERSITY OF MARYLAND
WIND TUNNEL OPERATIONS DEPT.
RUN NO. TEST NO. 02/27/73
1 656

AA = 4.0 AY = 0.0 Q = 38.53 PSF V = 122.73 MPH

TUBE NO	PRESS COEFF	TUBE NO	PRESS COEFF	TUBE NO	PRESS COEFF	TUBE NO	PRESS COEFF	TUBE NO	PRESS COEFF
1	-1.408	31	-.675	61	-.217	117	-.119	146	-.132
2	-1.571	32	-.666	62	-.241	118	-.119	147	-.142
3	-1.646	33	-.684	63	-.260	119	-.099	148	-.132
4	-1.752	34	-.772	64	-.018	120	-.119	149	-.059
5	-1.545	35	-.728	65	-.132	121	-.099	150	-.073
6	-1.518	36	-.724	66	-.170	122	-.034	151	-.109
7	-1.408	37	-.754	67	.014	123	-.009	152	-.114
8	-1.439	38	-.768	68	-.080	124	.009	153	-.123
9	-1.368	39	-.754	69	-.113	125	.014	154	-.132
10	-1.448	40	-.719	70	-.118	126	-.079	155	-.137
11	-1.417	41	-.507	71	.071	127	-.089	156	-.132
12	-1.183	42	-.141	72	.023	128	-.119	157	-.128
13	-1.267	43	-.080	73	-.009	129	-.124	158	-.032
14	-.935	44	-.284	74	-.028	130	-.119	159	-.054
15	-.988	45	-.412	101	.124	131	-.129	160	-.077
16	-.326	46	-.478	102	.189	132	-.094	161	-.087
17	-.485	47	-.502	103	.328	133	-.089	162	-.087
18	-.626	48	-.540	104	.423	134	-.089	163	-.073
19	-.732	49	-.094	105	.443	135	-.079	164	-.009
20	-.834	50	-.142	106	.562	136	-.079	165	-.041
21	-.838	51	-.274	107	.602	137	-.089	166	-.054
22	-.847	52	-.293	108	.662	138	-.089	167	0.000
23	-.887	53	-.388	109	.696	139	-.089	168	-.027
24	-.896	54	-.402	110	.726	140	-.099	169	-.027
25	-.940	55	-.421	111	.746	141	-.109	170	-.032
26	-.295	56	-.440	112	.826	142	-.114	171	.018
27	-.331	57	-.483	113	.796	143	-.032	172	.018
28	-.525	58	-.014	114	-.333	144	-.109	173	.009
29	-.556	59	-.104	115	-.034	145	-.132	174	-.004
30	-.609	60	-.165	116	-.089				

NASA OGEE TIP
UNIVERSITY OF MARYLAND
WIND TUNNEL OPERATIONS DEPT.
RUN NO. TEST NO. 02/27/73
1 656

AA = 6.0 AY = 0.0 Q = 38.53 PSF V = 122.73 MPH

TUBE NO	PRESS COEFF	TUBE NO	PRESS COEFF	TUBE NO	PRESS COEFF	TUBE NO	PRESS COEFF	TUBE NO	PRESS COEFF
1	-1.871	31	-.777	61	-.236	117	-.065	146	-.059
2	-2.022	32	-.781	62	-.274	118	-.040	147	-.063
3	-2.198	33	-.803	63	-.293	119	-.010	148	-.050
4	-2.388	34	-.874	64	-.023	120	.010	149	-.045
5	-2.295	35	-.856	65	-.151	121	.020	150	-.059
6	-2.105	36	-.856	66	-.184	122	.095	151	-.082
7	-2.048	37	-.865	67	.009	123	.145	152	-.072
8	-2.048	38	-.869	68	-.080	124	.155	153	-.072
9	-2.048	39	-.869	69	-.123	125	.065	154	-.072
10	-2.075	40	-.843	70	-.127	126	-.060	155	-.072
11	-2.154	41	-.596	71	.056	127	-.060	156	-.068
12	-1.841	42	-.167	72	.014	128	-.050	157	-.063
13	-2.026	43	-.094	73	-.014	129	-.050	158	-.036
14	-.944	44	-.317	74	-.028	130	-.040	159	-.045
15	-1.205	45	-.468	101	.330	131	-.035	160	-.054
16	-.326	46	-.544	102	.450	132	-.015	161	-.054
17	-.547	47	-.582	103	.510	133	.005	162	-.045
18	-.710	48	-.625	104	.595	134	.010	163	-.036
19	-.825	49	-.113	105	.655	135	.025	164	-.013
20	-.984	50	-.151	106	.770	136	.025	165	-.027
21	-1.006	51	-.303	107	.810	137	.030	166	-.031
22	-1.046	52	-.331	108	.865	138	.025	167	-.009
23	-1.068	53	-.431	109	.870	139	.015	168	-.009
24	-1.090	54	-.459	110	.905	140	.010	169	-.013
25	-1.161	55	-.483	111	.910	141	.005	170	-.013
26	-.313	56	-.502	112	.955	142	-.010	171	.004
27	-.362	57	-.540	113	.945	143	-.031	172	.022
28	-.591	58	-.028	114	-.265	144	-.072	173	.018
29	-.640	59	-.113	115	.125	145	-.077	174	.009
30	-.710	60	-.180	116	-.065				

NASA OGEE TIP
UNIVERSITY OF MARYLAND
WIND TUNNEL OPERATIONS DEPT.
RUN NO. TEST NO. 02/27/73
1 656

AA = 8.0 AY = 0.0 Q = 38.53 PSF V = 122.73 MPH

TUBE NO	PRESS COEFF	TUBE NO	PRESS COEFF	TUBE NO	PRESS COEFF	TUBE NO	PRESS COEFF	TUBE NO	PRESS COEFF
1	-2.351	31	-.883	61	-.250	117	-.020	146	0.000
2	-2.479	32	-.887	62	-.288	118	.045	147	.009
3	-2.628	33	-.914	63	-.311	119	.080	148	.018
4	-2.909	34	-.993	64	-.037	120	.120	149	-.046
5	-2.808	35	-.984	65	-.153	121	.140	150	-.050
6	-2.465	36	-.989	66	-.190	122	.226	151	-.050
7	-2.874	37	-1.006	67	-.004	123	.276	152	-.041
8	-2.975	38	-1.010	68	-.083	124	.286	153	-.023
9	-2.795	39	-.997	69	-.125	125	.125	154	-.023
10	-2.751	40	-.949	70	-.134	126	-.035	155	-.023
11	-2.782	41	-.646	71	.037	127	-.025	156	-.018
12	-2.536	42	-.145	72	.013	128	.010	157	-.004
13	-2.681	43	-.134	73	-.013	129	.015	158	-.059
14	-.980	44	-.334	74	-.037	130	.030	159	-.046
15	-1.375	45	-.511	101	.518	131	.055	160	-.041
16	-.276	46	-.604	102	.608	132	.060	161	-.027
17	-.589	47	-.655	103	.699	133	.105	162	-.018
18	-.760	48	-.706	104	.769	134	.105	163	-.009
19	-.892	49	-.125	105	.829	135	.130	164	-.023
20	-1.090	50	-.162	106	.880	136	.135	165	-.009
21	-1.156	51	-.329	107	.920	137	.130	166	-.004
22	-1.213	52	-.357	108	.950	138	.130	167	-.023
23	-1.270	53	-.469	109	.965	139	.120	168	0.000
24	-1.296	54	-.506	110	.980	140	.105	169	.004
25	-1.432	55	-.529	111	.980	141	.100	170	.004
26	-.320	56	-.552	112	.990	142	.080	171	-.018
27	-.378	57	-.594	113	.980	143	-.041	172	.023
28	-.650	58	-.055	114	-.211	144	-.046	173	.023
29	-.707	59	-.120	115	.256	145	-.027	174	.013
30	-.795	60	-.185	116	-.070				

NASA OGEE TIP
UNIVERSITY OF MARYLAND
WIND TUNNEL OPERATIONS DEPT.
RUN NO. TEST NO. 02/27/73
1 656

TUBE NO	PRESS COEFF	TUBE NO	PRESS COEFF	TUBE NO	PRESS COEFF	TUBE NO	PRESS COEFF	TUBE NO	PRESS COEFF
AA =	10.0	AY =	0.0	Q =	38.53 PSF	V =	122.73 MPH		
1	-2.658	31	-.965	61	-.268	117	.015	146	.069
2	-2.809	32	-.980	62	-.315	118	.106	147	.078
3	-2.995	33	-1.004	63	-.330	119	.151	148	.101
4	-3.156	34	-1.073	64	-.070	120	.222	149	-.046
5	-2.926	35	-1.082	65	-.165	121	.242	150	-.046
6	-3.004	36	-1.082	66	-.207	122	.348	151	-.018
7	-2.809	37	-1.117	67	-.033	123	.389	152	-.004
8	-3.409	38	-1.117	68	-.084	124	.414	153	.018
9	-3.439	39	-1.082	69	-.132	125	.176	154	.032
10	-3.458	40	-1.024	70	-.136	126	-.015	155	.046
11	-3.478	41	-.673	71	.004	127	.005	156	.046
12	-3.263	42	-.126	72	.004	128	.065	157	.055
13	-3.360	43	-.240	73	-.018	129	.091	158	-.073
14	-.931	44	-.334	74	-.033	130	.106	159	-.036
15	-1.531	45	-.546	101	.616	131	.146	160	-.023
16	-.307	46	-.660	102	.702	132	.146	161	0.000
17	-.585	47	-.716	103	.813	133	.192	162	.023
18	-.760	48	-.777	104	.879	134	.207	163	.027
19	-.936	49	-.183	105	.915	135	.217	164	-.032
20	-1.209	50	-.183	106	.970	136	.227	165	.009
21	-1.258	51	-.330	107	.985	137	.227	166	.013
22	-1.395	52	-.372	108	.995	138	.227	167	-.036
23	-1.463	53	-.499	109	1.001	139	.222	168	.013
24	-1.482	54	-.542	110	.995	140	.207	169	.027
25	-1.634	55	-.575	111	.985	141	.176	170	.027
26	-.346	56	-.598	112	.965	142	.166	171	-.046
27	-.370	57	-.636	113	.980	143	-.050	172	.018
28	-.682	58	-.103	114	-.202	144	-.013	173	.032
29	-.760	59	-.127	115	.369	145	.027	174	.018
30	-.863	60	-.193	116	-.091				

NASA OGEE TIP
UNIVERSITY OF MARYLAND
WIND TUNNEL OPERATIONS DEPT.
RUN NO. TEST NO. 02/27/73
1 656

AA = 12.0 AY = 0.0 Q = 38.53 PSF V = 122.73 MPH

TUBE NO	PRESS COEFF	TUBE NO	PRESS COEFF	TUBE NO	PRESS COEFF	TUBE NO	PRESS COEFF	TUBE NO	PRESS COEFF
1	-2.938	31	-1.013	61	-.270	117	.020	146	.119
2	-3.078	32	-1.061	62	-.326	118	.110	147	.142
3	-3.239	33	-1.094	63	-.355	119	.186	148	.169
4	-1.681	34	-1.164	64	-.184	120	.286	149	-.064
5	-1.611	35	-1.191	65	-.170	121	.321	150	-.054
6	-1.229	36	-1.202	66	-.208	122	.452	151	-.004
7	-2.398	37	-1.234	67	-.132	123	.503	152	.022
8	-3.417	38	-1.229	68	-.099	124	.513	153	.068
9	-3.536	39	-1.202	69	-.132	125	.226	154	.082
10	-4.237	40	-1.110	70	-.142	126	-.020	155	.091
11	-4.253	41	-.706	71	-.075	127	0.000	156	.096
12	-4.183	42	-.113	72	-.056	128	.105	157	.114
13	-4.199	43	-.473	73	-.033	129	.145	158	-.100
14	-.884	44	-.521	74	-.037	130	.171	159	-.032
15	-1.229	45	-.516	101	.724	131	.211	160	-.009
16	-.555	46	-.682	102	.799	132	.216	161	.032
17	-1.261	47	-.767	103	.870	133	.276	162	.050
18	-1.266	48	-.852	104	.875	134	.286	163	.064
19	-1.202	49	-.364	105	.880	135	.311	164	-.045
20	-1.013	50	-.360	106	.950	136	.316	165	.022
21	-1.229	51	-.402	107	.990	137	.326	166	.036
22	-1.504	52	-.378	108	.995	138	.326	167	-.054
23	-1.628	53	-.511	109	.975	139	.311	168	.013
24	-1.649	54	-.577	110	.945	140	.306	169	.036
25	-1.827	55	-.615	111	.920	141	.281	170	.036
26	-.873	56	-.644	112	.865	142	.266	171	-.073
27	-.857	57	-.682	113	.880	143	-.087	172	.009
28	-.663	58	-.217	114	-.191	144	0.000	173	.032
29	-.679	59	-.255	115	.392	145	.073	174	.041
30	-.857	60	-.236	116	-.110				

NASA OGEE TIP
UNIVERSITY OF MARYLAND
WIND TUNNEL OPERATIONS DEPT.
RUN NO. TEST NO. 02/27/73
1 656

TUBE NO	PRESS COEFF	TUBE NO	PRESS COEFF	TUBE NO	PRESS COEFF	TUBE NO	PRESS COEFF	TUBE NO	PRESS COEFF
AA =	14.0	AY =	0.0	Q =	38.53 PSF		V = 122.73 MPH		
1	-3.305	31	-.857	61	-.395	117	.045	146	.145
2	-3.650	32	-.916	62	-.333	118	.135	147	.186
3	-3.153	33	-.992	63	-.333	119	.201	148	.214
4	-1.757	34	-1.084	64	-.352	120	.286	149	-.100
5	-1.673	35	-1.227	65	-.318	121	.311	150	-.082
6	-1.631	36	-1.236	66	-.314	122	.482	151	-.009
7	-1.354	37	-1.337	67	-.252	123	.558	152	.027
8	-1.118	38	-1.337	68	-.276	124	.578	153	.077
9	-.958	39	-1.295	69	-.209	125	.271	154	.100
10	-2.682	40	-1.169	70	-.171	126	-.030	155	.127
11	-3.490	41	-.698	71	-.190	127	-.005	156	.132
12	-4.676	42	-.134	72	-.204	128	.110	157	.155
13	-5.063	43	-.780	73	-.199	129	.150	158	-.177
14	-.849	44	-.994	74	-.099	130	.191	159	-.072
15	-1.379	45	-.818	101	.799	131	.246	160	-.018
16	-.950	46	-.709	102	.860	132	.266	161	.027
17	-1.547	47	-.656	103	.910	133	.316	162	.059
18	-1.497	48	-.823	104	.930	134	.331	163	.082
19	-1.303	49	-.761	105	.925	135	.372	164	-.091
20	-1.135	50	-.799	106	.960	136	.377	165	.009
21	-.984	51	-.718	107	.970	137	.397	166	.027
22	-.958	52	-.690	108	.985	138	.402	167	-.113
23	-1.547	53	-.618	109	.995	139	.392	168	-.009
24	-1.648	54	-.561	110	.985	140	.372	169	.018
25	-1.976	55	-.542	111	.935	141	.357	170	.031
26	-1.185	56	-.594	112	.789	142	.331	171	-.132
27	-1.236	57	-.656	113	.774	143	-.118	172	-.036
28	-1.101	58	-.466	114	-.176	144	-.009	173	-.004
29	-.950	59	-.480	115	.427	145	.068	174	.013
30	-.899	60	-.433	116	-.115				

NASA OGEE TIP
UNIVERSITY OF MARYLAND
WIND TUNNEL OPERATIONS DEPT.
RUN NO. TEST NO. 02/27/73
2 656

AA = -2.0 AY = 0.0 Q = 56.64 PSF V = 148.81 MPH

TUBE NO	PRESS COEFF	TUBE NO	PRESS COEFF	TUBE NO	PRESS COEFF	TUBE NO	PRESS COEFF	TUBE NO	PRESS COEFF
1	-.071	31	-.334	61	-.122	117	-.297	146	-.326
2	-.185	32	-.285	62	-.122	118	-.393	147	-.332
3	-.173	33	-.303	63	-.132	119	-.427	148	-.307
4	-.216	34	-.294	64	.042	120	-.510	149	-.018
5	-.120	35	-.260	65	-.074	121	-.547	150	-.065
6	-.127	36	-.260	66	-.093	122	-.489	151	-.201
7	-.068	37	-.263	67	.071	123	-.448	152	-.214
8	-.086	38	-.263	68	-.045	124	-.455	153	-.254
9	0.000	39	-.257	69	-.058	125	-.174	154	-.276
10	-.006	40	-.260	70	-.071	126	-.178	155	-.251
11	.027	41	-.161	71	.090	127	-.215	156	-.264
12	.170	42	-.055	72	.038	128	-.352	157	-.282
13	.219	43	.003	73	.003	129	-.386	158	.074
14	-.427	44	-.161	74	-.012	130	-.407	159	-.052
15	-.365	45	-.252	101	-.718	131	-.427	160	-.136
16	-.219	46	-.261	102	-.633	132	-.359	161	-.161
17	-.254	47	-.255	103	-.544	133	-.369	162	-.152
18	-.337	48	-.226	104	-.516	134	-.369	163	-.149
19	-.362	49	-.016	105	-.520	135	-.356	164	.049
20	-.399	50	-.061	106	-.438	136	-.349	165	-.083
21	-.387	51	-.177	107	-.427	137	-.359	166	-.108
22	-.319	52	-.171	108	-.362	138	-.359	167	.074
23	-.281	53	-.216	109	-.308	139	-.366	168	-.043
24	-.254	54	-.219	110	-.314	140	-.356	169	-.062
25	-.260	55	-.206	111	-.318	141	-.356	170	-.065
26	-.176	56	-.216	112	-.150	142	-.314	171	.096
27	-.201	57	-.232	113	-.150	143	.024	172	.046
28	-.300	58	.067	114	-.585	144	-.214	173	0.000
29	-.312	59	-.042	115	-.592	145	-.304	174	-.024
30	-.334	60	-.113	116	-.243				

NASA OGEE TIP
UNIVERSITY OF MARYLAND
WIND TUNNEL OPERATIONS DEPT.
RUN NO. TEST NO. 02/27/73
2 656

AA = 2.0 AY = 0.0 Q = 40.42 PSF V = 125.71 MPH

TUBE NO	PRESS COEFF	TUBE NO	PRESS COEFF	TUBE NO	PRESS COEFF	TUBE NO	PRESS COEFF	TUBE NO	PRESS COEFF
1	-.880	31	-.520	61	-.170	117	-.165	146	-.202
2	-.980	32	-.481	62	-.175	118	-.222	147	-.194
3	-1.075	33	-.498	63	-.188	119	-.222	148	-.164
4	-1.179	34	-.494	64	.044	120	-.270	149	0.000
5	-1.010	35	-.477	65	-.103	121	-.284	150	-.047
6	-.954	36	-.468	66	-.130	122	-.217	151	-.146
7	-.888	37	-.490	67	.080	123	-.142	152	-.146
8	-.862	38	-.481	68	-.058	124	-.151	153	-.168
9	-.845	39	-.472	69	-.089	125	-.037	154	-.172
10	-.823	40	-.459	70	-.098	126	-.118	155	-.155
11	-.802	41	-.303	71	.107	127	-.142	156	-.151
12	-.572	42	-.121	72	.040	128	-.213	157	-.168
13	-.542	43	0.000	73	-.004	129	-.222	158	.069
14	-.702	44	-.233	74	-.026	130	-.246	159	-.038
15	-.732	45	-.346	101	-.056	131	-.236	160	-.099
16	-.273	46	-.368	102	0.000	132	-.184	161	-.107
17	-.385	47	-.377	103	.052	133	-.175	162	-.094
18	-.507	48	-.359	104	.198	134	-.180	163	-.086
19	-.602	49	-.031	105	.132	135	-.151	164	.047
20	-.654	50	-.080	106	.189	136	-.156	165	-.051
21	-.650	51	-.238	107	.241	137	-.151	166	-.069
22	-.620	52	-.247	108	.274	138	-.151	167	.060
23	-.589	53	-.314	109	.307	139	-.146	168	-.025
24	-.572	54	-.314	110	.326	140	-.161	169	-.034
25	-.576	55	-.305	111	.341	141	-.146	170	-.034
26	-.238	56	-.319	112	.454	142	-.142	171	.064
27	-.273	57	-.337	113	.440	143	.043	172	.051
28	-.424	58	.071	114	-.364	144	-.146	173	.012
29	-.450	59	-.058	115	-.246	145	-.207	174	-.008
30	-.498	60	-.143	116	-.142				

NASA OGEE TIP
UNIVERSITY OF MARYLAND
WIND TUNNEL OPERATIONS DEPT.
RUN NO. TEST NO. 02/27/73
2 656

AA = 4.0 AY = 0.0 Q = 43.25 PSF V = 130.03 MPH

TUBE NO	PRESS COEFF	TUBE NO	PRESS COEFF	TUBE NO	PRESS COEFF	TUBE NO	PRESS COEFF	TUBE NO	PRESS COEFF
1	-1.404	31	-.635	61	-.195	117	-.107	146	-.142
2	-1.518	32	-.587	62	-.207	118	-.134	147	-.138
3	-1.603	33	-.595	63	-.220	119	-.129	148	-.097
4	-1.708	34	-.643	64	.050	120	-.147	149	-.004
5	-1.611	35	-.582	65	-.118	121	-.161	150	-.044
6	-1.530	36	-.578	66	-.148	122	-.076	151	-.117
7	-1.445	37	-.582	67	.084	123	-.008	152	-.113
8	-1.408	38	-.587	68	-.063	124	-.008	153	-.121
9	-1.412	39	-.574	69	-.101	125	.013	154	-.126
10	-1.429	40	-.566	70	-.110	126	-.085	155	-.105
11	-1.372	41	-.404	71	.114	127	-.102	156	-.101
12	-1.048	42	-.178	72	.038	128	-.156	157	-.109
13	-1.069	43	-.004	73	-.008	129	-.161	158	.048
14	-.850	44	-.267	74	-.029	130	-.174	159	-.032
15	-.975	45	-.398	101	.192	131	-.156	160	-.085
16	-.295	46	-.445	102	.259	132	-.098	161	-.085
17	-.461	47	-.453	103	.299	133	-.085	162	-.069
18	-.607	48	-.453	104	.428	134	-.085	163	-.060
19	-.704	49	-.038	105	.362	135	-.053	164	.040
20	-.813	50	-.084	106	.429	136	-.044	165	-.040
21	-.805	51	-.263	107	.456	137	-.044	166	-.048
22	-.769	52	-.280	108	.501	138	-.044	167	.044
23	-.769	53	-.356	109	.519	139	-.044	168	-.016
24	-.736	54	-.364	110	.537	140	-.049	169	-.024
25	-.769	55	-.364	111	.555	141	-.053	170	-.024
26	-.263	56	-.373	112	.617	142	-.044	171	.052
27	-.307	57	-.403	113	.635	143	.004	172	.048
28	-.502	58	.080	114	-.259	144	-.121	173	.016
29	-.534	59	-.059	115	-.080	145	-.158	174	.004
30	-.578	60	-.152	116	-.107				

NASA OGEE TIP
UNIVERSITY OF MARYLAND
WIND TUNNEL OPERATIONS DEPT.
RUN NO. TEST NO. 02/27/73
2 656

AA = 6.0 AY = 0.0 Q = 44.33 PSF V = 131.65 MPH

TUBE NO	PRESS COEFF	TUBE NO	PRESS COEFF	TUBE NO	PRESS COEFF	TUBE NO	PRESS COEFF	TUBE NO	PRESS COEFF
1	-1.804	31	-.729	61	-.214	117	-.061	146	-.083
2	-1.975	32	-.690	62	-.230	118	-.065	147	-.063
3	-2.070	33	-.702	63	-.247	119	-.039	148	-.023
4	-2.435	34	-.749	64	.049	120	-.039	149	.007
5	-2.344	35	-.698	65	-.127	121	-.048	150	-.031
6	-2.003	36	-.694	66	-.164	122	.043	151	-.087
7	-2.193	37	-.710	67	.086	123	.105	152	-.079
8	-2.122	38	-.710	68	-.069	124	.114	153	-.075
9	-2.026	39	-.702	69	-.102	125	.057	154	-.075
10	-2.019	40	-.694	70	-.115	126	-.048	155	-.047
11	-2.023	41	-.487	71	.107	127	-.065	156	-.039
12	-1.626	42	-.222	72	.037	128	-.083	157	-.055
13	-1.701	43	-.020	73	-.008	129	-.092	158	.047
14	-.860	44	-.292	74	-.032	130	-.096	159	-.027
15	-1.174	45	-.448	101	.369	131	-.083	160	-.067
16	-.226	46	-.506	102	.417	132	-.026	161	-.055
17	-.507	47	-.526	103	.487	133	-.004	162	-.031
18	-.694	48	-.518	104	.619	134	0.000	163	-.019
19	-.813	49	-.045	105	.545	135	.035	164	.039
20	-.955	50	-.094	106	.589	136	.039	165	-.019
21	-.975	51	-.284	107	.606	137	.048	166	-.023
22	-.948	52	-.312	108	.628	138	.043	167	.051
23	-.955	53	-.395	109	.637	139	.039	168	-.003
24	-.932	54	-.415	110	.650	140	.026	169	-.003
25	-.987	55	-.411	111	.668	141	.035	170	-.003
26	-.289	56	-.419	112	.707	142	.026	171	.055
27	-.345	57	-.448	113	.720	143	.015	172	.051
28	-.575	58	.074	114	-.206	144	-.091	173	.019
29	-.614	59	-.065	115	.061	145	-.099	174	.011
30	-.674	60	-.164	116	-.123				

NASA OGEE TIP
UNIVERSITY OF MARYLAND
WIND TUNNEL OPERATIONS DEPT.
RUN NO. TEST NO. 02/27/73
2 656

TUBE NO	PRESS COEFF	TUBE NO	PRESS COEFF	TUBE NO	PRESS COEFF	TUBE NO	PRESS COEFF	TUBE NO	PRESS COEFF
AA =	8.0	AY =	0.0	Q =	44.33 PSF		V = 131.65 MPH		
1	-2.048	31	-.825	61	-.229	117	-.034	146	-.031
2	-2.190	32	-.797	62	-.246	118	0.000	147	-.007
3	-2.396	33	-.805	63	-.266	119	.030	148	.035
4	-2.327	34	-.854	64	.049	120	.052	149	0.000
5	-2.611	35	-.809	65	-.135	121	.056	150	-.027
6	-2.595	36	-.813	66	-.172	122	.151	151	-.063
7	-2.506	37	-.817	67	.082	123	.212	152	-.051
8	-3.008	38	-.829	68	-.069	124	.221	153	-.035
9	-2.914	39	-.813	69	-.106	125	.104	154	-.031
10	-2.647	40	-.789	70	-.114	126	-.043	155	-.003
11	-2.672	41	-.566	71	.110	127	-.047	156	.007
12	-2.311	42	-.259	72	.036	128	-.034	157	.007
13	-2.327	43	-.036	73	-.008	129	-.021	158	.035
14	-.623	44	-.315	74	-.024	130	-.026	159	-.019
15	-1.384	45	-.492	101	.446	131	-.004	160	-.055
16	-.311	46	-.561	102	.507	132	.034	161	-.043
17	-.514	47	-.586	103	.[illegible]76	133	.073	162	-.007
18	-.744	48	-.586	104	.711	134	.078	163	.003
19	-.890	49	-.057	105	.637	135	.112	164	.031
20	-1.097	50	-.102	106	.659	136	.117	165	-.007
21	-1.117	51	-.303	107	.676	137	.134	166	-.011
22	-1.133	52	-.336	108	.685	138	.134	167	.043
23	-1.129	53	-.430	109	.689	139	.125	168	0.000
24	-1.113	54	-.451	110	.689	140	.130	169	.007
25	-1.186	55	-.455	111	.698	141	.112	170	.007
26	-.291	56	-.471	112	.702	142	.112	171	.047
27	-.356	57	-.496	113	.732	143	.003	172	.055
28	-.635	58	.069	114	-.242	144	-.055	173	.027
29	-.692	59	-.069	115	.173	145	-.059	174	.019
30	-.765	60	-.172	116	-.160				

NASA OGEE TIP
UNIVERSITY OF MARYLAND
WIND TUNNEL OPERATIONS DEPT.
RUN NO. TEST NO. 02/27/73
2 656

TUBE NO	PRESS COEFF	TUBE NO	PRESS COEFF	TUBE NO	PRESS COEFF	TUBE NO	PRESS COEFF	TUBE NO	PRESS COEFF
AA =	10.0	AY =	0.0	Q =	44.33 PSF		V = 131.65 MPH		
1	-2.171	31	-.894	61	-.241	117	-.186	146	.019
2	-2.167	32	-.872	62	-.262	118	-.082	147	.051
3	-1.641	33	-.885	63	-.282	119	-.004	148	.103
4	-.616	34	-.939	64	.041	120	.104	149	-.051
5	-.584	35	-.899	65	-.143	121	.125	150	-.067
6	-.580	36	-.912	66	-.176	122	.251	151	-.051
7	-2.041	37	-.930	67	.073	123	.320	152	-.043
8	-2.958	38	-.926	68	-.073	124	.325	153	-.003
9	-3.237	39	-.903	69	-.098	125	.147	154	.007
10	-3.394	40	-.876	70	-.118	126	-.138	155	.043
11	-3.309	41	-.636	71	.102	127	-.134	156	.051
12	-3.116	42	-.301	72	.036	128	-.021	157	.051
13	-2.967	43	-.528	73	0.000	129	.013	158	.007
14	-.714	44	-.389	74	-.024	130	.030	159	-.019
15	-.800	45	-.541	101	.464	131	.065	160	-.047
16	-.809	46	-.610	102	.485	132	.104	161	-.011
17	-.741	47	-.647	103	.485	133	.156	162	.023
18	-.647	48	-.656	104	.581	134	.164	163	.039
19	-.647	49	-.164	105	.520	135	.195	164	.023
20	-1.047	50	-.184	106	.659	136	.203	165	.007
21	-1.160	51	-.336	107	.724	137	.221	166	.011
22	-1.258	52	-.364	108	.711	138	.221	167	.039
23	-1.294	53	-.455	109	.689	139	.216	168	.007
24	-1.276	54	-.487	110	.672	140	.208	169	.023
25	-1.362	55	-.492	111	.667	141	.203	170	.031
26	-.674	56	-.504	112	.637	142	.203	171	.043
27	-.665	57	-.537	113	.680	143	-.150	172	.055
28	-.656	58	.041	114	-.281	144	-.091	173	.027
29	-.723	59	-.077	115	.169	145	-.027	174	.027
30	-.813	60	-.184	116	-.307				

NASA OGEE TIP
UNIVERSITY OF MARYLAND
WIND TUNNEL OPERATIONS DEPT.
RUN NO. TEST NO. 02/27/73
2 656

AA = 12.0 AY = 0.0 Q = 44.33 PSF V = 131.65 MPH

TUBE NO	PRESS COEFF	TUBE NO	PRESS COEFF	TUBE NO	PRESS COEFF	TUBE NO	PRESS COEFF	TUBE NO	PRESS COEFF
1	-2.222	31	-.982	61	-.266	117	-.193	146	.063
2	-2.153	32	-.982	62	-.278	118	-.060	147	.098
3	-1.581	33	-1.003	63	-.291	119	-.008	148	.154
4	-2.195	34	-1.024	64	-.102	120	.077	149	-.173
5	-3.066	35	-1.010	65	-.159	121	.141	150	-.169
6	-1.121	36	-1.052	66	-.188	122	.313	151	-.047
7	-.668	37	-1.059	67	.020	123	.382	152	-.023
8	-.780	38	-1.059	68	-.082	124	.404	153	.011
9	-.808	39	-1.045	69	-.098	125	.184	154	.035
10	-3.205	40	-1.017	70	-.106	126	-.193	155	.082
11	-3.825	41	-.752	71	.053	127	-.180	156	.090
12	-3.965	42	-.383	72	.016	128	-.038	157	.098
13	-3.965	43	-.672	73	0.000	129	.021	158	-.122
14	-.564	44	-.664	74	-.024	130	.081	159	-.051
15	-.613	45	-.565	101	.498	131	.124	160	-.055
16	-.857	46	-.656	102	.507	132	.154	161	-.011
17	-.717	47	-.697	103	.511	133	.214	162	.039
18	-.634	48	-.717	104	.597	134	.232	163	.059
19	-.627	49	-.422	105	.546	135	.262	164	-.011
20	-1.310	50	-.344	106	.644	136	.275	165	.011
21	-1.344	51	-.364	107	.687	137	.296	166	.023
22	-1.233	52	-.545	108	.683	138	.300	167	-.015
23	-1.442	53	-.487	109	.717	139	.296	168	.003
24	-1.463	54	-.520	110	.679	140	.292	169	.039
25	-1.581	55	-.528	111	.576	141	.279	170	.039
26	-.703	56	-.549	112	.503	142	.275	171	.023
27	-.780	57	-.561	113	.550	143	-.276	172	.043
28	-.794	58	-.307	114	-.296	144	-.122	173	.019
29	-.794	59	-.282	115	.197	145	-.003	174	.031
30	-.808	60	-.200	116	-.352				

NASA OGEE TIP
UNIVERSITY OF MARYLAND
WIND TUNNEL OPERATIONS DEPT.
RUN NO. TEST NO. 02/27/73
2 656

TUBE NO	PRESS COEFF	TUBE NO	PRESS COEFF	TUBE NO	PRESS COEFF	TUBE NO	PRESS COEFF	TUBE NO	PRESS COEFF
AA =	14.0	AY =	0.0	Q =	43.77 PSF		V = 130.81 MPH		
1	-1.111	31	-.776	61	-.288	117	-.146	146	.076
2	-1.153	32	-.933	62	-.280	118	-.057	147	.129
3	-1.951	33	-.997	63	-.293	119	.004	148	.206
4	-1.851	34	-1.054	64	-.301	120	.115	149	-.242
5	-2.585	35	-1.082	65	-.188	121	.159	150	-.214
6	-1.217	36	-1.132	66	-.192	122	.368	151	-.101
7	-.591	37	-1.153	67	-.146	123	.465	152	-.056
8	-.612	38	-1.160	68	-.104	124	.478	153	.032
9	-.584	39	-1.146	69	-.104	125	.217	154	.060
10	-2.699	40	-1.132	70	-.113	126	-.226	155	.117
11	-3.945	41	-.840	71	-.012	127	-.190	156	.133
12	-4.586	42	-.462	72	-.029	128	-.026	157	.149
13	-4.843	43	-.770	73	-.025	129	.017	158	-.222
14	-.740	44	-.703	74	-.046	130	.093	159	-.117
15	-.633	45	-.690	101	.501	131	.155	160	-.085
16	-.690	46	-.561	102	.527	132	.203	161	-.004
17	-.804	47	-.695	103	.598	133	.266	162	.060
18	-.776	48	-.749	104	.709	134	.274	163	.085
19	-.705	49	-.607	105	.611	135	.332	164	-.1[illegible]
20	-.648	50	-.636	106	.589	136	.337	165	-.008
21	-.569	51	-.661	107	.638	137	.376	166	.020
22	-1.089	52	-.670	108	.674	138	.372	167	-.068
23	-1.488	53	-.498	109	.713	139	.368	168	-.008
24	-1.531	54	-.527	110	.687	140	.372	169	.040
25	-1.723	55	-.544	111	.620	141	.359	170	.040
26	-.861	56	-.565	112	.407	142	.354	171	-.044
27	-.861	57	-.586	113	.350	143	-.344	172	.008
28	-.641	58	-.473	114	-.341	144	-.161	173	.008
29	-.690	59	-.510	115	.186	145	-.024	174	.024
30	-.733	60	-.355	116	-.301				

NASA OGEE TIP
UNIVERSITY OF MARYLAND
WIND TUNNEL OPERATIONS DEPT.
RUN NO. TEST NO. 02/27/73
3 656

TUBE NO	PRESS COEFF	TUBE NO	PRESS COEFF	TUBE NO	PRESS COEFF	TUBE NO	PRESS COEFF	TUBE NO	PRESS COEFF
AA =	-2.0	AY =	0.0	Q =	47.20 PSF		V = 135.84 MPH		
1	-.114	31	-.357	61	-.127	117	-.353	146	-.353
2	-.178	32	-.325	62	-.131	118	-.434	147	-.372
3	-.185	33	-.325	63	-.147	119	-.459	148	-.357
4	-.264	34	-.328	64	.027	120	-.552	149	-.048
5	-.092	35	-.303	65	-.077	121	-.585	150	-.100
6	-.096	36	-.293	66	-.100	122	-.540	151	-.219
7	-.042	37	-.303	67	.054	123	-.500	152	-.230
8	-.021	38	-.303	68	-.042	124	-.495	153	-.271
9	.035	39	-.307	69	-.065	125	-.195	154	-.301
10	.010	40	-.296	70	-.077	126	-.199	155	-.286
11	.060	41	-.189	71	.089	127	-.239	156	-.301
12	.203	42	-.071	72	.034	128	-.373	157	-.309
13	.268	43	-.015	73	0.000	129	-.402	158	.037
14	-.457	44	-.189	74	-.015	130	-.418	159	-.067
15	-.375	45	-.267	101	-.845	131	-.447	160	-.134
16	-.250	46	-.278	102	-.703	132	-.394	161	-.171
17	-.282	47	-.282	103	-.646	133	-.402	162	-.167
18	-.357	48	-.259	104	-.613	134	-.414	163	-.171
19	-.382	49	-.038	105	-.589	135	-.406	164	.029
20	-.421	50	-.077	106	-.475	136	-.406	165	-.093
21	-.403	51	-.189	107	-.479	137	-.418	166	-.122
22	-.332	52	-.189	108	-.382	138	-.422	167	.063
23	-.300	53	-.232	109	-.357	139	-.426	168	-.052
24	-.289	54	-.240	110	-.308	140	-.430	169	-.070
25	-.296	55	-.232	111	-.313	141	-.414	170	-.074
26	-.200	56	-.232	112	-.134	142	-.382	171	.081
27	-.225	57	-.259	113	-.174	143	-.003	172	.040
28	-.310	58	.042	114	-.666	144	-.234	173	.003
29	-.332	59	-.058	115	-.638	145	-.327	174	-.022
30	-.350	60	-.108	116	-.247				

NASA OGEE TIP
UNIVERSITY OF MARYLAND
WIND TUNNEL OPERATIONS DEPT.
RUN NO. TEST NO. 02/27/73
3 656

AA = 2.0 AY = 0.0 Q = 38.45 PSF V = 122.60 MPH

TUBE NO	PRESS COEFF	TUBE NO	PRESS COEFF	TUBE NO	PRESS COEFF	TUBE NO	PRESS COEFF	TUBE NO	PRESS COEFF
1	-.892	31	-.555	61	-.184	117	-.211	146	-.215
2	-1.063	32	-.533	62	-.198	118	-.246	147	-.215
3	-1.050	33	-.547	63	-.213	119	-.251	148	-.206
4	-1.221	34	-.555	64	.023	120	-.296	149	-.022
5	-.945	35	-.529	65	-.113	121	-.306	150	-.073
6	-.962	36	-.529	66	-.142	122	-.236	151	-.160
7	-.857	37	-.551	67	.061	123	-.176	152	-.160
8	-.849	38	-.542	68	-.061	124	-.176	153	-.183
9	-.844	39	-.542	69	-.094	125	-.050	154	-.192
10	-.844	40	-.529	70	-.108	126	-.140	155	-.183
11	-.814	41	-.363	71	.099	127	-.155	156	-.178
12	-.560	42	-.161	72	.037	128	-.231	157	-.192
13	-.599	43	-.028	73	-.004	129	-.251	158	.032
14	-.743	44	-.255	74	-.028	130	-.251	159	-.054
15	-.757	45	-.364	101	-.171	131	-.261	160	-.100
16	-.271	46	-.402	102	-.050	132	-.211	161	-.119
17	-.415	47	-.402	103	.010	133	-.206	162	-.109
18	-.538	48	-.402	104	.125	134	-.211	163	-.109
19	-.603	49	-.056	105	.115	135	-.186	164	.022
20	-.673	50	-.104	106	.231	136	-.181	165	-.054
21	-.682	51	-.255	107	.256	137	-.191	166	-.077
22	-.656	52	-.260	108	.326	138	-.191	167	.050
23	-.643	53	-.336	109	.342	139	-.201	168	-.032
24	-.608	54	-.341	110	.382	140	-.196	169	-.041
25	-.660	55	-.345	111	.377	141	-.196	170	-.045
26	-.262	56	-.355	112	.533	142	-.171	171	.054
27	-.288	57	-.378	113	.492	143	.013	172	.041
28	-.446	58	.047	114	-.422	144	-.160	173	.013
29	-.472	59	-.075	115	-.271	145	-.215	174	-.009
30	-.533	60	-.142	116	-.171				